(Oligo-)Thiophene Functionalized Tetraazaperopyrenes: Donor–Acceptor Dyes and Ambipolar Organic Semiconductors

Lena Hahn,[†] André Hermannsdorfer,[†] Benjamin Günther,[†] Tobias Wesp,[†] Bastian Bühler,[†] Ute Zschieschang,[‡] Hubert Wadepohl,[†] Hagen Klauk,[‡] and Lutz H. Gade*,[†]

[†]Anorganisch-Chemisches Institut, Universität Heidelberg, Im Neuenheimer Feld 270, 69120 Heidelberg, Germany
[‡]Max Planck Institute for Solid State Research, Heisenbergstr.1, 70569 Stuttgart, Germany

Ⓢ *Supporting Information*

ABSTRACT: Tetraazaperopyrenes (TAPPs) have been functionalized with thiophene and terthiophene units of different architecture resulting in a variety of organic donor–acceptor (D–A) compounds. The influence of the connection of the thiophenes to the TAPP core on their structural, photophysical and electrochemical properties has been studied in detail by a combination of X-ray crystallography, UV–vis and fluorescence spectroscopy as well as cyclic voltammetry, which allowed the establishment of structure–property relationships. The HOMO–LUMO gap is significantly decreased upon substitution of the TAPP core with electron-donating thiophene units, the extent of which is strongly influenced by the orientation of the thiophene units. The latter also crucially directs the molecular packing in the solid. Linkage at the α-position allows both inter- and intramolecular N···S interaction, whereas linkage in the β-position prevents intramolecular N···S interaction, resulting in a less pronounced conjugation of the TAPP core and the thiophene units. The new TAPP derivatives were processed as semiconductors in organic thin-film transistors (TFTs) that show ambipolar behavior. The insight into band gap and structure engineering may open up new possibilities to tailor the electronic properties of TAPP-based materials for certain desired applications.
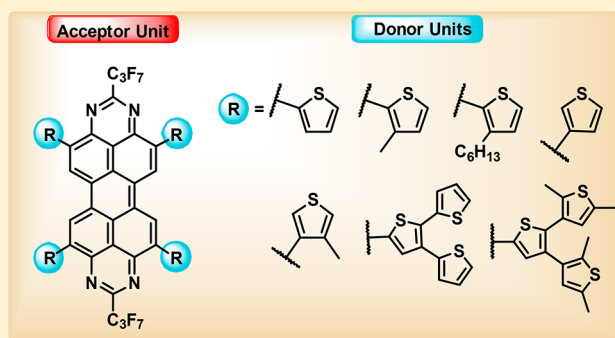
INTRODUCTION

Ambipolar behavior in organic semiconductors employed in electronic devices may be achieved by appropriate choice of the device architecture by, for example, applying nonsymmetric work-function electrodes,[1] electrode surface modifications[2] or depositing bilayer/blend semiconductor films.[3,4] However, the use of intrinsically ambipolar semiconducting materials would greatly simplify the fabrication of such devices. Donor–acceptor (D–A) conjugated molecules have been of interest for manifold applications in optoelectronics, including donor–acceptor conjugated polymer-based[5–11] as well as small molecule-based[12–18] ambipolar organic TFTs. Although polymer-based ambipolar organic TFTs tend to display greater electron and hole mobilities than their small molecule-based analogues, the latter have the possible advantage of potentially smaller batch-to-batch variations.[19]

The frontier orbital energies of the semiconducting material are key parameters determining whether electrons or holes will predominantly be injected into the transistor channel. In order to transport both electrons and holes, the organic semiconductor must usually possess both sufficiently low LUMO levels and at the same time close HOMO and LUMO frontier orbitals with an energy gap in the range of 2.0 eV[3,20] which is a significant challenge, explaining why only a few small molecules

with ambipolar charge-transport that operate under ambient conditions are known to date.[21–24]

Due to their electron-rich character and resulting electrochemical properties along with their excellent charge-transport properties, thiophene or oligothiophene units are often employed as the electron-donating moieties in D–A systems.[25–30] Thiophene moieties attached to electron-poor perylene diimide (PDI) and naphthalene diimide (NDI) units have been the focus of a number of recent studies.[27,28,31–48] These types of D–A ensembles have shown potential as materials for ambipolar organic TFTs, organic solar cells and dye-sensitized solar cells.[33]

We have developed an efficient synthetic route to a class of functional dyes which possess photophysical and redox-chemical properties that are in many respects comparable to those of PDIs. The 1,3,8,10-tetraazaperopyrenes (TAPPs) are readily accessible poly-N-heterocyclic species obtained either from the oxidative coupling of 1,8-diaminonaphthaline or by derivatization of perylenes.[49,50] The structure of TAPP is related to the structure of PDI with the two carboximido units at the perylene core being replaced by two fused pyrimidine rings. While PDIs are certainly the most intensely studied class

of organic dyes, due to the variety of their applications as for example pigments, biosensors, and as organic semiconductors in organic light emitting diodes as well as in thin film transistors,[51−55] the full potential of TAPPs has yet to be explored.

TAPPs are characterized by a compact and chemically relatively inert poly-N-heterocyclic core structure which alone has been shown to be a potent electron acceptor unit. Substitution of the TAPP core provides a means of modifying the frontier orbital energy levels and thus of fine-tuning the properties of TAPP-based materials.[56,57] These include, inter alia, water-soluble dyes that have been employed as fluorescence markers in cells[58] and a variety of TAPP derivatives which have been applied as semiconductors in n-channel organic TFTs.[59−61]

Here we present the synthesis of a range of thiophene- and oligothiophene-functionalized tetraazaperopyrene derivatives which has given rise to new types of D−A systems. Structure−property relationships are derived from detailed investigations of their molecular packing motifs in the solid as well as their optical, electrochemical and charge-transport properties.

RESULTS AND DISCUSSION

Synthesis of Thiophene-Functionalized Tetraazapero-pyrenes. Using a previously reported core-brominated TAPP derivative as the starting material,[60] compounds 1−5 were obtained as purple solids in moderate to good yields (53−75%) by Suzuki coupling with the corresponding boronic acid pinacol ester-substituted thiophenes using Pd(dppf)Cl₂ as catalyst (Scheme 1). Except for derivative 1, all compounds exhibit

Scheme 1. Synthesis of Compounds 1−5 via Suzuki Reaction
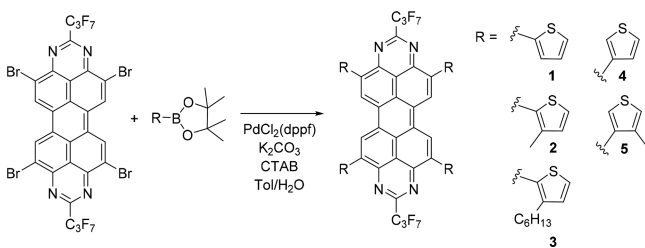
good solubility in common organic solvents such as chloroform or THF and thus allowed complete characterization by mass spectrometry, ¹H and ¹³C NMR as well as the investigation of their photophysical and electrochemical properties.

Crystal Structures of Compounds 2−5. In a comparative investigation of the solid-state structures of the new TAPP derivatives, single-crystals of the soluble compounds 2−5 suitable for X-ray diffraction were grown from solutions in organic solvents (see SI).

As expected, all derivatives have an only slightly distorted TAPP core, represented by the torsion angle Φ (Figure 1), with the distortion of the polycyclic core being slightly more pronounced in the β-thienyl-linked TAPP 5 than in the α-linked thienyl derivatives (with reference to the minimum Φ). In the case of 3, the steric hindrance of the hexyl group prevents the expected planarity, resulting in an enlarged Φ. In contrast to the core twisting, the rotation of the thienyl substituents, represented by the dihedral angle δ, differs greatly, with α-linkage generally leading to a significantly lower out-of-plane rotation. The compounds featuring the latter exhibit
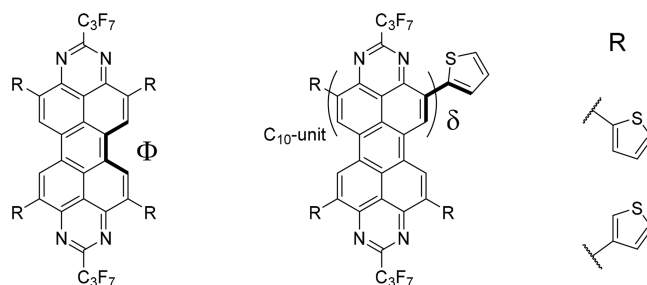
Figure 1. Torsion angles Φ (left) and δ (right) as the key features of the molecular structures.

relatively short N···S distances, leading in all cases to a "head-to-head" arrangement in the solid-state structures. This can be attributed to possible N···S interactions, as exemplified by the N···S distances of 2.729 and 2.989 Å in **2** (sum of the Van-der-Waals radii being 3.35 Å), which is comparable to other N−S interactions described previously in literature (Figure 2).[62,63]
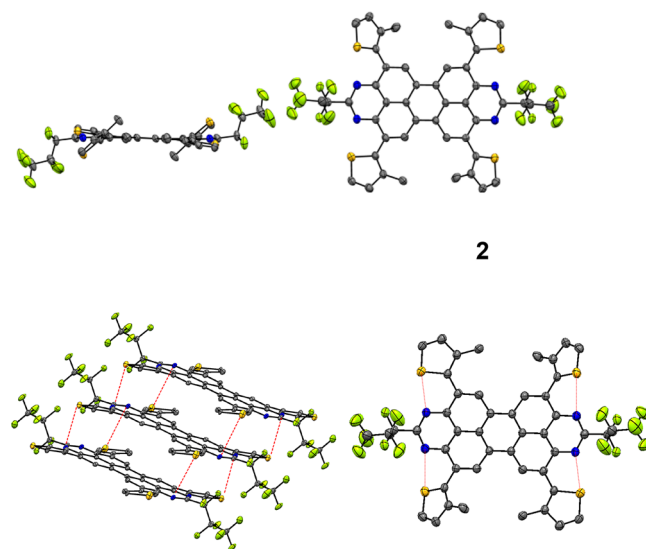
Figure 2. Top: Molecular structure of compound **2**. Bottom: Inter- and intramolecular N···S interactions in compound **2**. Thermal ellipsoids are drawn at 50% probability level. Hydrogen atoms are omitted for reasons of clarity. Only one of the independent molecules is shown.

In the case of derivative **3**, only two of the thienyl groups are coplanar with respect to the TAPP core, whereas the other two are rotated significantly due to the steric hindrance of the hexyl groups (Figure 3). In contrast, for the β-linked derivatives **4** and **5** no N−S interactions are possible, and the rotation angle of the thienyl units with respect to the TAPP core is thus determined by the sterics of other substituents of the S-heterocycle, as evident in compound **5**. A summary of the different distortion and rotation angles is given in Table 1.

The packing pattern of compounds **2−4** is similar to most other previously synthesized TAPP derivatives. It is characterized by a slip-stacked face-to-face arrangement of the molecules with π−π plane distances of 3.44−3.47 Å (Table 1). This pattern is exemplified for compound **2** in Figure 4 (top). An exception is the packing pattern of compound **3** that forms trimeric subaggregates which probably result from the orientational effect of the hexyl groups (Figure 4, bottom).
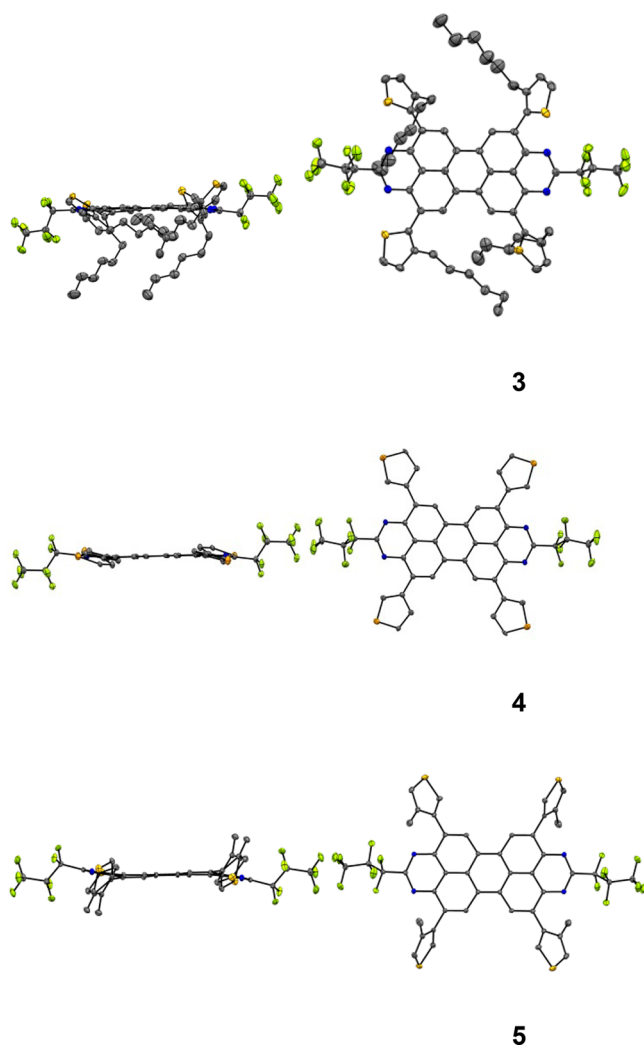
3

4

5

Figure 3. Molecular structures of **3**−**5** observed in the solid state. Thermal ellipsoids are drawn at 50% probability level. Hydrogen atoms are omitted for reasons of clarity.

Table 1. Important Geometric Parameters of TAPP Compounds 2−5

	Φ [deg]		δ [deg][a]		rmsd of mean TAPP core plane [Å]	π−π plane distance [Å]
	min.	max.	min.	max.		
2	0.9(9)	2.7(9)	10.2(2)	42.4(2)	0.043, 0.061	3.45
3	1.8(4)	9.7(4)	33.34(8)	57.02(7)	0.101, 0.013	3.44
4	0.8(3)		17.3(2)	20.2(1)	0.080	3.47
5	4.7(2)		47.83(6)	68.33(5)	0.108	

[a]Interplanar angle between thiophene substituent and C_{10}-unit of TAPP core (C1 through C10).

The molecules of **3** have small π−π plane distances of 3.44 Å within the trimeric subaggregate, but large distances of approximately 10 Å between these units. For TAPP derivative **5**, the crystals contained solvent molecules in the lattice preventing the comparison of the solid-state structures in terms of the packing pattern and π−π plane distance.

Photophysical and Redox-Chemical Properties of the Thienyl-TAPP Compounds 2−5. The UV−vis spectra of compounds **2**−**5** along with the UV−vis spectrum of the parent
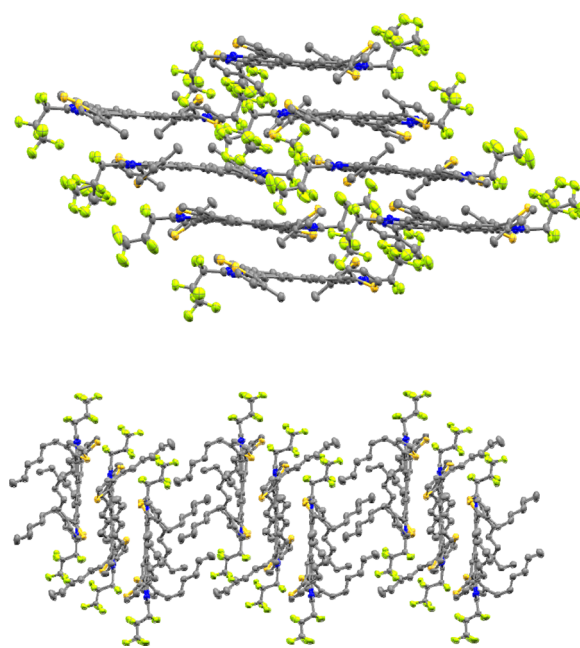

Figure 4. Regular packing pattern of compound **2** (top) and aggregation in the form of trimeric units in case of compound **3** (bottom).

TAPP compound 2,9-bis(heptafluoropropyl)-1,3,8,10-tetraazaperopyrene (**TAPP-H**) recorded in THF are depicted in Figure 5. The thienyl TAPPs exhibit absorption maxima at 493−538 nm, with similar extinction coefficients (log $\varepsilon \approx 4.60$), that can be attributed to the $S_1 \leftarrow S_0$ transition. Compared to the parent compound, the absorption maxima of **2**−**5** exhibit a bathochromic shift, which is the result of the reduced HOMO−LUMO gap, due to the presence of the donor groups. The effect is most pronounced for the derivatives with the smallest interplanar angle δ, and least for **5**, in which the rotation out of the TAPP plane prevents an effective conjugation of the thienyl rings and the TAPP core, minimizing the donating effect of the peripheral units. Furthermore, all the TAPPs **2**−**5** exhibit broadened absorption bands compared to **TAPP-H** due to the orientational mobility, resulting in a reduced resolution of the vibronic fine structure. The high-energy absorption bands at wavelengths below 400 nm are primarily assigned to excitations localized on the thiophene moieties.

The emission spectra of compounds **2**−**5** were recorded in THF, with emission maxima in the range of 551 to 627 nm. The α-linked compounds **2** and **3** (2848 and 3245 cm^{-1}) exhibit considerably larger Stokes shifts than the β-linked derivatives **4** and **5** (1166 and 2135 cm^{-1}). This indicates that the molecular geometry of the ground state and the excited state differs significantly for α-linked TAPPs, whereas the difference appears to be less pronounced in the β-linked derivatives. With the exception of compound **5** (ϕ_{em} = 0.33) the thienyl-substituted TAPPs show intense fluorescence in solution, with fluorescence quantum yields of 62 to 70%. The observed large Stokes shifts are indicative of significant structural differences of the energy minima in the ground state and the first excited state. The absorption and emission maxima as well as the fluorescence quantum yields are listed and related to the interplanar angle δ in Table 2.

The frontier orbital energies are key parameters determining whether an organic compound is suitable as a semiconductor in organic electronics and whether electrons or holes will
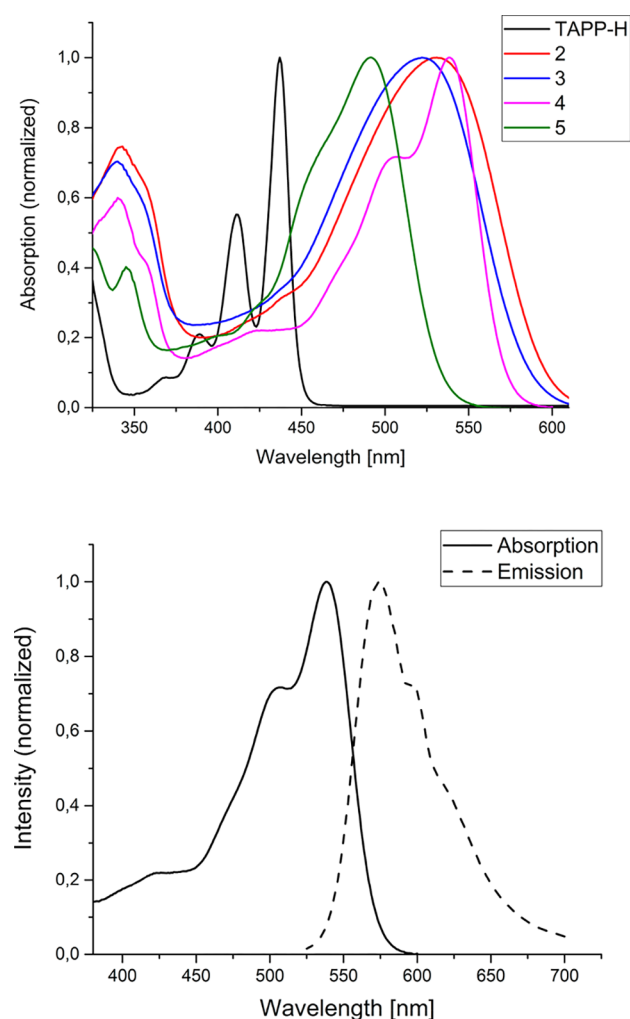
Figure 5. Top: Absorption spectra of compounds **2**−**5** and TAPP-H, recorded in THF. Bottom: Absorption and emission bands of **4** recorded in THF.

predominantly be injected into the transistor channel. Therefore, in a first step, the frontier orbital molecular energies and electron affinities of compounds **1**−**5** were modeled by DFT. The B3LYP functional[64−66] and a def2-SVP basis set[67] were used for geometry optimization, the molecular orbital energies and the other properties were calculated based on that geometry using a def2-QZVPP basis set.[68]

The combination of donor−acceptor units in compounds **1**−**5** strongly affects the energy levels of the frontier orbitals. The calculated HOMO and LUMO energies of **TAPP-H** as well as compounds **1**−**5** are summarized in Table 3.

The Kohn−Sham frontier orbitals of **2** are shown in Figure 6 and closely resemble the corresponding MOs of the other thiophene-substituted TAPP derivatives reported in this work. As expected, substitution of the TAPP core with electron-donating thienyl moieties leads to a significant destabilization of the HOMO level compared to the unsubstituted **TAPP-H**, while the energy of the LUMO, which is localized almost entirely on the TAPP core, is only slightly affected. This results in reduced HOMO−LUMO gaps between 2.51 and 2.00 eV. The observation that the destabilization of the HOMO level is least pronounced for compound **5** is in agreement with a strong torsion of the thiophene units out of the TAPP core plane due to steric repulsion. Experimental estimates of the LUMO levels were obtained for soluble compounds **2**−**5** by means of cyclic voltammetry (CV) measurements using Fc/Fc$^+$ as an internal standard, setting E_{HOMO} (Fc) = −4.8 eV. The CVs of compounds **2**−**5** display two reversible reduction waves, indicating the formation of a monoanion and a dianion, respectively (see CV of compound **4** in Figure 7). The LUMO levels deduced from the CV measurements are in good agreement with the calculated values, which has also been observed previously for other TAPP derivatives. The oxidation potentials could not be measured by CV, due to the highly irreversible nature of the oxidation processes.

Charge-Transport Properties in Thin-Film Transistors. Core-halogenated TAPP-derivatives have been successfully employed as semiconductors in n-channel organic TFTs that displayed field-effect mobilities of up to 0.17 cm^2/(V s).[61] As in these previous studies, the electrical properties of compounds **1**−**5** were studied in TFTs with a bottom-gate, top-contact architecture and a vacuum-deposited semiconductor layer.

Electron mobilities (μ_e, determined in the saturation regime), on/off current ratios (I_{on}/I_{off}), subthreshold swings (SS), and threshold voltages (V_{th}) were extracted from the measured transfer characteristics. Electron mobilities observed for transistors fabricated with **1**−**5** as the semiconductor along with the predicted properties and the solid-state-structure characteristics are summarized in Table 4. TFTs based on all five derivatives display n-channel behavior, with electron mobilities ranging from 2×10^{-4} to 6×10^{-3} cm^2/(V s). In addition to the n-channel behavior, which is characteristic for most TAPP derivatives reported so far, p-channel behavior was observed for compounds **1**, **2** and **4**, with hole mobilities in the range of 7×10^{-4} to 0.015 cm^2/(V s). This ambipolar transistor behavior is related to the electron-donating thienyl substituents that result in a relatively small HOMO−LUMO gap which allows both electrons and holes to be injected from the gold source and drain contacts into the semiconductor (Table 4).

The p-channel behavior is most pronounced for compound **4** with a hole mobility of 0.015 cm^2/(V s). In contrast, compounds **3** and **5** display only weak n-channel and no

Table 2. Interplanar Angles and Photophysical Properties of TAPP-Compounds 2−5 in THF

	δ [deg]^a		λ_{max} [nm] (log ε)	λ_{em} [nm]	Stokes shift [cm^{-1}]	ϕ_{Em}
	min.	max.				
2	10.2(2)	42.4(2)	532 (4.59)	627	2848	0.70
3	33.34(8)	57.02(7)	521 (4.58)	627	3245	0.65
4	17.3(2)	20.2(1)	538 (4.65)	574	1166	0.62
5	47.83(6)	68.33(5)	493 (4.65)	551	2135	0.33
TAPP-H	−	−	436	448	938	0.51

^{a}Interplanar angle between thiophene substituent and C$_{10}$ unit of TAPP core (C1 through C10).

Table 3. Electrochemical Properties of TAPP-H and Compounds 1−5

	$E_{\text{HOMO (DFT)}}$ [eV]	$E_{\text{LUMO (DFT)}}$ [eV]	$E_{\text{LUMO (CV)}}$ [eV]	$\Delta E_{\text{HOMO−LUMO}}$ [eV]	$EA_{\text{(DFT)}}$ [eV]
1	−5.70	−3.72	−	1.98	2.77
2	−5.73	−3.57	−3.76	2.16	2.34
3[a]	−5.73	−3.57	−3.75	2.16	2.67
4	−5.76	−3.56	−3.78	2.20	2.67
5	−6.15	−3.64	−3.70	2.51	2.71
TAPP-H	−6.61	−3.66	−	2.95	2.62

[a]Hexyl-groups of the thiophene units were simplified to methyl-groups to reduce computational cost (→ 2 = 3!).
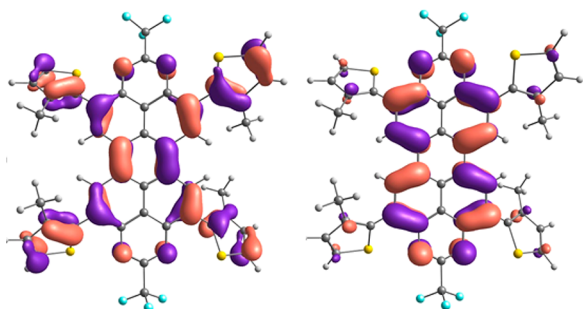

Figure 6. HOMO (left) and LUMO (right) of **2**, calculated with B3LYP/def2-SVP//B3LYP/def2-QZVPP. As previously reported[50,57,59−61] the substituents in 2- and 9-position have no significant influence in orbital energies, thus C_3F_7 groups were reduced to CF_3 groups to reduce computational cost.
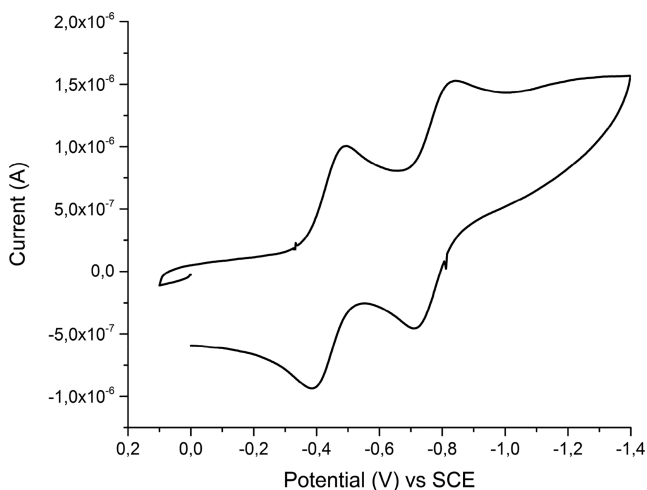

Figure 7. Cyclic voltammogram of compound **4** recorded in THF (sweep rate 50 mV s^{-1}; supporting electrolyte Bu_4NPF_6, reference SCE).

Table 4. Comparison of Predictive Semiconductor Properties, Solid State Structure Characteristics as Well as Electron and Hole Mobility of Compounds 1−5

	$\pi-\pi$ distance	μ_e [cm^2/(V s)]	μ_h [cm^2/(V s)]
1	−	1×10^{-3}	7×10^{-4}
2	3.45	6×10^{-3}	4×10^{-4}
3	3.44	3×10^{-3}	−
4	3.47	1.5×10^{-3}	1.5×10^{-2}
5	−	2×10^{-4}	−

chemical properties. In case of **3** we attribute this observation to the trimeric packing pattern described above which is characterized by large distances between the trimer units, preventing efficient charge-transport. In addition, the degree of torsion of the thiophene substituents with respect to the TAPP core, which was found to be most pronounced in the case of compounds **3** and **5**, could be a possible reason for the diminished charge transport capability. In contrast, in compounds **2** and **4**, the thienyl substituents are almost coplanar with respect to the TAPP core, resulting in a significant interaction of the electron-rich thienyl units and the electron-poor TAPP core, which could explain the ambipolar TFT behavior observed for these compounds. The current−voltage characteristics of organic TFTs fabricated using compound **4** as the semiconductor are shown in Figure 8.
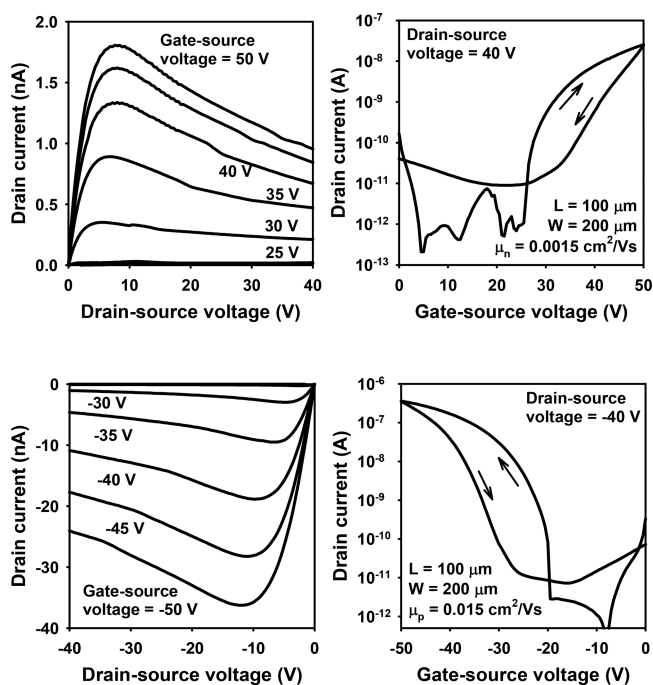

Figure 8. Current−voltage characteristics of organic TFTs using compound **4** as the semiconductor, showing n-channel transistor behavior (top) and p-channel transistor behavior (bottom).

In addition to the intrinsic materials properties the processability and the morphological properties of the TAPP derivatives also have an important influence on the TFT performance. To evaluate the morphology of the vacuum-deposited semiconductor layer, atomic force microscopy (AFM) analysis was conducted; the results are shown in Figure 9. While clearly differing in crystalinity, all four materials give rise to relatively uniform thin film. However, compound **5**
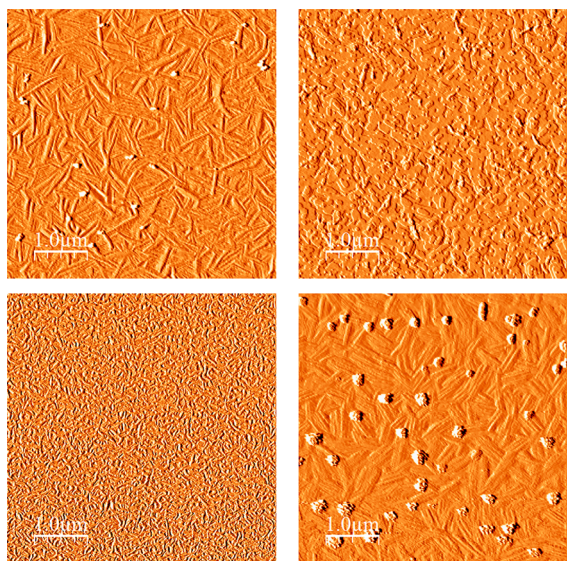
measurable p-channel characteristics. The predominantly n-channel behavior of compounds **3** and **5** seems surprising when considering compounds **3** and **2** possess very similar electro-

Figure 9. AFM graphs of transistor surfaces of compounds **2** (top left), **3** (top right), **4** (bottom left) and **5** (bottom right).

shows clear formation of aggregated islands which could explain the considerable decrease of mobility in comparison to compounds **1–4**.

Synthesis of Oligothiophene-Functionalized Tetra-azaperopyrenes. In addition to the thiophene-substituted TAPP derivatives **1–5**, the terthiophene-substituted compounds **8–10** and **12** were synthesized via two different routes. Reacting the tetrabromo-TAPP with boronic acid pinacol esters **6** and **7** lead to the formation of compounds **8** and **9** in yields of 34% and 59%, respectively.[32,69] In the case of **9**, the trimethylsilyl substituted boronic pinacol ester was used in order to provide sufficient solubility to ensure the 4-fold substitution. Desilylation of compound **9** with TBAF in THF afforded compound **10** in 72% yield (Scheme 2).

For the synthesis of **12** a different approach was chosen. In the first step, compound **4** was reacted with bromine at room temperature, to give the octabrominated compound **11** in a high yield of 82%. Conversion of **11** with 2-thiophene boronic acid pinacol ester resulted in the formation of TAPP derivative **12** with 45% yield (Scheme 3).

Photophysical and Electrochemical Properties of Compounds 8, 10 and 12. The UV–vis spectra of compounds **8**, **10** and **12** along with the UV–vis spectrum of **TAPP-H** recorded in THF are depicted in Figure 10 (and the SI). There are significant differences in the absorption spectra of terthiophene-linked compounds **8**, **10** and **12** compared to those of compounds **2–5**. The absorption spectra display three absorption maxima, two maxima in the range of 330 to 490 nm and a broad low-energy absorption at 662 nm (**8**), 660 nm (**10**) and 524 nm (**12**), respectively. The absorption bands at 483 nm (**8**), 482 nm (**10**) and 461 nm (**12**) are assigned to $\pi^* \leftarrow \pi$ transitions localized on the TAPP-core (λ_{max}(**TAPP-H**) = 436 nm). The high-energy bands between 330 and 390 nm can be assigned to $\pi^* \leftarrow \pi$ transitions localized on the terthiophene units (λ_{max} (terthiophene) = 354 nm),[70] whereas the broad low-energy absorption band is due to a terthiophene–TAPP charge transfer transition.

The absorption maxima of α-linked compounds **8** and **10** are red-shifted compared to the corresponding absorption bands of the β-linked compound **12**. This may be explained by the β-

Scheme 2. Synthesis of the Terthiophene-Substituted Compounds 8–10
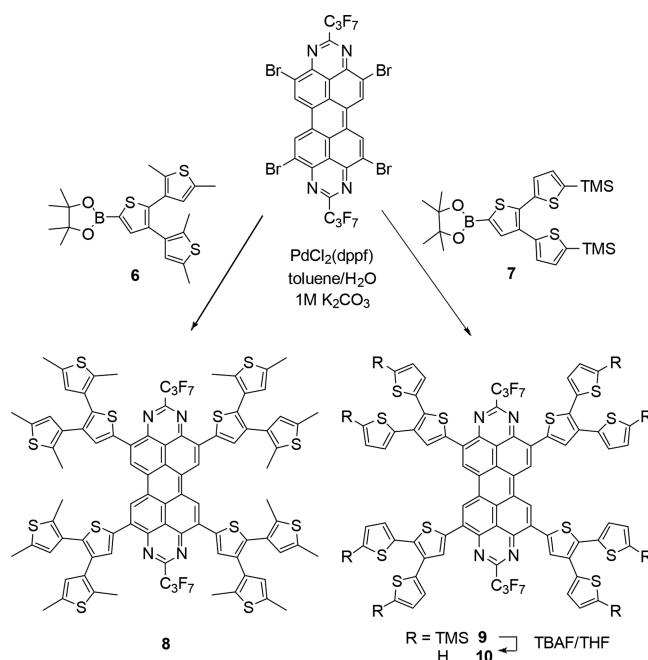
Scheme 3. Synthesis of the TAPP Derivative 12
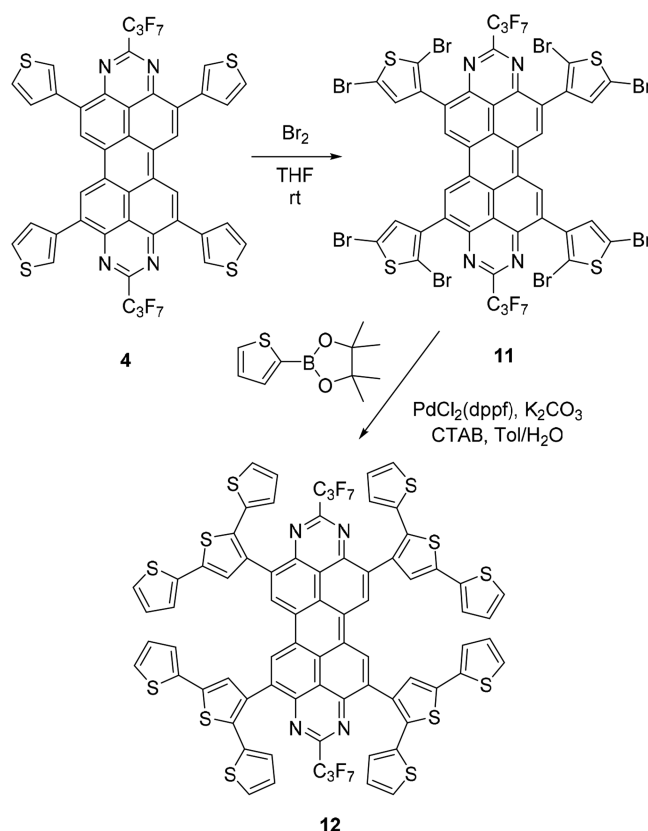
linkage of the terthiophene unit in compound **12** leading to an increased repulsion of the terthiophene units and causing these substituent units to twist out of the TAPP plane. The result is a less pronounced conjugation of the donor units with the TAPP core. On the other hand, in the case of compounds **8** and **10** it is reasonable to argue that the α-linkage allows intramolecular
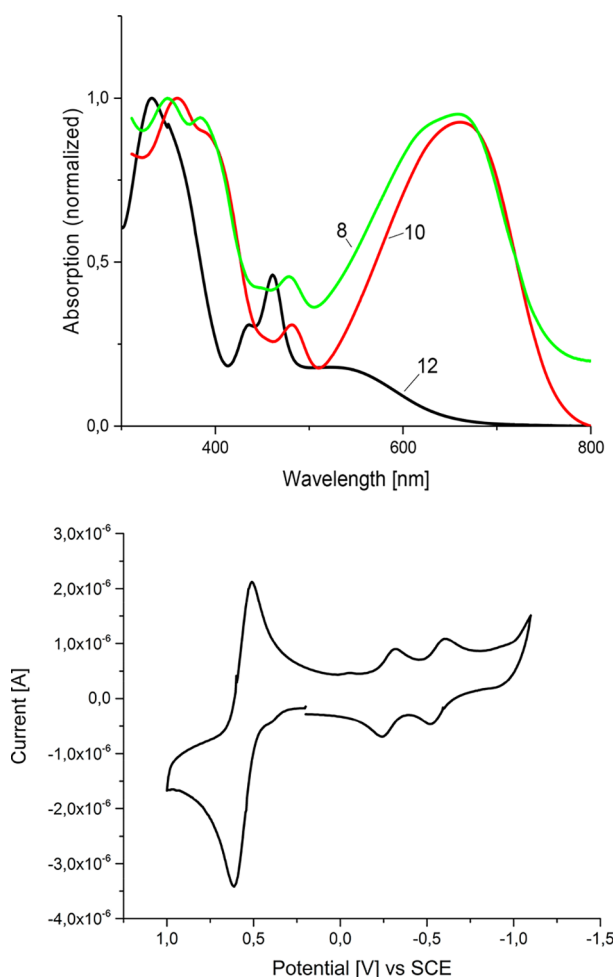
Figure 10. Top: UV−vis absorption spectra of compounds 8 and 10. Bottom: Cyclic voltammogram of compound 8 recorded in THF (sweep rate 50 mV s^{-1}; supporting electrolyte Bu$_4$NPF$_6$, reference SCE).

nitrogen−sulfur interactions (as observed for compounds 2 and 3), favoring a coplanar orientation of the terthiophene units which results in an effective conjugation of the electron-donating and electron-accepting units. This would also explain the observation that the intensity of the charge transfer band is much greater for compounds 8 and 10 than for compound 12. While TAPP derivatives 2−5 show moderate to strong fluorescence in solution, no fluorescence was observed for compounds 8, 10 and 12. We attribute this to the possibility of photoinduced intramolecular electron transfer (PET) between the donor and acceptor moieties, which has also been described for donor-substituted PDIs in literature.[27,28,31,32,34] The clear-cut intramolecular donor−acceptor character of these three TAPP derivatives is also illustrated by the distinct spatial separation of the HOMO and LUMO Kohn−Sham orbitals of compound 12 which are displayed in Figure 11. Whereas the HOMO is situated on the terthiophene-units, the LUMO is localized on the TAPP core.

The cyclic voltammograms of the terthiophene-substituted TAPPs feature reversible reduction waves while all oxidations were found to be highly irreversible. Thus, the experimental determination of the LUMO levels for compounds 8, 10 and 12 by means of cyclic voltammetry (CV) was carried out using Fc/Fc$^+$ as an internal standard, setting E_{HOMO}(Fc) = −4.8 eV.
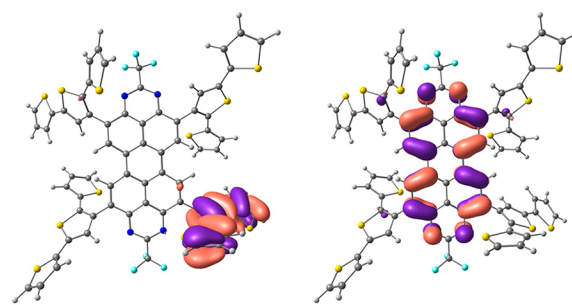

Figure 11. Visualization of HOMO (left) and LUMO (right) of compound 12; for clarity reasons the LUMO was visualized only on one of the four terthiophene units.

The two reversible reduction waves indicate the formation of a monoanion and a dianion, respectively (see CV of compound 8 in Figure 10). The LUMO energy levels thus determined via this method were found to be in good agreement with the values calculated by DFT (Table 5).

As described for the thienyl-substituted TAPP derivatives 1−5, compounds 8, 10 and 12 were processed as semiconductor materials in organic TFTs. While compounds 8 and 12 displayed no measurable charge-carrier mobilities, compound 10 was found to show small electron and hole mobilities of 1 × 10^{-5} cm^2/(V s) and 1 × 10^{-4} cm^2/(V s), respectively. We attribute these poor charge-carrier mobilities to the large and rather flexible terthiophene substituents which may prevent close packing in their solid-state structures, resulting in a decrease of intermolecular electronic coupling between neighboring molecules in the bulk material. In the case of compound 10, the substituents will most likely be oriented in a way that allows intramolecular S···N interactions, as observed for compounds 2 and 3, owing to the α-linkage of the thiophene unit to the TAPP core. This would lead to a decrease in flexibility and would therefore explain the slightly better TFT performance compared to compounds 8 and 12. The electrochemical, photophysical as well as semiconducting properties of compounds 8, 10 and 12 are summarized in Table 5.

CONCLUSIONS

We have presented a first study on the impact of donor functionalization of the tetraazaperopyrene core on the properties of such donor−acceptor based organic functional materials. It was demonstrated that the HOMO−LUMO gap is significantly decreased by substitution of the TAPP core with donor units resulting in a remarkable bathochromic shift of the TAPP-centered absorption maxima relative to that of the unsubstituted parent compound. The decrease of the HOMO−LUMO gap and therefore the influence on the photophysical and electrochemical properties was found to depend strongly on the type of linkage between the thiophene unit and the TAPP core. For derivatives with linkages in the α-position both intra- and intermolecular nitrogen sulfur interactions were observed in the solid state structure leading to an almost coplanar orientation of the thiophene unit with respect to the TAPP core. In the case of β-linkage only intermolecular N−S interactions were observed, and the thiophene units are tilted out of the TAPP plane. Finally, the TAPP-derivatives were employed in organic TFTs. While the terthiophenyl-coupled TAPPs display no or only low n- and p-channel mobility, the

Table 5. Electrochemical, Photophysical as Well as Electron and Hole Mobility of Compounds 8, 10 and 12

	E_{LUMO} (CV) [eV]	E_{LUMO} (DFT) [eV]	E_{HOMO} (DFT) [eV]	gap (DFT) [eV]	$\lambda_{1(max)}$ [nm]	$\lambda_{2(max)}$ [nm]	$\lambda_{3(max)}$ [nm]	μ_e [cm^2/(V s)]	μ_h [cm^2/(V s)]
8	−3.80	−3.52	−5.36	1.84	347	483	662	−	−
10	−3.96	−3.67	−5.36	1.69	360	482	660	1×10^{-5}	1×10^{-4}
12	−3.83	−3.54	−5.51	1.97	332	461	524	−	−

monothienyl derivatives exhibit moderate charge-carrier mobilities and in some cases even ambipolar behavior.

■ EXPERIMENTAL SECTION

The syntheses were performed under dried argon in standard Schlenk glassware, which was flame-dried prior to use. Solvents were dried according to standard procedures. The ^{1}H and ^{13}C NMR spectra were recorded with Bruker AVANCE 400 and 600II+ spectrometers equipped with variable-temperature units.

2,9-Bisheptafluoropropyl-4,7,11,14-tetrabromo-1,3,8,10-tetraaza-peropyrene (II) **TAPP-Br** was synthesized according to the literature procedures.[60] All other starting materials were obtained commercially and used without further purification.

Preparation of Compound 1. A flame-dried Schlenk flask was charged with 2,9-Bisheptafluoropropyl-4,7,11,14-tetrabromo-1,3,8,10-tetra-azaperopyrene (100 mg, 0.10 mmol), 2-thienyl boronic acid (102 mg, 0.80 mmol), PdCl$_2$(dppf) (30 mg, 0.04 mmol), and cetyltrimethylammonium bromide (2 mg). After the addition of 10 mL of toluene and 10 mL of aqueous K$_2$CO$_3$ solution (1 M) the suspension was heated to 105 °C for 2 days. The reaction mixture was allowed to cool to room temperature, the solvent was removed in vacuo and the obtained solid was washed with water, methanol and pentane to give **1** as a blue solid (59 mg, 60%) which was practically insoluble in all organic solvents and therefore could not be characterized by NMR spectroscopy. mp > 300 °C (decomposition). HRMS (MALDI⁻-TOF) calcd. for C$_{44}$H$_{16}$F$_{14}$N$_4$S$_4$ [M]⁻: 994.0034, found 994.0029.

Preparation of Compound 2. A flame-dried Schlenk flask was charged with 2,9-Bisheptafluoropropyl-4,7,11,14-tetrabromo-1,3,8,10-tetraazaperopyrene (150 mg, 0.15 mmol), 3-methylthiophene-2-boronic acid pinacol ester (274 mg, 1.22 mmol), PdCl$_2$(dppf) (45 mg, 0.06 mmol), and cetyltrimethylammonium bromide (2 mg). After the addition of 15 mL of toluene and 15 mL of aqueous K$_2$CO$_3$ solution (1 M) the suspension was heated to 105 °C for 2 days. The reaction mixture was allowed to cool to room temperature, the aqueous layer was extracted three times with chloroform (30 mL). The combined organic layer was dried over MgSO$_4$, the solvent was removed under vacuum and the obtained solid was washed with methanol and pentane to give **2** as a violet solid (120 mg, 74%). mp > 300 °C (dec.). ^{1}H NMR (600.13 MHz, CD$_2$Cl$_2$ 295 K) δ (ppm) = 9.97 (s, 4 H, H-3), 7.76 (d,$^3J_{HH}$ = 5.2 Hz,4 H, H-11), 7.26 (d, $^3J_{HH}$ = 5.2 Hz, 4 H, H-10), 2.54 (s, 12 H, H-12). ^{13}C NMR (150.90 MHz, CD$_2$Cl$_2$ 295 K) δ (ppm) = 153.7 (C-1), 138.7 (C-9), 135.2 (C-2), 133.1 (C-3), 132.2 (C-8), 131.2 (C-10), 127.7 (C-11), 127.0 (C-4), 120.7 (C-5), 16.6 (C-12) perfluorinated carbon atoms and C-7 were not detected at the attainable S/N ratio. ^{19}F NMR (376.27 MHz, CD$_2$Cl$_2$, 295 K) δ (ppm) = −81.51 (t, $^3J_{FF}$ = 9.3 Hz, 6 F, CF$_3$), −113.59 (m, 4 F, CF$_2$), −125.36 (m, 4 F, CF$_2$). HRMS (MALDI⁻-TOF) calcd. for C$_{48}$H$_{24}$F$_{14}$N$_4$S$_4$ [M]⁻: 1050.0660, found 1050.0653.

Preparation of Compound 3. A flame-dried Schlenk flask was charged with 2,9-Bisheptafluoropropyl-4,7,11,14-tetrabromo-1,3,8,10-tetraazaperopyrene (150 mg, 0.15 mmol), 3-hexylthiophene-2-boronic acid pinacol ester (360 mg, 1.22 mmol), PdCl$_2$(dppf) (45 mg, 0.06 mmol), and cetyltrimethylammonium bromide (2 mg). After the addition of 15 mL of toluene and 15 mL of aqueous K$_2$CO$_3$ solution (1 M) the suspension was heated to 105 °C for 2 days. The reaction mixture was allowed to cool to room temperature, the aqueous layer was extracted three times with chloroform (30 mL). The combined organic layer was dried over MgSO$_4$, the solvent was removed under vacuum and the obtained solid was washed with methanol. Further purification by column chromatography (silica, PE:EE 30:1) afforded **3**

as a violet solid (108 mg, 53%). mp > 300 °C (dec.). ^{1}H NMR (600.13 MHz, CD$_2$Cl$_2$ 295 K) δ (ppm) = 9.93 (s, 4 H, H-3), 7.76 (d,$^3J_{HH}$ = 5.2 Hz,4 H, H-11), 7.30 (d, $^3J_{HH}$ = 5.3 Hz, 4 H, H-10), 2.82 (t, $^3J_{HH}$ = 7.8 Hz 8 H, H-12), 1.69 (quint. $^3J_{HH}$ = 7.1 Hz, 8 H, H-13), 1.19 (quint, $^3J_{HH}$ = 7.3 Hz, 8 H, H-14), 1.06 (m, 16 H, H-15/16), 0.64 (m; 12H, H-17) ^{13}C NMR (150.90 MHz, CD$_2$Cl$_2$ 295 K) δ (ppm) = 153.9 (C-7), 153.6 (C-1), 143.4 (C-9), 135.6 (C-2), 132.6 (C-3), 131.6 (C-8), 129.3 (C-10), 127.4 (C-11), 126.6 (C-4), 120.6 (C-5), 117.4 (C-6), 31.7 (C-15), 31.0 (C-13), 30.0 (C-12), 29.3 (C-14), 22.6 (C-16), 14.1 (C-17) perfluorinated carbon atoms were not detected at the attainable S/N ratio. ^{19}F NMR (376.27 MHz, CD$_2$Cl$_2$, 295 K) δ (ppm) = −81.12 (t, $^3J_{FF}$ = 9.1 Hz, 6 F, CF$_3$), −113.12 (m, 4 F, CF$_2$), −125.07 (m, 4 F, CF$_2$). HRMS (MALDI⁻-TOF) calcd. for C$_{68}$H$_{64}$F$_{14}$N$_4$S$_4$ [M]⁻: 1330.3790, found 1330.3759.

Preparation of Compound 4. A flame-dried Schlenk flask was charged with 2,9-Bisheptafluoropropyl-4,7,11,14-tetrabromo-1,3,8,10-tetraazaperopyrene (100 mg, 0.10 mmol), 3-thienyl boronic acid (102 mg, 0.80 mmol), PdCl$_2$(dppf) (30 mg, 0.04 mmol), and cetyltrimethylammonium bromide (2 mg). After the addition of 10 mL of toluene and 10 mL of aqueous K$_2$CO$_3$ solution (1 M) the suspension was heated to 105 °C for 2 days. The reaction mixture was allowed to cool to room temperature, the aqueous layer was extracted three times with chloroform (30 mL). The combined organic layer was dried over MgSO$_4$, the solvent was removed under vacuum and the obtained solid was washed with methanol and pentane to obtain **4** as a blue solid (75 mg, 75%). mp > 300 °C (dec.). ^{1}H NMR (600.13 MHz, THF-d_8, 295 K) δ (ppm) = 10.47 (s, 4 H, H-3), 8.87 (dd,$^3J_{HH}$ = 3.0 Hz, $^4J_{HH}$ = 1.3 Hz, 4 H, H-9), 8.38 (dd, $^3J_{HH}$ = 5.1 Hz, $^4J_{HH}$ = 1.3 Hz, 4 H, H-11), 7.73 (dd, $^3J_{HH}$ = 5.1 Hz, $^4J_{HH}$ = 3.0 Hz, 4 H, H-10). ^{13}C NMR (150.90 MHz, THF-d_8, 323 K) δ (ppm) = 153.8 (C-1), 138.2 (C-8), 135.5 (C-2), 131.0 (C-3), 130.2 (C-11), 128.6 (C-4), 128.0 (C-9), 125.7 (C-10), 120.6 (C-5), 118.5 (C-6) perfluorinated carbon atoms and C-7 were not detected at the attainable S/N ratio. ^{19}F NMR (376.27 MHz, THF-d_8, 295 K) δ (ppm) = −81.09 (t, $^3J_{FF}$ = 9.1 Hz, 6 F, CF$_3$), −113.81 (m, 4 F, CF$_2$), −126.10 (m, 4 F, CF$_2$). HRMS (MALDI⁺-TOF) calcd. for C$_{44}$H$_{17}$F$_{14}$N$_4$S$_4$ [M + H]⁺•: 995.0112, found 995.0149.

Preparation of Compound 5. A flame-dried Schlenk flask was charged with 2,9-Bisheptafluoropropyl-4,7,11,14-tetrabromo-1,3,8,10-tetraazaperopyrene (150 mg, 0.15 mmol), 4-methylthiophene-3-boronic acid pinacol ester (274 mg, 1.22 mmol), PdCl$_2$(dppf) (45 mg, 0.06 mmol), and cetyltrimethylammonium bromide (2 mg). After the addition of 15 mL of toluene and 15 mL of aqueous K$_2$CO$_3$ solution (1 M) the suspension was heated to 105 °C for 2 days. The reaction mixture was allowed to cool to room temperature, the aqueous layer was extracted three times with chloroform (30 mL). The combined organic layer was dried over MgSO$_4$, the solvent was removed under vacuum and the obtained solid was washed with methanol. Further purification by column chromatography (silica, CHCl$_3$:PE 1:1) afforded **5** as a violet solid (108 mg, 53%). mp > 300 °C (dec.). ^{1}H NMR (600.13 MHz, CD$_2$Cl$_2$ 295 K) δ (ppm) = 9.93 (s, 4 H, H-3), 7.81 (d,$^3J_{HH}$ = 3.2 Hz, 4 H, H-9), 7.32−7.31 (m, 4 H, H-11), 2.32 (d, $^4J_{HH}$ = 0.6 Hz, 12 H, H-12). ^{13}C NMR (150.90 MHz, CD$_2$Cl$_2$ 295 K) δ (ppm) = 153.9 (C-1), 139.1 (C-8), 138.7 (C-10), 137.8 (C-2), 132.8 (C-3), 127.3 (C-9), 127.2 (C-4), 122.4 (C-11), 121.0 (C-5), 117.6 (C-6), 15.7 (C-12) perfluorinated carbon atoms and C-7 were not detected at the attainable S/N ratio. ^{19}F NMR (376.27 MHz, CD$_2$Cl$_2$, 295 K) δ (ppm) = −80.48 (t, $^3J_{FF}$ = 9.3 Hz, 6 F, CF$_3$), −113.44 (m, 4 F, CF$_2$), −125.34 (m, 4 F, CF$_2$). HRMS (MALDI⁻-TOF) calcd. for C$_{48}$H$_{24}$F$_{14}$N$_4$S$_4$ [M]⁻: 1050.0660, found 1050.0655.

Preparation of Compound 8. A flame-dried Schlenk flask was charged with 2,9-Bisheptafluoropropyl-4,7,11,14-tetrabromo-1,3,8,10-tetraazaperopyrene (100 mg, 0.10 mmol), boronic acid pinacol ester **6** (395 mg, 9.17 mmol), $PdCl_2(dppf)$ (30 mg, 0.04 mmol), and cetyltrimethylammonium bromide (2 mg). After the addition of 10 mL of toluene and 10 mL aqueous Cs_2CO_3 solution (2 M) the suspension was heated to 105 °C for 3 days. The mixture was allowed to cool to room temperature and extracted with $CHCl_3$ (3 × 50 mL). The combined organic layers were washed with water (3 × 50 mL), dried over anhydrous magnesium sulfate and filtered. The solvent was removed under reduced pressure and the crude product was purified by column chromatography (silica, PE:EE 10:1) to give the product as a dark green solid (64.6 mg, 34.4 μmol, 34%). mp > 300 °C (dec.). ^{1}H NMR (600.13 MHz, $CDCl_3$, 295 K) δ (ppm) = 10.2 (s, 4H), 8.50 (s, 4H, H4 thienyl), 6.66 (s, 4H), 6.63 (s, 4H), 2.46 (s, 24H), 2.28 (s, 12H), 2.27 (s, 12H). ^{13}C NMR (150.90 MHz, $CDCl_3$, 295 K) δ (ppm) = 151.9 (C-1), 139.4 (C-10), 135.7 (C 8), 135.6 (C-12), 135.5 (C-11), 135.3 (C-2), 135.0 (C-15), 133.3 (C-18), 133.1 (C-22), 133.0 (C-19), 132.2 (C-9), 130.4 (C-13), 127.5 (C-21), 127.2 (C 14), 126.5 (C-3), 126.4 (C-4), 119.5 (C-5), 117.6 (C-6), 15.3 (C-23), 15.3 (C-20), 14.2 (C-17), 13.9 (C-16), perfluorinated carbon atoms and C-7 were not detected at the attainable S/N ratio. ^{19}F NMR (376.27 MHz, $CDCl_3$, 295 K) δ (ppm) = −80.10 (t, $^3J_{FF}$ = 9.0 Hz, 6 F, CF_3), −113.48 (m, 4 F, CF_2), −125.36 (m, 4 F, CF_2). HRMS (MALDI$^-$-TOF) calcd. for $C_{92}H_{64}F_{14}N_4S_{12}$ [M]$^-$: 1874.1556, found 1874.1580.

Preparation of Compound 9. A flame-dried Schlenk flask was charged with 2,9-Bisheptafluoropropyl-4,7,11,14-tetrabromo-1,3,8,10-tetraazaperopyrene (110 mg, 0.11 mmol), boronic acid pinacol ester **7** (508 mg, 1.1 mmol), $PdCl_2(dppf)$ (33 mg, 0.044 mmol), and cetyltrimethylammonium bromide (2 mg). After the addition of 10 mL of toluene and 10 mL of aqueous K_2CO_3 solution (1 M) the suspension was heated to 105 °C for 2 days. The reaction mixture was allowed to cool to room temperature; the aqueous layer was extracted three times with chloroform (30 mL). The combined organic layer was dried over $MgSO_4$, the solvent was removed under vacuum and the obtained crude product was purified by column chromatography (silica, PE:CHCl$_3$ 10:1) to obtain **9** as dark green solid (147 mg, 59%) mp > 300 °C (dec.). ^{1}H NMR (600.13 MHz, $CDCl_3$, 295 K) δ (ppm) = 10.02 (s, 4 H, H-3), 8.62 (s, 4 H, H-9), 7.36 (d, $^3J_{HH}$ = 3.2 Hz, 4 H, H-14/H-19), 7.29 (d, $^3J_{HH}$ = 3.2 Hz, 4 H, H-14/19), 7.23−7.20 (m, 8 H, H-13/18), 0.37−0.35 (m, 72 H, TMS). ^{13}C NMR (150.90 MHz, $CDCl_3$, 295 K) δ (ppm) = 152.0 (C-1), 143.2 (C-15/20), 142.7 (C-12/13), 141.5 (C-15/20), 140.3 (C-12/13), 137.2 (C-10/11), 135.9 (C-10/11), 134.7 (C-13/18), 134.6 (C-13/18), 133.1 (C-9), 132.9 (C-8), 132.8 (C-2), 129.4 (C-14/19), 128.5 (C-14/19), 126.9 (C-4), 126.7 (C-3), 119.9 (C-5), 117.6 (C-6), 0.35 (TMS), 0.29 (TMS), perfluorinated carbon atoms and C-7 were not detected at the attainable S/N ratio. ^{19}F NMR (376.27 MHz, $CDCl_3$, 295 K) δ (ppm) = −81.02 (t, $^3J_{FF}$ = 9.1 Hz, 6 F, CF_3), −113.49 (m, 4 F, CF_2), −125.95 (m, 4 F, CF_2). HRMS (MALDI$^-$-TOF) calcd. for $C_{100}H_{96}F_{14}N_4S_{12}Si_8$ [M]$^-$: 2226.2214, found 2226.2209.

Preparation of Compound 10. In a flame-dried Schlenk flask compound **9** (80 mg, 0.037 mmol) was dissolved in 15 mL of THF and TBAF (1 M in THF, 0.78 mL, 0.78 mmol) was added dropwise. After stirring at room temperature for 2 h, 20 mL of water were added. The aqueous phase was extracted three times with chloroform (150 mL). The combined organic layer was dried over $MgSO_4$, after filtration the solvent was removed in vacuo. The crude product was thus washed three times with both methanol and pentane to obtain **10** as a green solid (21 mg, 72%). mp > 300 °C (dec.). ^{1}H NMR (600.13 MHz, THF-d_8, 333 K) δ (ppm) = 10.70 (s, 4 H, H-3), 8.75 (s, 4 H, H-9), 7.48 (m, 8 H, H-15/20), 7.34 (m, 4 H, H-14/19), 7.30 (m, 4 H, H-14/19), 7.11 (m, 8 H, H-13/18). The low solubility of the compound precluded the recording of ^{13}C NMR data. ^{19}F NMR (376.27 MHz, THF-d_8, 295 K) δ (ppm) = −81.01 (t, $^3J_{FF}$ = 8.9 Hz, 6 F, CF_3), −113.60 (m, 4 F, CF_2), −126.17 (m, 4 F, CF_2). HRMS (MALDI$^-$-TOF) calcd. for $C_{76}H_{32}F_{14}N_4S_{12}$ [M]$^-$: 1649.9051, found 1649.9046.

Preparation of Compound 11. A flame-dried Schlenk flask was charged with compound **4** (200 mg, 0.02 mmol). After the addition of 20 mL of THF bromine (0.13 mL, 0.24 mmol) was added and the

reaction mixture was stirred for 24 h at room temperature. After removal of the solvent the crude product was purified by means of column chromatography (silica, CHCl$_3$:PE 3:2). The product **11** was thus obtained as a red solid (266 mg, 82%). mp > 300 °C (dec.). ^{1}H NMR (600.13 MHz, $CDCl_3$) δ (ppm) = 10.13 (s, 4 H, H-3), 7.70 (s, 4 H, H-8). ^{13}C NMR (150.9 MHz, $CDCl_3$) δ (ppm) = 153.0 (C-1), 137.3 (C-9), 134.1 (C-2), 133.8 (C-10), 133.0 (C-3), 126.9 (C-4), 120.9 (C-5), 117.5 (C-6), 112.4 (C-8/11), 111.4 (C-8/11). ^{19}F NMR (376.27 MHz, CD_3Cl, 295 K) δ (ppm) = −81.04 (t, $^3J_{FF}$ = 9.0 Hz, 6 F, CF_3), −113.1 (m, 4 F, CF_2), −125.3 (m, 4 F, CF_2). HRMS (MALDI$^-$-TOF) calcd. for $C_{44}H_8{}^{79}Br_4{}^{81}Br_4F_{14}N_4S_4$ [M]$^-$: 1625.2793, found 1625.2788.

Preparation of Compound 12. A flame-dried Schlenk flask was charged with compound **11** (50 mg, 0.03 mmol), 2-thienyl boronic acid (102 mg, 0.80 mmol), $Pd(PPh_3)_2Cl_2$ (12 mg, 0.017 mmol), and cetyltrimethylammonium bromide (2 mg). After the addition of 10 mL of toluene and 10 mL of aqueous K_2CO_3 solution (1 M) the suspension was heated to 105 °C for 2 days. The reaction mixture was allowed to cool to room temperature, the aqueous layer was extracted three times with chloroform (30 mL). The combined organic layer was dried over $MgSO_4$, the solvent was removed under vacuum and the crude product was purified by column chromatography (silica PE:CHCl$_3$:Toluene 2:1:1) to obtain **12** as a dark violet solid (37 mg, 45%) mp > 300 °C (dec.). ^{1}H NMR (600.13 MHz, THF-d_8, 295 K) δ (ppm) = 10.21 (s, 4 H, H-3), 7.76 (s, 4 H, H-14), 7.42 (dd, $^3J_{HH}$ = 5.1 Hz, $^4J_{HH}$ = 1.0 Hz, 4 H, H-19), 7.40 (dd, $^3J_{HH}$ = 3.6 Hz, $^4J_{HH}$ = 1.0 Hz, 4 H, H-17), 7.10−7.11 (m, 8 H, H-8/H-18), 7.03 (dd, $^3J_{HH}$ = 5.1 Hz, $^4J_{HH}$ = 1.0 Hz, 4 H, H-10), 6.78 (dd, $^3J_{HH}$ = 5.0 Hz, $^3J_{HH}$ = 3.8 Hz, 4 H, H-9). ^{13}C NMR (150.90 MHz, THF-d_8, 295 K) δ (ppm) = 154.2 (C-1), 137.3 (C-16), 137.1 (C-13), 136.0 (C-15), 135.2 (C-12), 135.1 (C-12), 134.8 (C-3), 129.0 (C-14), 128.7 (C-18), 128.0 (C-14), 127.7 (C-9), 127.3 (C-8), 126.8 (C-10), 125.8 (C-19), 124.8 (C-17), 121.6 (C-5), 117.9 (C-6) perfluorinated carbon atoms and C-7 were not detected at the attainable S/N ratio. ^{19}F NMR (376.27 MHz, THF-d_8, 295 K) δ (ppm) = −82.93 (t, $^3J_{FF}$ = 8.9 Hz, 6 F, CF_3), −113.35 (m, 4 F, CF_2), −127.72 (m, 4 F, CF_2). HRMS (MALDI$^-$-TOF) calcd. for $C_{76}H_{32}F_{14}N_4S_{12}$ [M]$^-$: 1649.9052, found 1649.9048.

■ ASSOCIATED CONTENT

Ⓢ Supporting Information

The Supporting Information is available free of charge on the ACS Publications website at DOI: 10.1021/acs.joc.7b02286.

> NMR, Absorption, Fluorescence spectra, DFT modeling (PDF)
>
> X-ray diffraction studies of compounds **2−5** and **11** (CIF)
>
> Coordinates of the DFT modeled structures (XYZ)

■ AUTHOR INFORMATION

Corresponding Author

*E-mail: lutz.gade@uni-heidelberg.de.

ORCID Ⓞ

Lutz H. Gade: 0000-0002-7107-8169

Notes

The authors declare no competing financial interest.

■ REFERENCES

(1) Rost, C.; Gundlach, D. J.; Karg, S.; Rieß, W. *J. Appl. Phys.* **2004**, 95, 5782−5787.

(2) Baeg, K.-J.; Kim, J.; Khim, D.; Caironi, M.; Kim, D.-Y.; You, I.-K.; Quinn, J. R.; Facchetti, A.; Noh, Y.-Y. *ACS Appl. Mater. Interfaces* **2011**, *3*, 3205−3214.

(3) Cornil, J.; Brédas, J.-L.; Zaumseil, J.; Sirringhaus, H. *Adv. Mater.* **2007**, *19*, 1791−1799.

(4) Xu, X.; Xiao, T.; Gu, X.; Yang, X.; Kershaw, S. V.; Zhao, N.; Xu, J.; Miao, Q. *ACS Appl. Mater. Interfaces* **2015**, *7*, 28019−28026.

(5) Kim, F. S.; Guo, X.; Watson, M. D.; Jenekhe, S. A. *Adv. Mater.* **2010**, *22*, 478−482.

(6) Stalder, R.; Puniredd, S. R.; Hansen, M. R.; Koldemir, U.; Grand, C.; Zajaczkowski, W.; Müllen, K.; Pisula, W.; Reynolds, J. R. *Chem. Mater.* **2016**, *28*, 1286−1297.

(7) Chaing, C.-J.; Chen, J.-C.; Kuo, Y.-J.; Tsao, H.-Y.; Wu, K.-Y.; Wang, C.-L. *RSC Adv.* **2016**, *6*, 8628−8638.

(8) Gsänger, M.; Bialas, D.; Huang, L.; Stolte, M.; Würthner, F. *Adv. Mater.* **2016**, *28*, 3615−3645.

(9) Kan, J.; Chen, Y.; Qi, D.; Liu, Y.; Jiang, J. *Adv. Mater.* **2012**, *24*, 1755−1758.

(10) Khim, D.; Cheon, Y. R.; Xu, Y.; Park, W.-T.; Kwon, S.-K.; Noh, Y.-Y.; Kim, Y.-H. *Chem. Mater.* **2016**, *28*, 2287−2294.

(11) Steckler, T. T.; Zhang, X.; Hwang, J.; Honeyager, R.; Ohira, S.; Zhang, X.-H.; Grant, A.; Ellinger, S.; Odom, S. A.; Sweat, D.; Tanner, D. B.; Rinzler, A. G.; Barlow, S.; Brédas, J.-L.; Kippelen, B.; Marder, S. R.; Reynolds, J. R. *J. Am. Chem. Soc.* **2009**, *131*, 2824−2826.

(12) Anthopoulos, T. D.; Tanase, C.; Setayesh, S.; Meijer, E. J.; Hummelen, J. C.; Blom, P. W. M.; de Leeuw, D. M. *Adv. Mater.* **2004**, *16*, 2174−2179.

(13) Chesterfield, R. J.; Newman, C. R.; Pappenfus, T. M.; Ewbank, P. C.; Haukaas, M. H.; Mann, K. R.; Miller, L. L.; Frisbie, C. D. *Adv. Mater.* **2003**, *15*, 1278−1282.

(14) Kang, W.; Jung, M.; Cha, W.; Jang, S.; Yoon, Y.; Kim, H.; Son, H. J.; Lee, D.-K.; Kim, B.; Cho, J. H. *ACS Appl. Mater. Interfaces* **2014**, *6*, 6589−6597.

(15) Lin, G.; Qin, Y.; Zhang, J.; Guan, Y.-S.; Xu, H.; Xu, W.; Zhu, D. *J. Mater. Chem. C* **2016**, *4*, 4470−4477.

(16) Mei, J.; Diao, Y.; Appleton, A. L.; Fang, L.; Bao, Z. *J. Am. Chem. Soc.* **2013**, *135*, 6724−6746.

(17) Pitayatanakul, O.; Higashino, T.; Kadoya, T.; Tanaka, M.; Kojima, H.; Ashizawa, M.; Kawamoto, T.; Matsumoto, H.; Ishikawa, K.; Mori, T. *J. Mater. Chem. C* **2014**, *2*, 9311−9317.

(18) Zhang, Y.; Kim, C.; Lin, J.; Nguyen, T.-Q. *Adv. Funct. Mater.* **2012**, *22*, 97−105.

(19) Katz, H. E.; Bao, Z.; Gilat, S. L. *Acc. Chem. Res.* **2001**, *34*, 359−369.

(20) Riaño, A.; Burrezo, P. M.; Mancheño, M. J.; Timalsina, A.; Smith, J.; Facchetti, A.; Marks, T. J.; Navarrete, J. T. L.; Segura, J. L.; Casado, J.; Ortiz, R. P. *J. Mater. Chem. C* **2014**, *2*, 6376−6386.

(21) Zhou, K.; Dong, H.; Zhang, H.; Hu, W. *Phys. Chem. Chem. Phys.* **2014**, *16*, 22448−22457.

(22) Chase, D. T.; Fix, A. G.; Kang, S. J.; Rose, B. D.; Weber, C. D.; Zhong, Y.; Zakharov, L. N.; Lonergan, M. C.; Nuckolls, C.; Haley, M. M. *J. Am. Chem. Soc.* **2012**, *134*, 10349−10352.

(23) Guo, J.; Liu, D.; Zhang, J.; Zhang, J.; Miao, Q.; Xie, Z. *Chem. Commun.* **2015**, *51*, 12004−12007.

(24) Özdemir, R.; Choi, D.; Özdemir, M.; Kwon, G.; Kim, H.; Sen, U.; Kim, C.; Usta, H. *J. Mater. Chem. C* **2017**, *5*, 2368−2379.

(25) Zaumseil, J.; Sirringhaus, H. *Chem. Rev.* **2007**, *107*, 1296−1323.

(26) Ando, S.; Nishida, J.; Tada, H.; Inoue, Y.; Tokito, S.; Yamashita, Y. *J. Am. Chem. Soc.* **2005**, *127*, 5336−5337.

(27) Chen, S.; Liu, Y.; Qiu, W.; Sun, X.; Ma, Y.; Zhu, D. *Chem. Mater.* **2005**, *17*, 2208−2215.

(28) Huang, J.; Fu, H.; Wu, Y.; Chen, S.; Shen, F.; Zhao, X.; Liu, Y.; Yao, J. *J. Phys. Chem. C* **2008**, *112*, 2689−2696.

(29) Mishra, A.; Ma, C.-Q.; Bäuerle, P. *Chem. Rev.* **2009**, *109*, 1141−1276.

(30) Yoon, M.-H.; DiBenedetto, S. A.; Facchetti, A.; Marks, T. J. *J. Am. Chem. Soc.* **2005**, *127*, 1348−1349.

(31) Balaji, G.; Kale, T. S.; Keerthi, A.; Della Pelle, A. M.; Thayumanavan, S.; Valiyaveettil, S. *Org. Lett.* **2011**, *13*, 18−21.

(32) Fischer, M. K. R.; Kaiser, T. E.; Würthner, F.; Bäuerle, P. *J. Mater. Chem.* **2009**, *19*, 1129−1141.

(33) Segura, J. L.; Herrera, H.; Bäuerle, P. *J. Mater. Chem.* **2012**, *22*, 8717−8733.

(34) Wonneberger, H.; Ma, C.-Q.; Gatys, M. A.; Li, C.; Bäuerle, P.; Müllen, K. *J. Phys. Chem. B* **2010**, *114*, 14343−14347.

(35) Zhan, X.; Tan, Z.; Domercq, B.; An, Z.; Zhang, X.; Barlow, S.; Li, Y.; Zhu, D.; Kippelen, B.; Marder, S. R. *J. Am. Chem. Soc.* **2007**, *129*, 7246−7247.

(36) Zhang, X.; Lu, Z.; Ye, L.; Zhan, C.; Hou, J.; Zhang, S.; Jiang, B.; Zhao, Y.; Huang, J.; Zhang, S.; Liu, Y.; Qiang, S.; Yunqi, L.; Yao, J. *Adv. Mater.* **2013**, *25*, 5791−5797.

(37) Zhang, Q.; Cirpan, A.; Russell, T.; Emrick, T. *Macromolecules* **2009**, *42*, 1079−1082.

(38) Zhou, E.; Cong, J.; Wie, Q.; Tajima, K.; Yang, C.; Hashimoto, K. *Angew. Chem., Int. Ed.* **2011**, *50*, 2799−2803.

(39) Choi, H.; Paek, S.; Song, J.; Kim, C.; Cho, N.; Ko, J. *Chem. Commun.* **2011**, *47*, 5509−5511.

(40) Huang, J.; Wu, Y.; Fu, H.; Zhan, X.; Yao, J.; Barlow, S.; Marder, S. R. *J. Phys. Chem. A* **2009**, *113*, 5039−5046.

(41) Yuan, Z.; Xiao, Y.; Yang, Y.; Xiong, T. *Macromolecules* **2011**, *44*, 1788−1791.

(42) Fang, K.; Huang, Y.; Chang, G.; Yang, J.; Shen, Y.; Ye, X. *Macromol. Res.* **2015**, *23*, 545−551.

(43) Schwartz, P.-O.; Biniek, L.; Zaborova, E.; Heinrich, B.; Brinkmann, M.; Leclerc, N.; Méry, S. *J. Am. Chem. Soc.* **2014**, *136*, 5981−5992.

(44) Deng, P.; Wu, B.; Lei, Y.; Zhou, D.; Ho, C. H. Y.; Zhu, F.; Ong, B. S. *Dyes Pigm.* **2017**, *146*, 20−26.

(45) Cremer, J.; Mena-Osteritz, E.; Pschierer, N. G.; Müllen, K.; Bäuerle, P. *Org. Biomol. Chem.* **2005**, *3*, 985−995.

(46) Zhang, C.; Zhao, G.; Zeng, W.; Tian, K.; Dong, H.; Hu, W.; Qin, J.; Yang, C. *Org. Electron.* **2015**, *16*, 101−108.

(47) Cremer, J.; Bäuerle, P. *Eur. J. Org. Chem.* **2005**, *17*, 3715−3723.

(48) Usta, H.; Facchetti, A.; Marks, T. J. *Acc. Chem. Res.* **2011**, *44*, 501−510.

(49) Riehm, T.; De Paoli, G.; Konradsson, A. E.; De Cola, L.; Wadepohl, H.; Gade, L. H. *Chem. - Eur. J.* **2007**, *13*, 7317−7329.

(50) Martens, S. C.; Riehm, T.; Geib, S.; Wadepohl, H.; Gade, L. H. *J. Org. Chem.* **2011**, *76*, 609−617.

(51) Würthner, F.; Saha-Möller, C. R.; Fimmel, B.; Ogi, S.; Leowanawat, P.; Schmidt, D. *Chem. Rev.* **2016**, *116*, 962−1052.

(52) Würthner, F.; Stolte, M. *Chem. Commun.* **2011**, *47*, 5109−5115.

(53) Anthony, J. E.; Facchetti, A.; Heeney, M.; Marder, S. R.; Zhan, X. *Adv. Mater.* **2010**, *22*, 3876−3892.

(54) Würthner, F. *Chem. Commun.* **2004**, 1564−1579.

(55) Selected references: (a) Laquindanum, J. G.; Katz, H. E.; Dodabalapur, A.; Lovinger, A. J. *J. Am. Chem. Soc.* **1996**, *118*, 11331. (b) Lee, S. K.; Zu, Y.; Herrmann, A.; Geerts, Y.; Müllen, K.; Bard, A. J. *J. Am. Chem. Soc.* **1999**, *121*, 3513. (c) Quante, H.; Müllen, K. *Angew. Chem., Int. Ed. Engl.* **1995**, *34*, 1323. (d) Schmidt-Mende, L.; Fechtenkötter, A.; Müllen, K.; Moons, E.; Friend, R. H.; MacKenzie, J. D. *Science* **2001**, *293*, 1119. (e) Ahrens, M. J.; Fuller, M. J.; Wasielewski, M. R. *Chem. Mater.* **2003**, *15*, 2684. (f) Qu, J.; Kohl, C.; Pottek, M.; Müllen, K. *Angew. Chem., Int. Ed.* **2004**, *43*, 1528−1521. (g) Jones, B. A.; Ahrens, M. J.; Yoon, M.-H.; Facchetti, A.; Marks, T. J.; Wasielewski, M. R. *Angew. Chem., Int. Ed.* **2004**, *43*, 6363. (h) Zhan, X.; Tan, Z. A.; Domercq, B.; An, Z.; Zhang, X.; Barlow, S.; Li, Y.; Zhu, D.; Kippelen, B.; Marder, S. R. *J. Am. Chem. Soc.* **2007**, *129*, 7246. (i) Franceschin, M.; Pascucci, E.; Alvino, A.; D'Ambrosio, D.; Bianco, A.; Ortaggi, G.; Savino, M. *Bioorg. Med. Chem. Lett.* **2007**, *17*, 2515−2522. (j) Tan, Z. A.; Zhou, E. J.; Zhan, X. W.; Wang, X.; Li, Y. F.; Barlow, S.; Marder, S. R. *Appl. Phys. Lett.* **2008**, *93*, 073309. (k) Li, Y.; Tan, L.; Wang, Z.; Qian, H.; Shi, Y.; Hu, W. *Org. Lett.* **2008**, *10*, 529−532. (l) Liu, C.; Liu, Z.; Lemke, H. T.; Tsao, H. N.; Naber, R. C. G.; Li, Y.; Banger, K.; Müllen, K.; Nielsen, M. M.; Sirringhaus, H. *Chem. Mater.* **2010**, *22*, 2120. (m) Gsänger, M.; Oh, J. H.; Könemann, M.; Höffken, H. W.; Krause, A.-M.; Bao, Z.; Würthner, F. *Angew. Chem.,*

Int. Ed. **2010**, *49*, 740. (n) Anthony, J. E. *Chem. Mater.* **2011**, *23*, 583−590.

(56) Geib, S.; Martens, S. C.; Märken, M.; Rybina, A.; Wadepohl, H.; Gade, L. H. *Chem. - Eur. J.* **2013**, *19*, 13811−13822.

(57) Hahn, L.; Wadepohl, H.; Gade, L. H. *Org. Lett.* **2015**, *17*, 2266−2269.

(58) (a) Hahn, L.; Öz, S.; Wadepohl, H.; Gade, L. H. *Chem. Commun.* **2014**, *50*, 4941−4943. (b) Hahn, L.; Buurma, N. J.; Gade, L. H. *Chem. - Eur. J.* **2016**, *22*, 6314−6322.

(59) Martens, S. C.; Zschieschang, U.; Wadepohl, H.; Klauk, H.; Gade, L. H. *Chem. - Eur. J.* **2012**, *18*, 3498−3509.

(60) Geib, S.; Zschieschang, U.; Gsänger, M.; Stolte, M.; Würthner, F.; Wadepohl, H.; Klauk, H.; Gade, L. H. *Adv. Funct. Mater.* **2013**, *23*, 3866−3874.

(61) Hahn, L.; Maaß, F.; Bleith, T.; Zschieschang, U.; Wadepohl, H.; Klauk, H.; Tegeder, P.; Gade, L. H. *Chem. - Eur. J.* **2015**, *21*, 17691−17700.

(62) Pati, P. B.; Zade, S. S. *Cryst. Growth Des.* **2014**, *14*, 1695−1700.

(63) Appleton, A. L.; Miao, S.; Brombosz, S. M.; Berger, N. J.; Barlow, S.; Marder, S. R.; Lawrence, B. M.; Hardcastle, K. I.; Bunz, U. H. F. *Org. Lett.* **2009**, *11*, 5222−5225.

(64) Becke, A. D. *J. Chem. Phys.* **1993**, *98*, 1372−1377.

(65) Becke, A. D. *J. Chem. Phys.* **1993**, *98*, 5648−5652.

(66) Lee, C.; Yang, W.; Parr, R. G. *Phys. Rev. B: Condens. Matter Mater. Phys.* **1988**, *37*, 785−789.

(67) Weigend, F.; Häser, M.; Patzelt, H.; Ahlrichs, R. *Chem. Phys. Lett.* **1998**, *294*, 143−152.

(68) Weigend, F.; Ahlrichs, R. *Phys. Chem. Chem. Phys.* **2005**, *7*, 3297−3305.

(69) Ma, C.-Q.; Mena-Osteritz, E.; Debaerdemaeker, T.; Wienk, M. M.; Janssen, R. A.; Bäuerle, P. *Angew. Chem., Int. Ed.* **2007**, *46*, 1679−1683.

(70) Seixas de Melo, J.; Burrows, H. D.; Svensson, M.; Andersson, M. R.; Monkman, A. P. *J. Chem. Phys.* **2003**, *118*, 1550−1556.

Supporting Information

(Oligo-)Thiophene Functionalized Tetraazaperopyrenes: Donor-Acceptor Dyes and Ambipolar Organic Semiconductors

Lena Hahn,[†] André Hermannsdorfer,[†] Benjamin Günther,[†] Tobias Wesp,[†] Bastian Bühler,[†] Ute Zschieschang,[‡] Hubert Wadepohl,[†] Hagen Klauk,[‡] Lutz H. Gade*[†]

[†]Anorganisch-Chemisches Institut, Universität Heidelberg, Im Neuenheimer Feld 270, 69120 Heidelberg (Germany), Fax: (+49)6221545609

[‡]Max Planck Institute for Solid State Research, Heisenbergstr.1, 70569 Stuttgart (Germany)
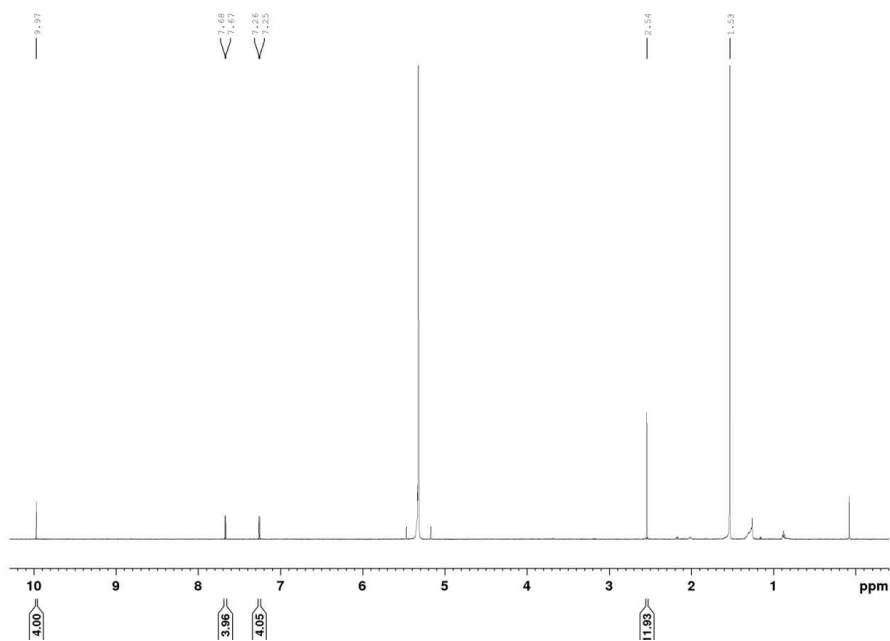
E-Mail: lutz.gade@uni-heidelberg.de

Table of contents:

The ¹H, ¹³C and ¹⁹F NMR Spectra of Compounds 2-5, 8-12

Compound 2:
¹H-NMR (600.13 MHz, CD₂Cl₂, 295 K):

¹³C-NMR (150.90 MHz, CD₂Cl₂, 295 K):
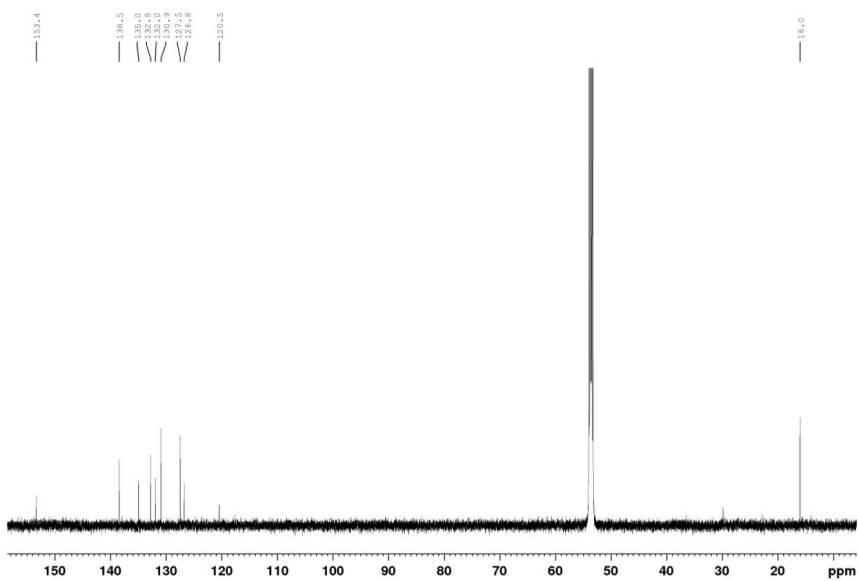
^{19}F-NMR (376.27 MHz, CD$_2$Cl$_2$, 295 K):

Compound 3:
^{1}H-NMR (600.13 MHz, CD$_2$Cl$_2$, 295 K):

^{13}C-NMR (150.90 MHz, CD$_2$Cl$_2$, 295 K):

^{19}F-NMR (376.27 MHz, CD$_2$Cl$_2$, 295 K):
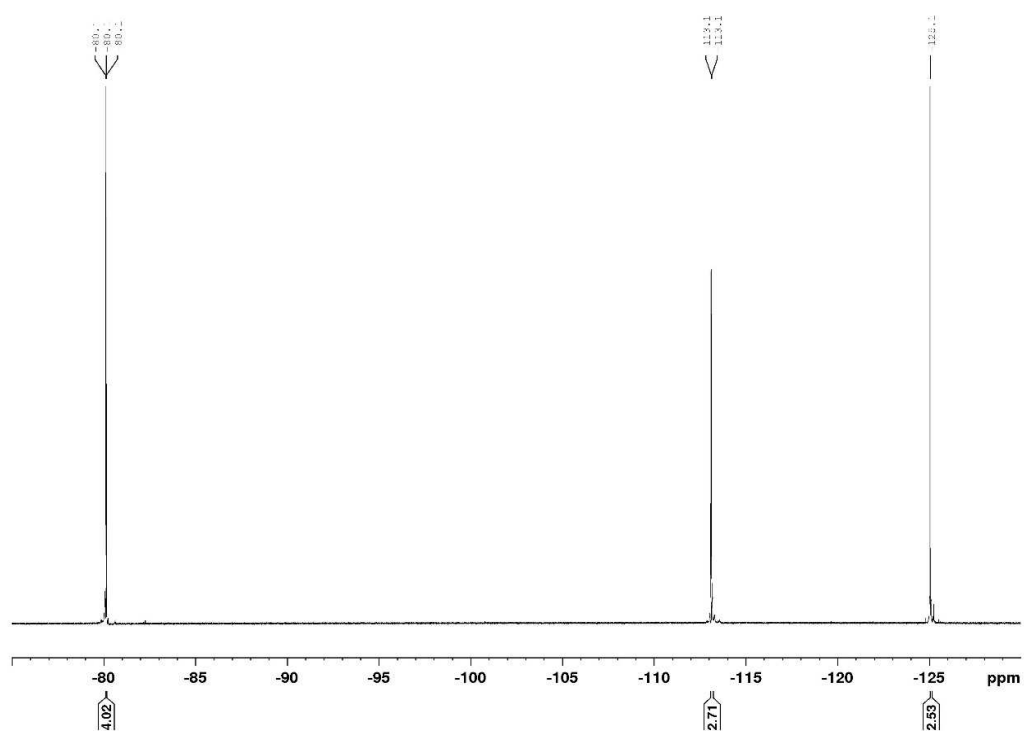
Compound 4:
^{1}H-NMR (600.13 MHz, THF-d$_8$, 295 K):
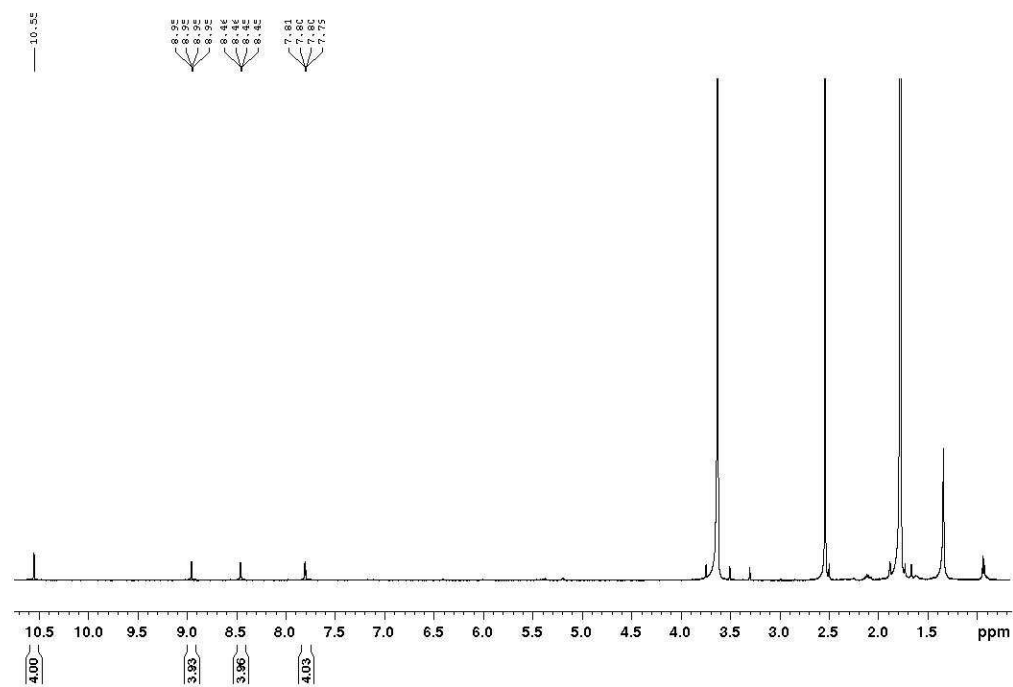
^{13}C-NMR (150.90 MHz, THF-d$_8$, 295 K):
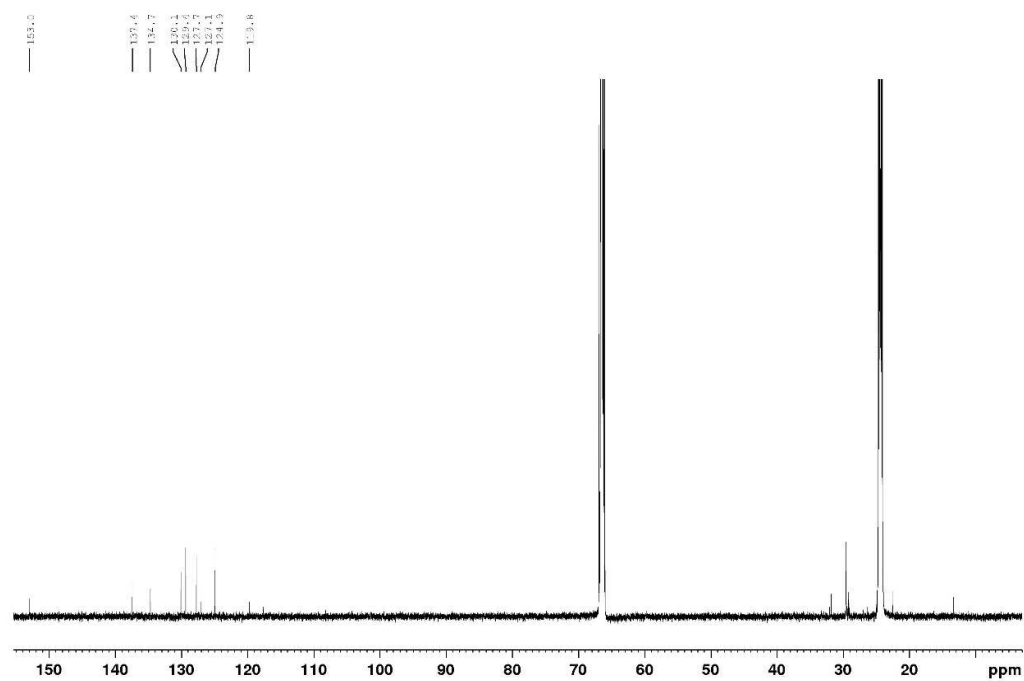
^{19}F-NMR (376.27 MHz, THF-d_8, 295 K):
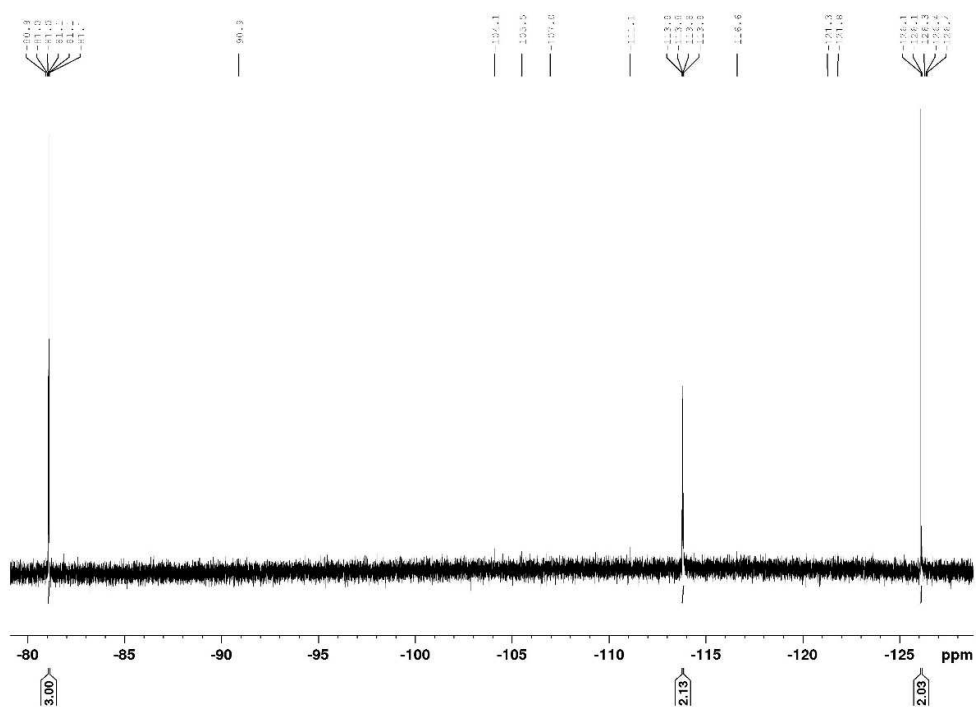
Compound 5:
^{1}H-NMR (600.13 MHz, CD$_2$Cl$_2$, 295 K):
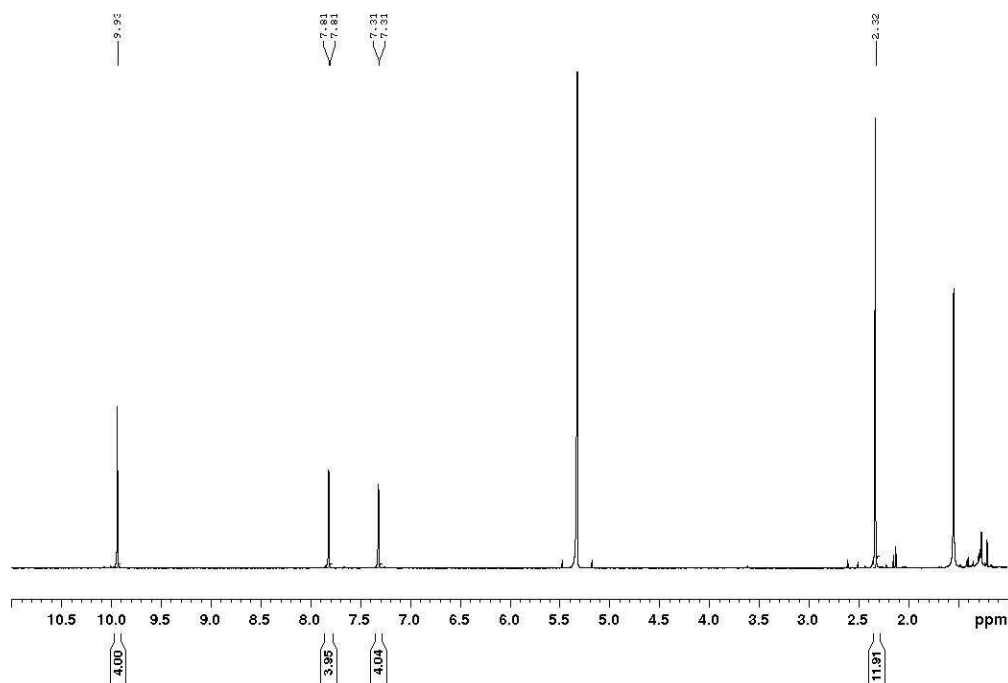
^{13}C-NMR (150.90 MHz, CD$_2$Cl$_2$, 295 K):
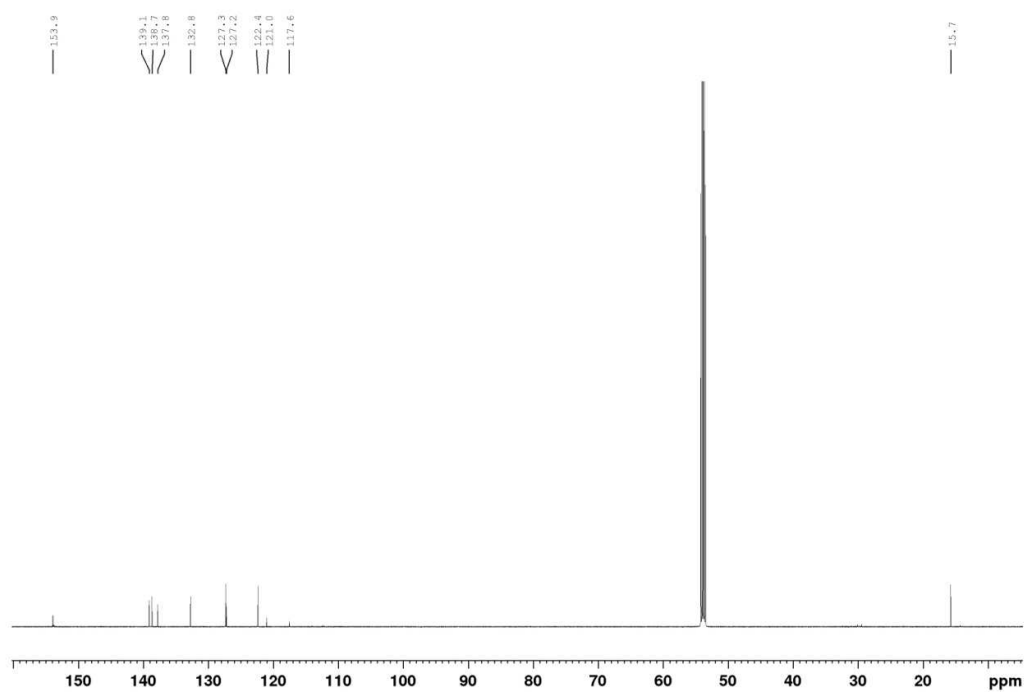
^{19}F-NMR (376.27 MHz, CD$_2$Cl$_2$, 295 K):
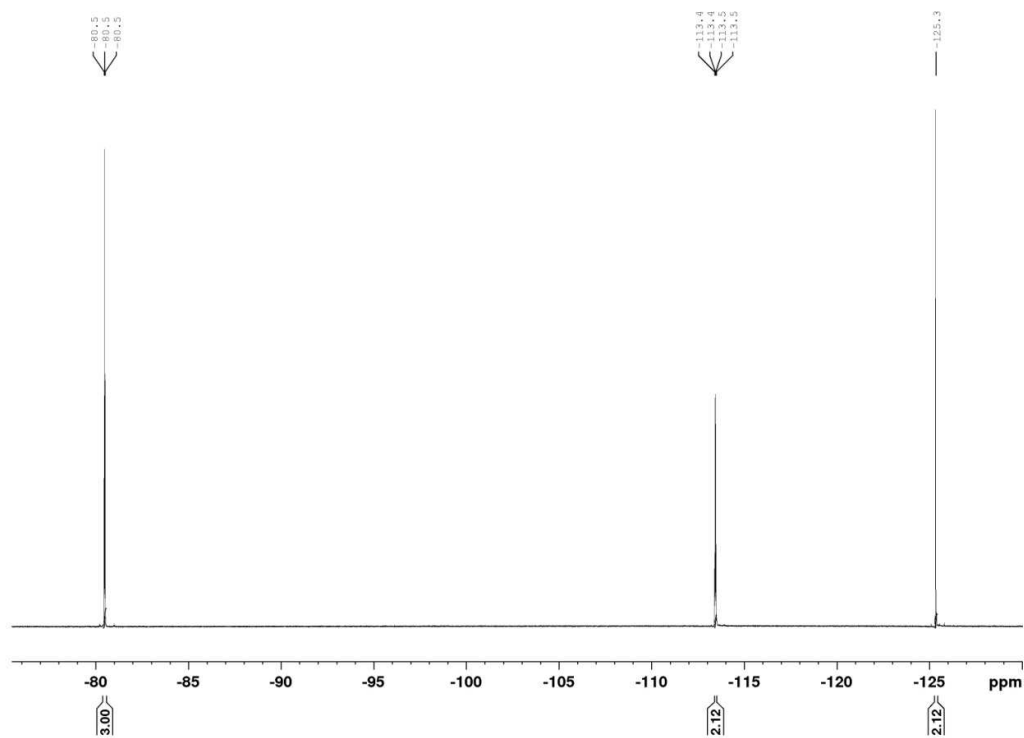
Compound 8:

^{1}H-NMR (600.13 MHz, CDCl$_3$, 295 K):
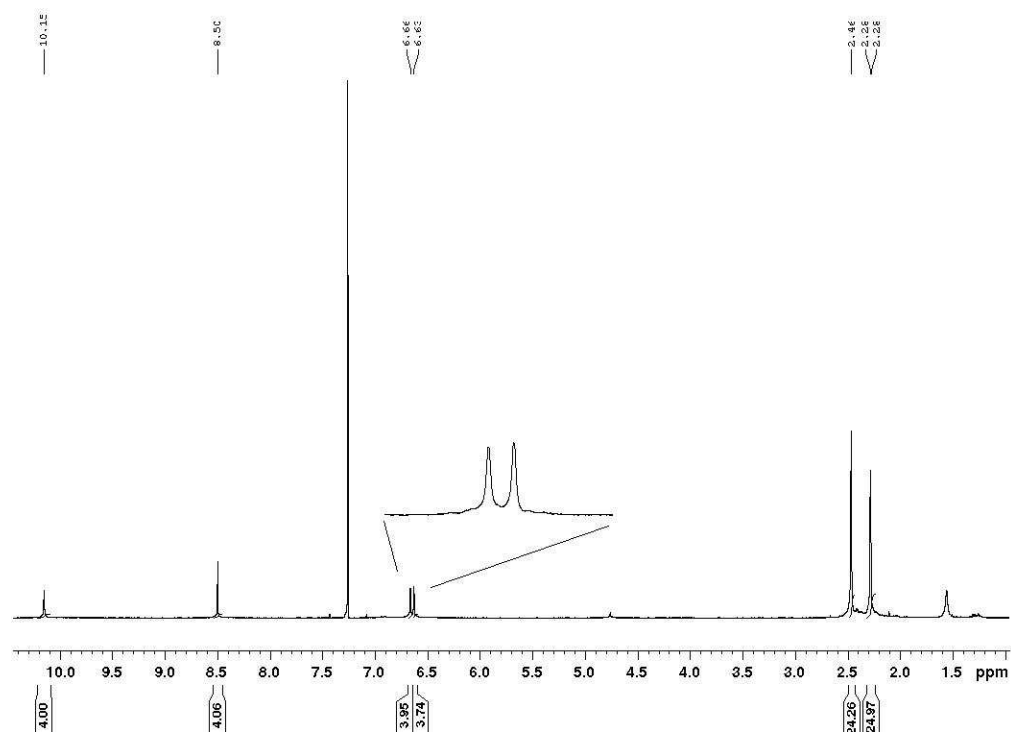
^{13}C-NMR (150.90 MHz, CDCl$_3$, 295 K):
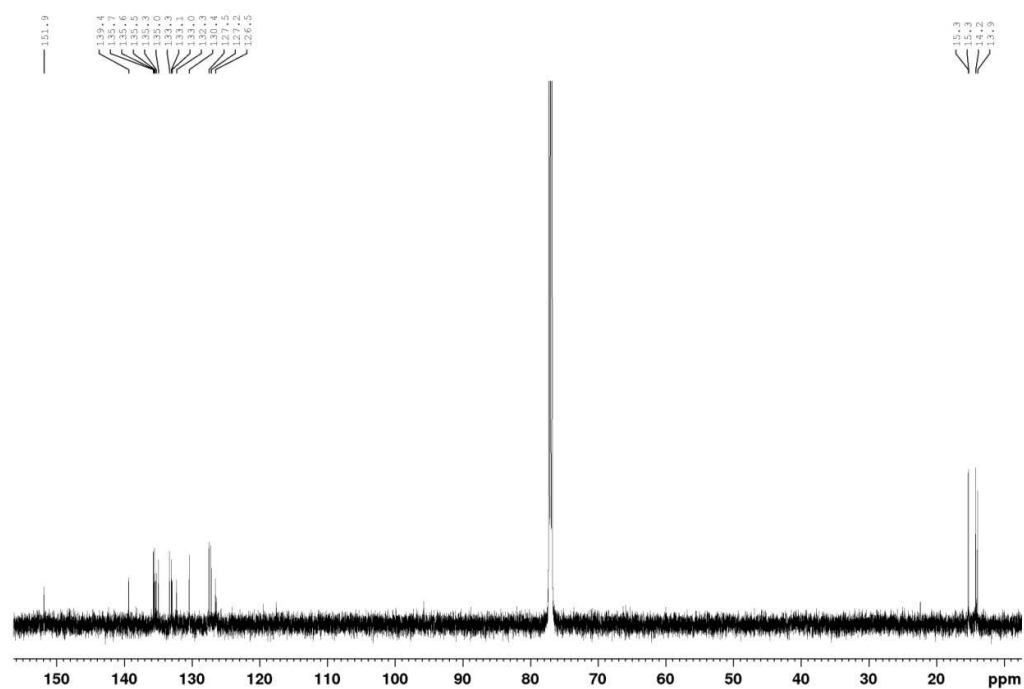
^{19}F-NMR (376.27 MHz, CDCl$_3$, 295 K):
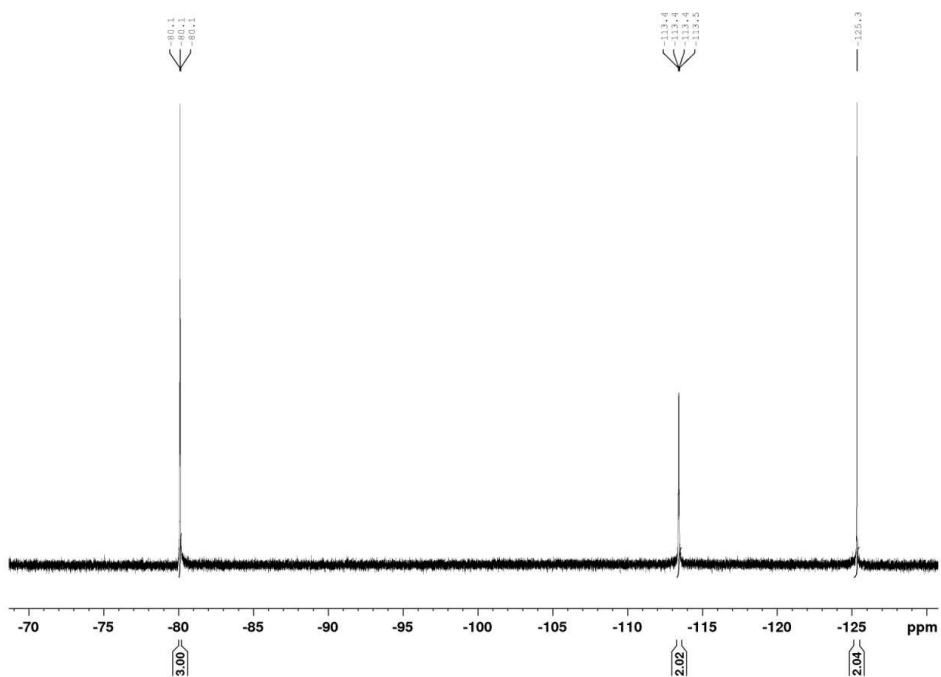
Compound 9:
^{1}H-NMR (600.13 MHz, CDCl$_3$, 295 K):
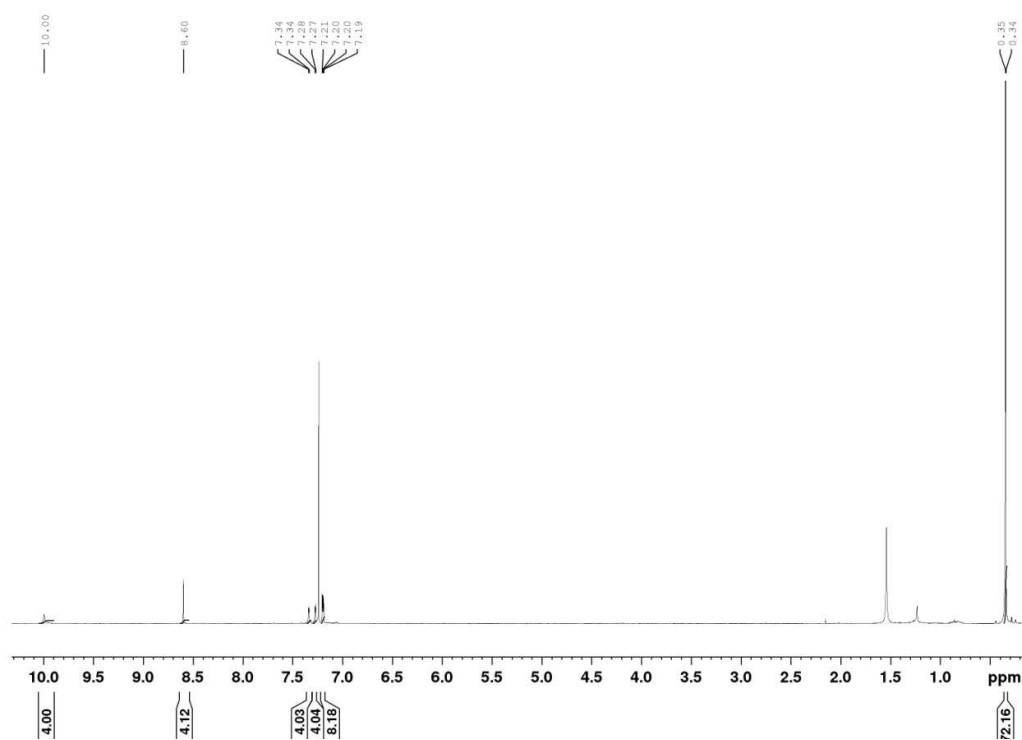
^{13}C-NMR (150.90 MHz, CDCl$_3$, 295 K):
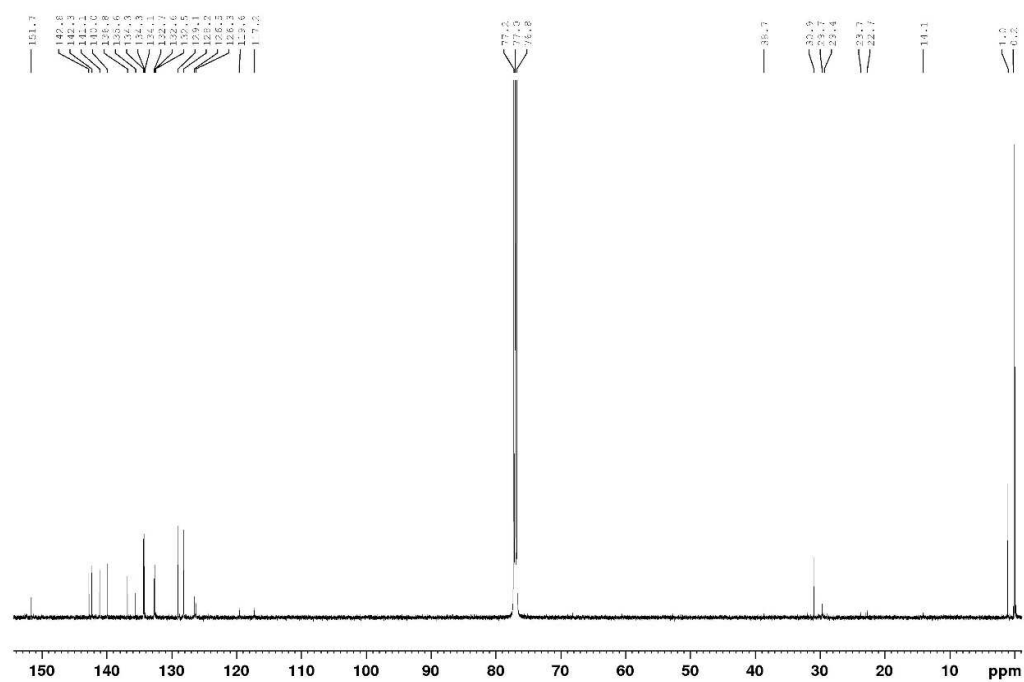
^{19}F-NMR (376.27 MHz, CDCl$_3$, 295 K):
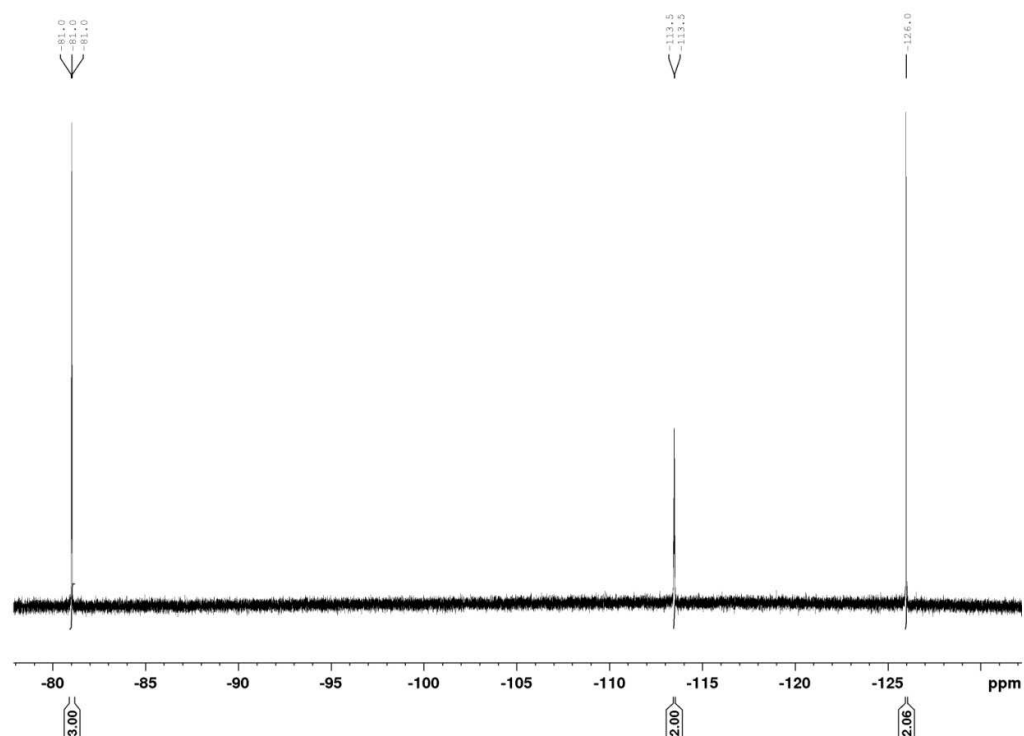
Compound 10:
^{1}H-NMR (600.13 MHz, THF-d$_8$, 295 K):

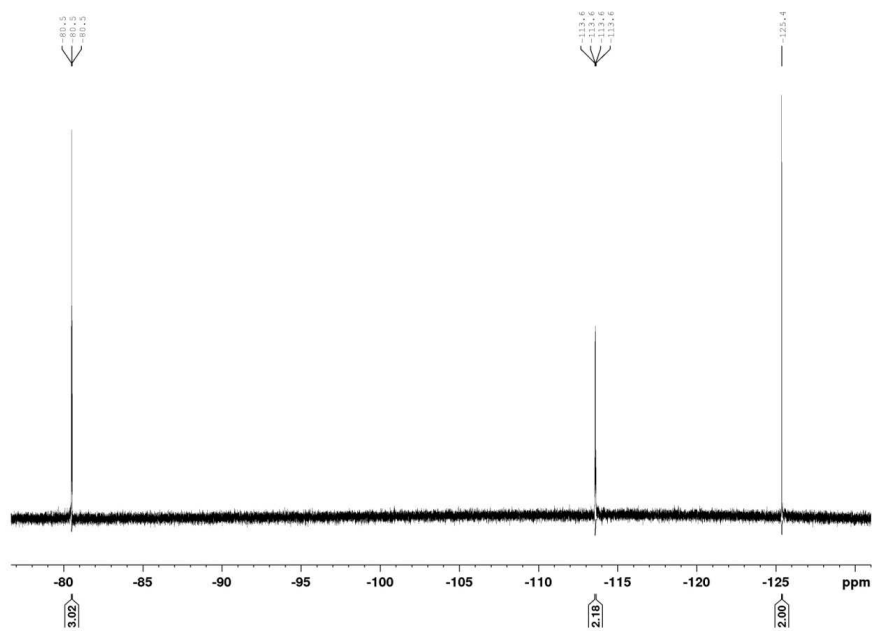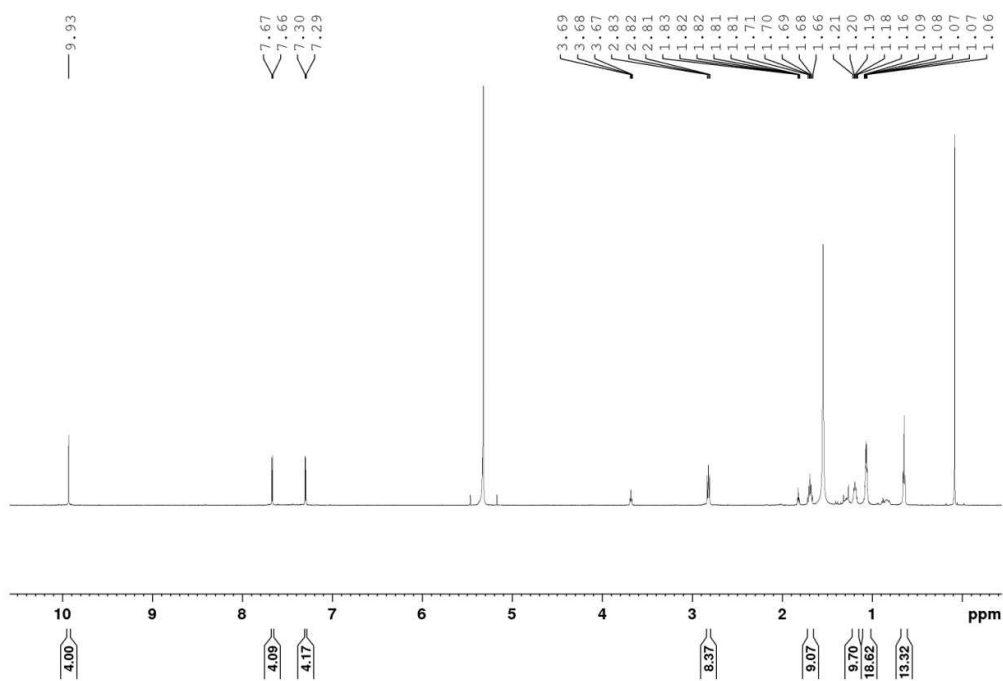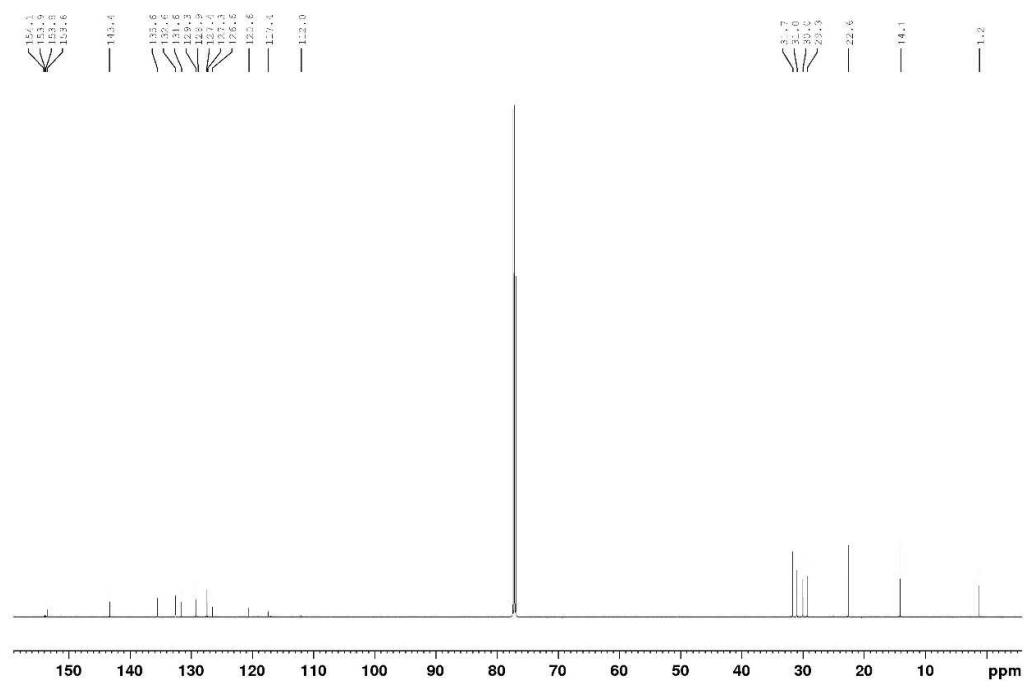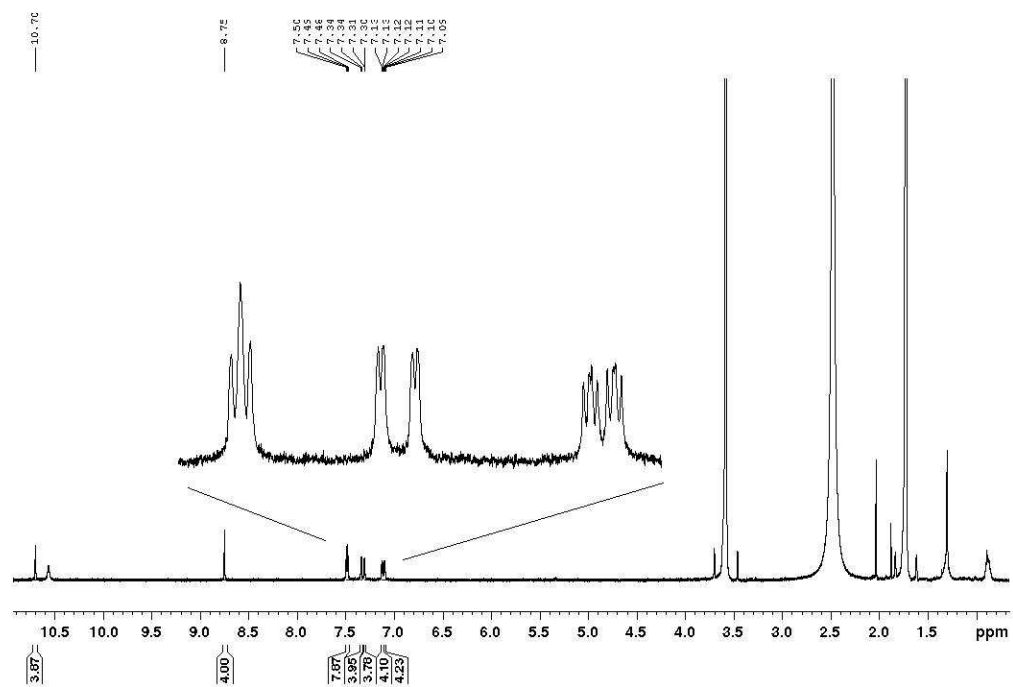^{19}F-NMR (376.27 MHz, THF-d$_8$, 295 K):
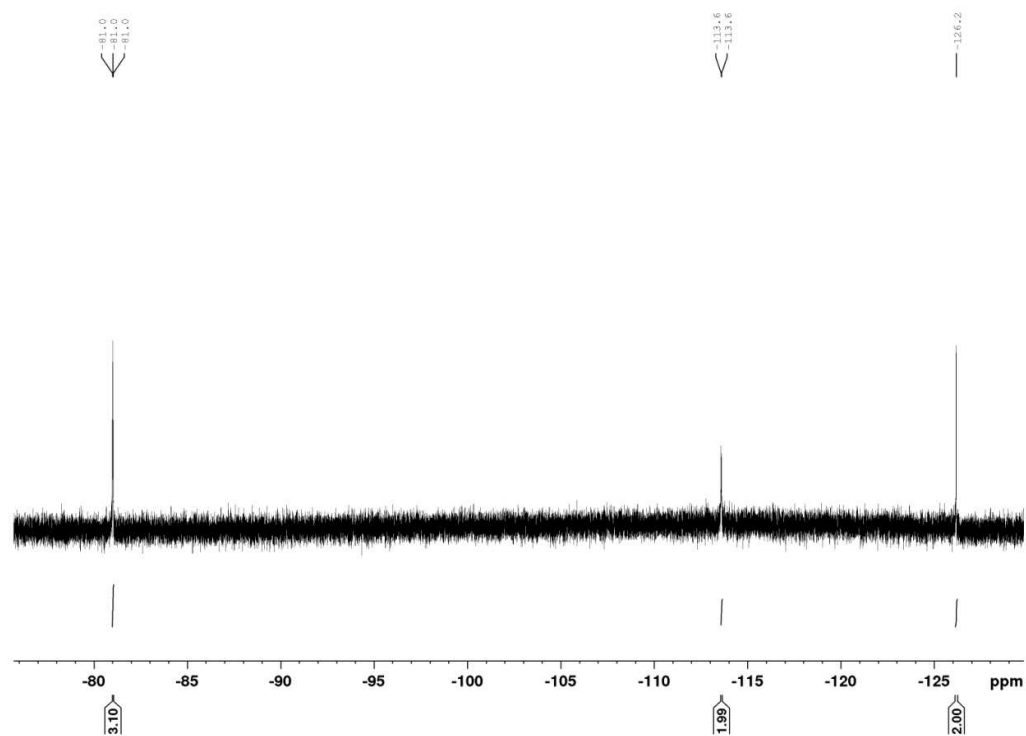
Compound 11:

^{1}H-NMR (600.13 MHz, CDCl$_3$, 295 K):
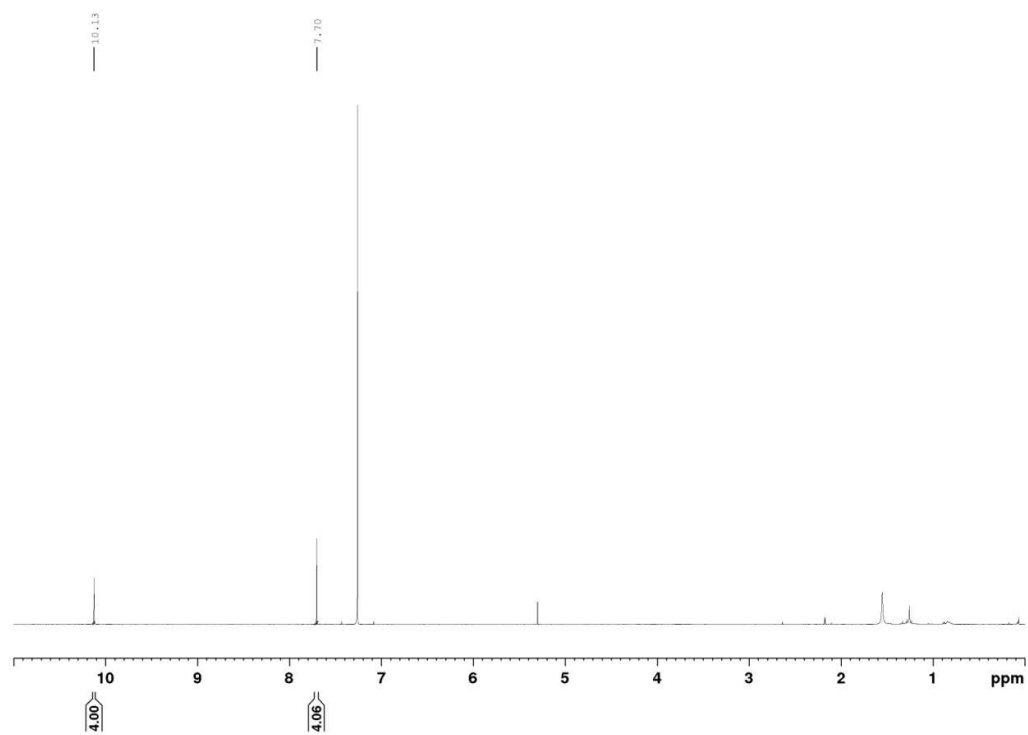
^{13}C-NMR (150.90 MHz, CDCl$_3$, 295 K):
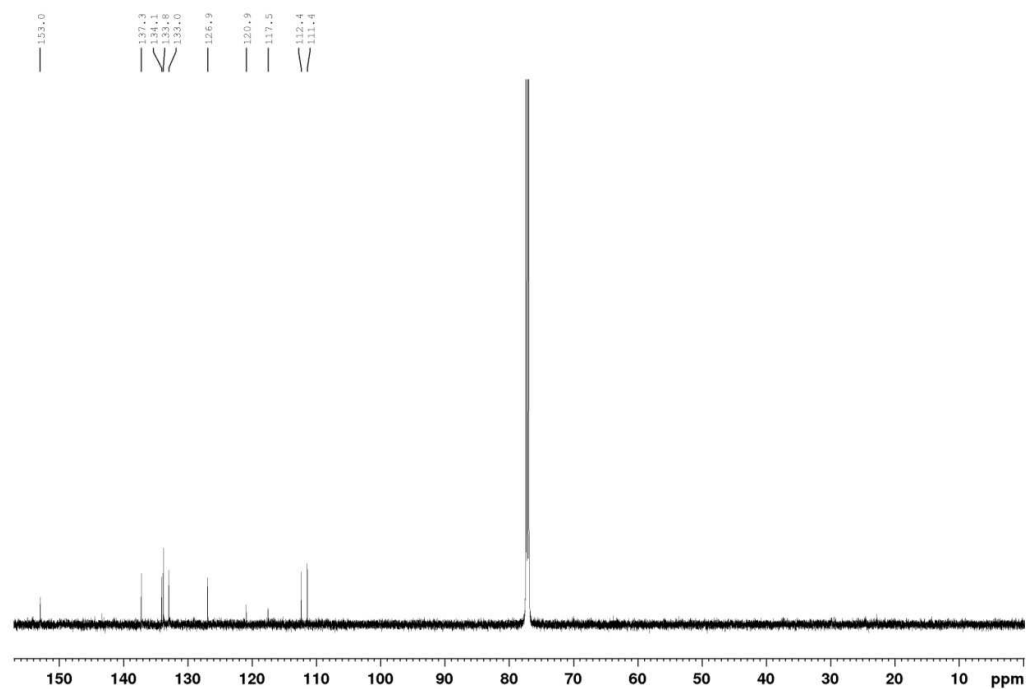
^{19}F-NMR (376.27 MHz, CDCl$_3$, 295 K):
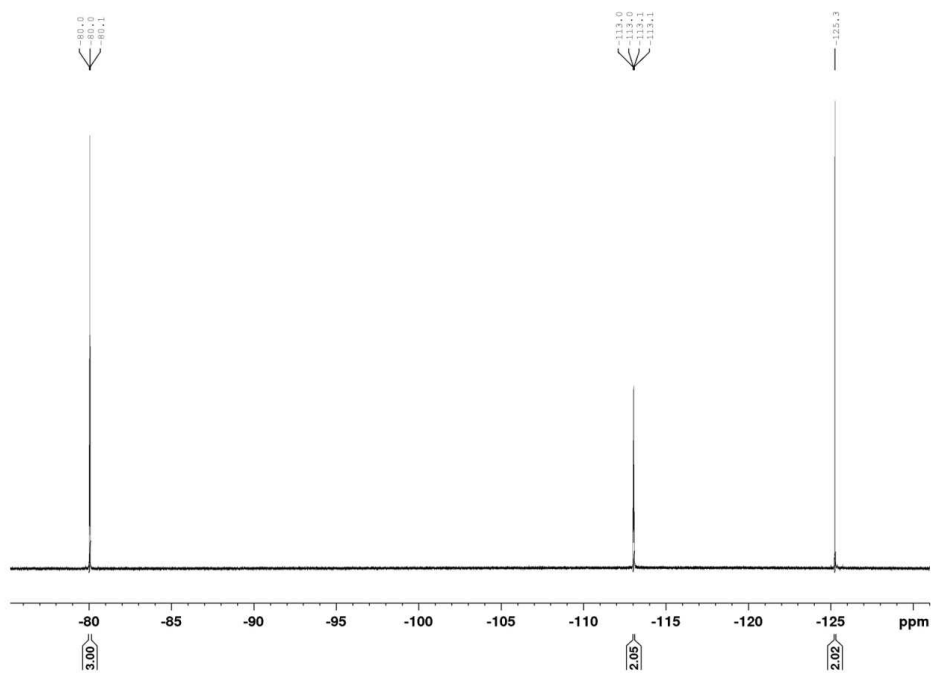
Compound 12:
^{1}H-NMR (600.13 MHz, THF-d$_8$, 295 K):

¹³C-NMR (150.90 MHz, THF-d₈, 295 K):
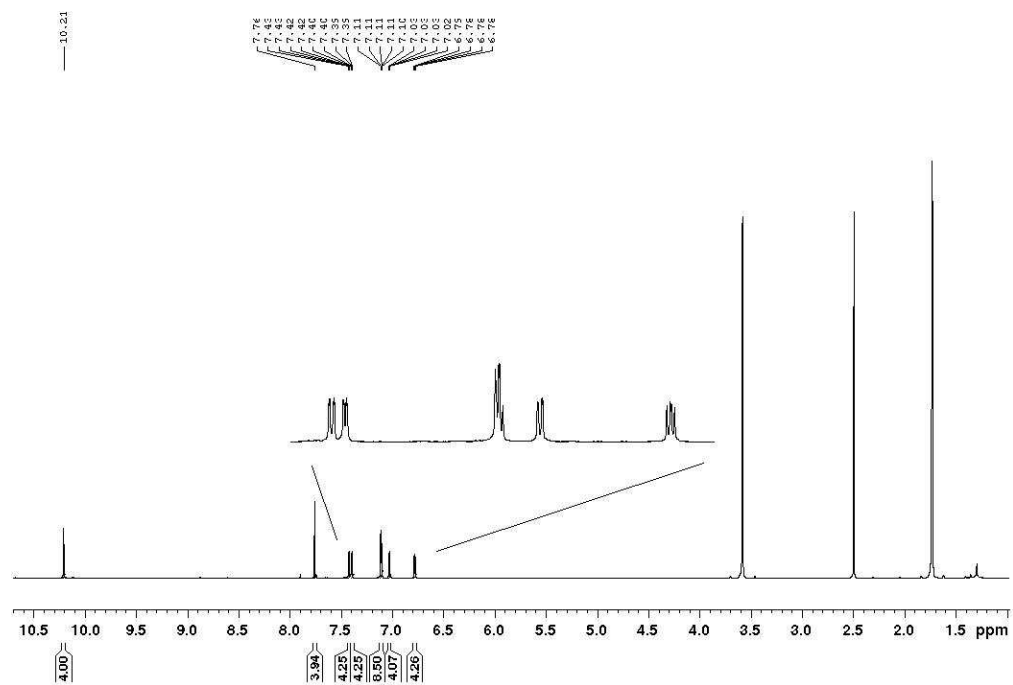
^{13}C-NMR (150.90 MHz, THF-d$_8$, 295 K):
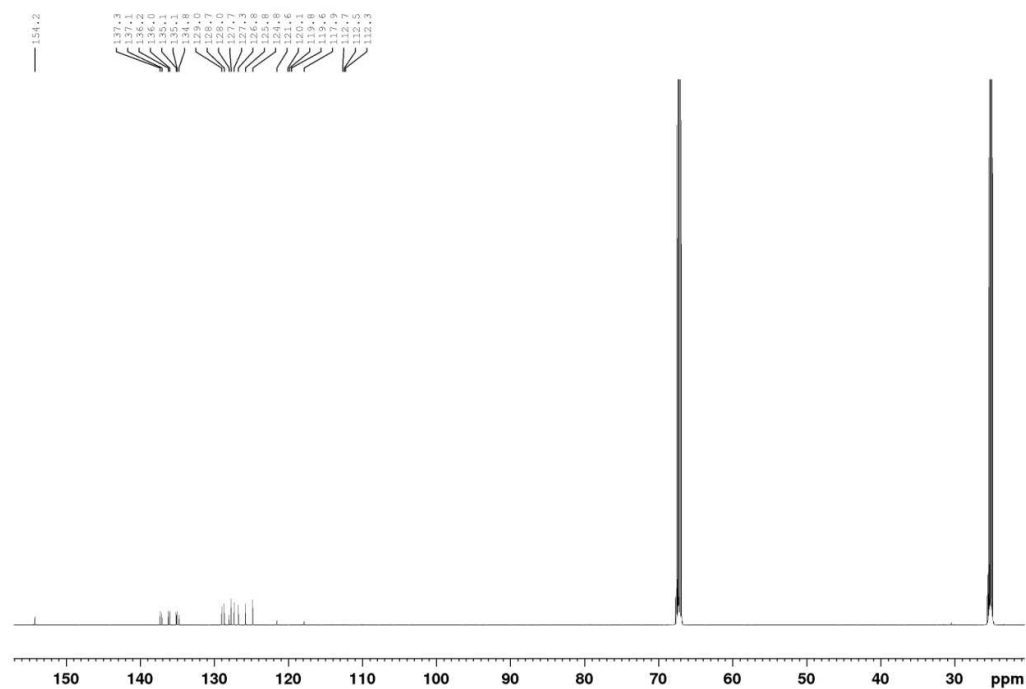
^{19}F-NMR (376.27 MHz, THF-d$_8$, 295 K):

Absorption Spectra of Compounds 2-5, 8, 10, 12
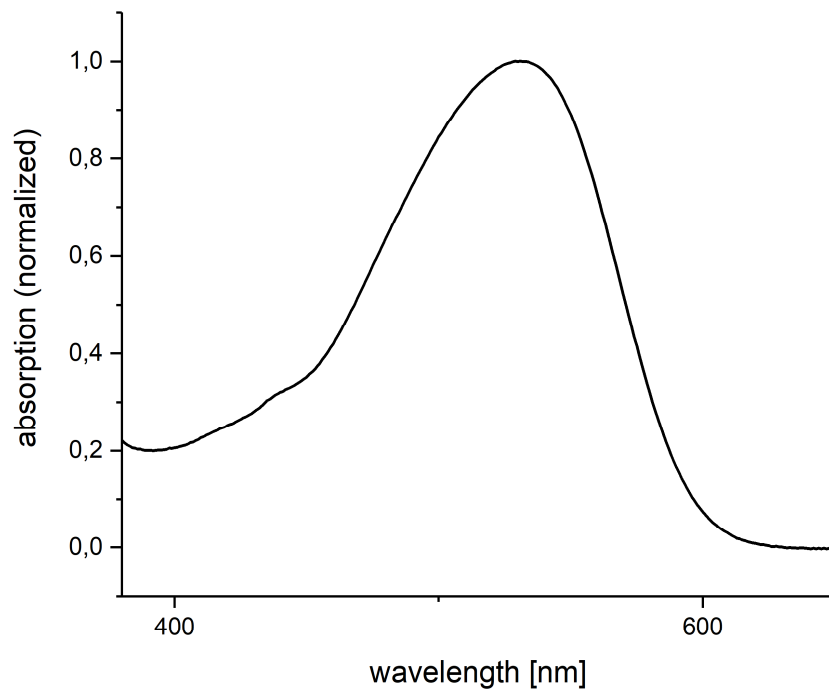
Compound 2:
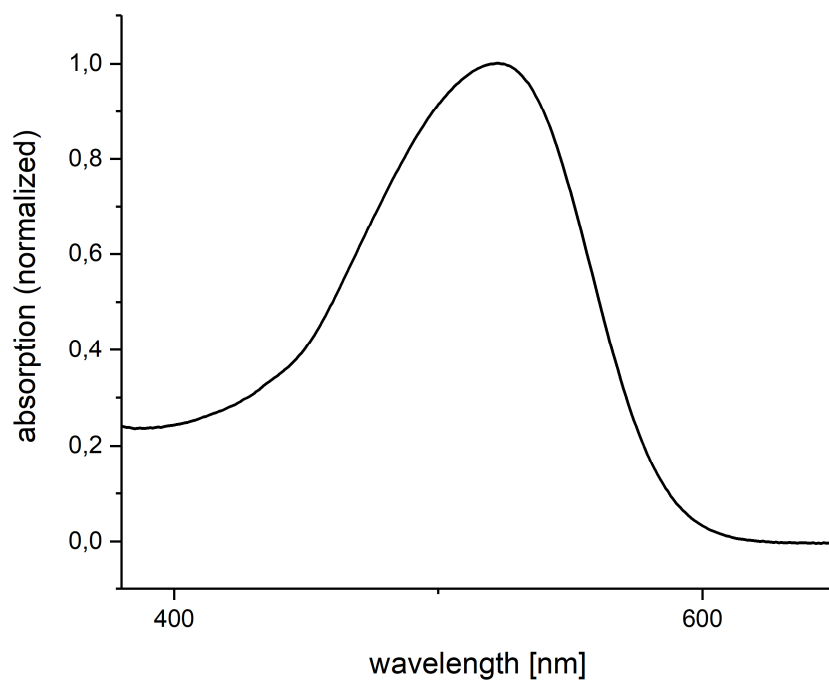
Compound 3:
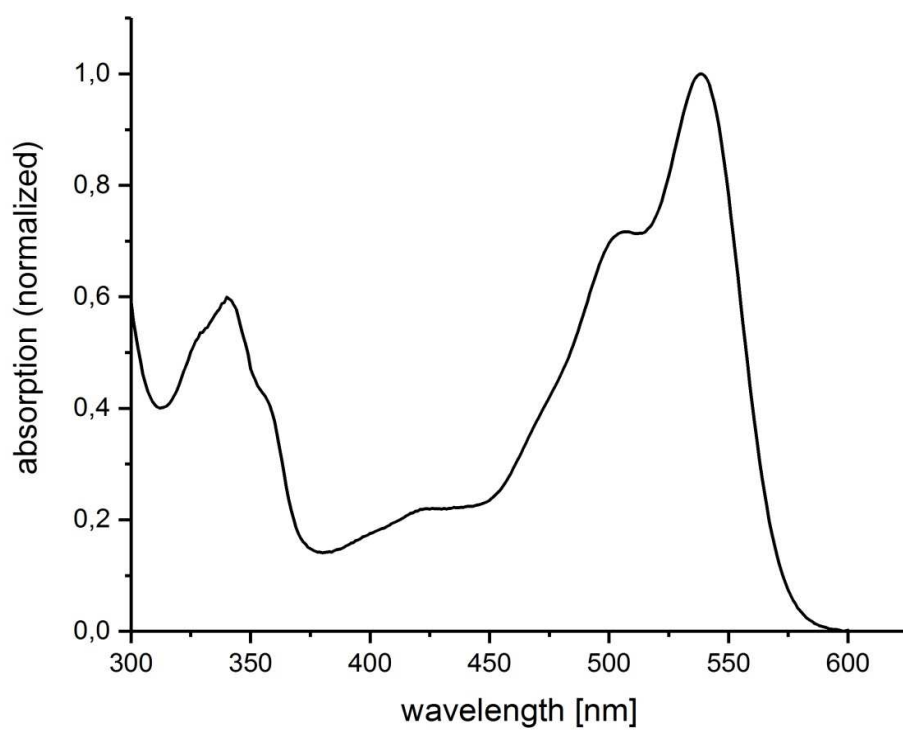
Compound 4:
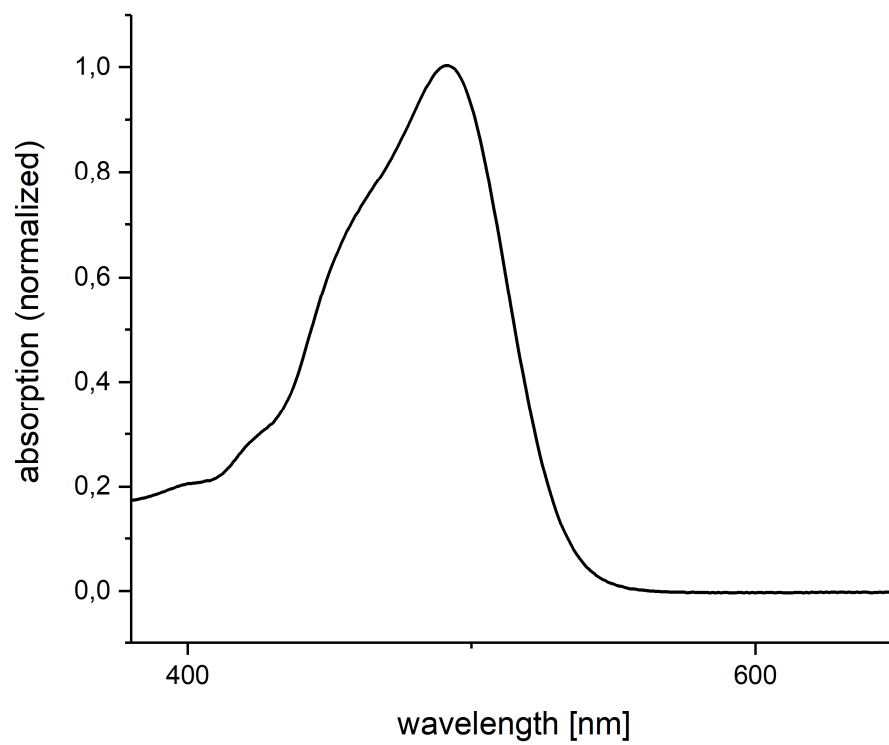
Compound 5:
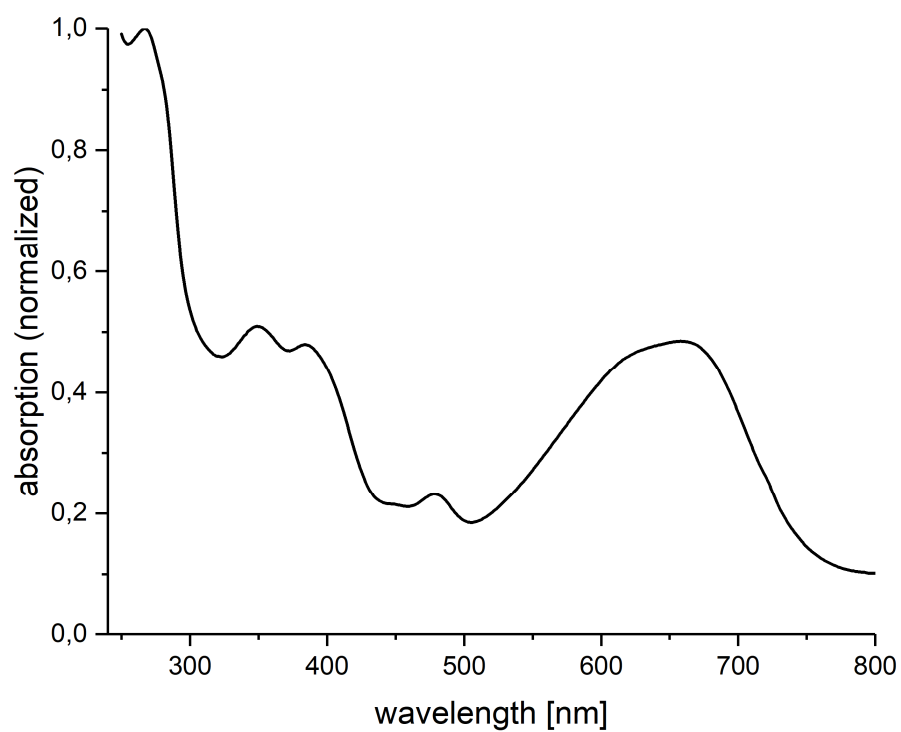
Compound 8:
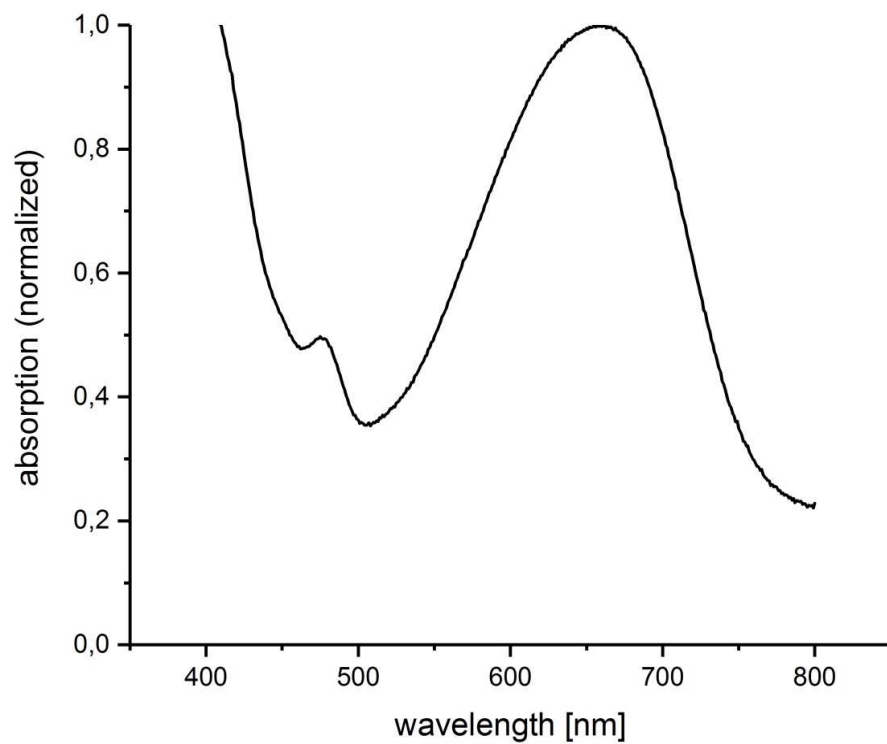
Compound 10:
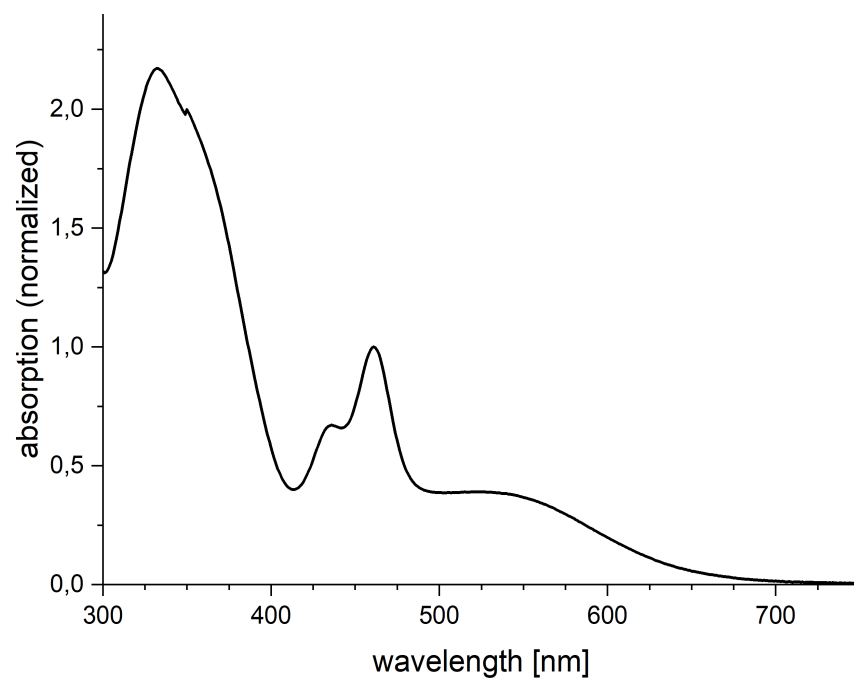
Compound 12:

Emission Spectra of Compounds 2-5

Compound 2:
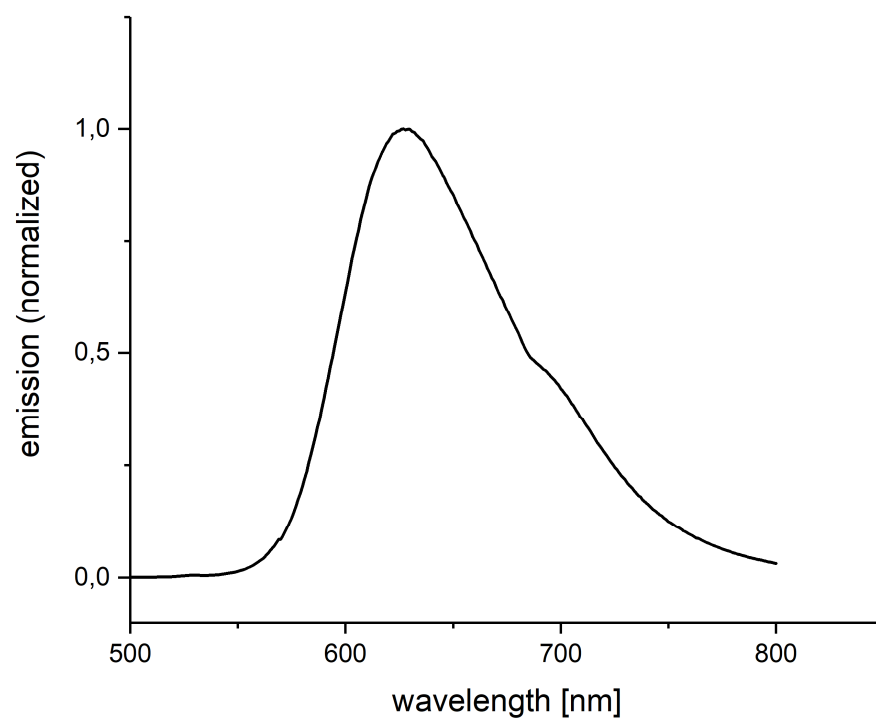
Compound 3:
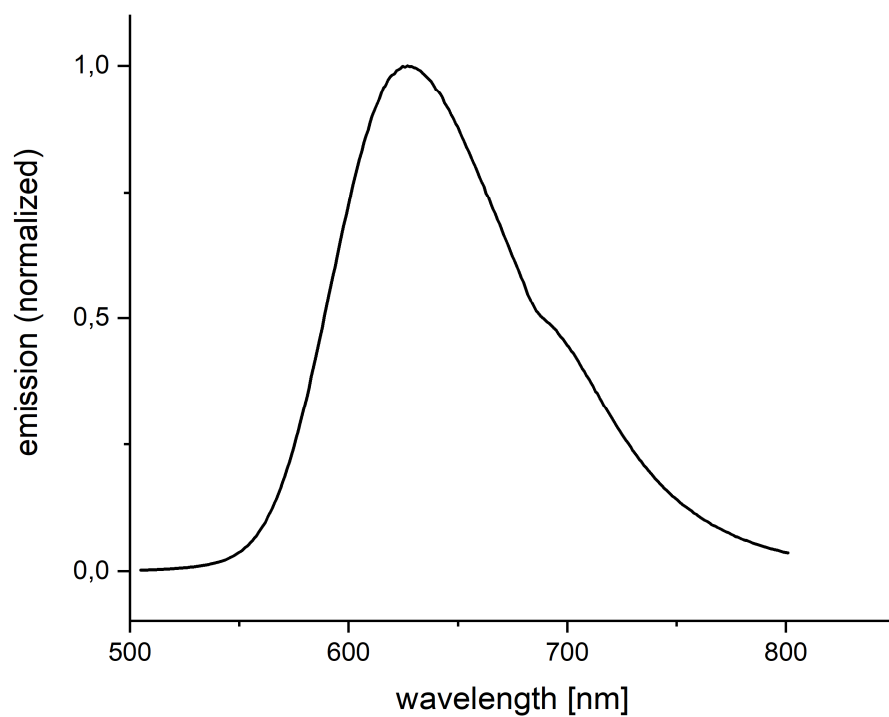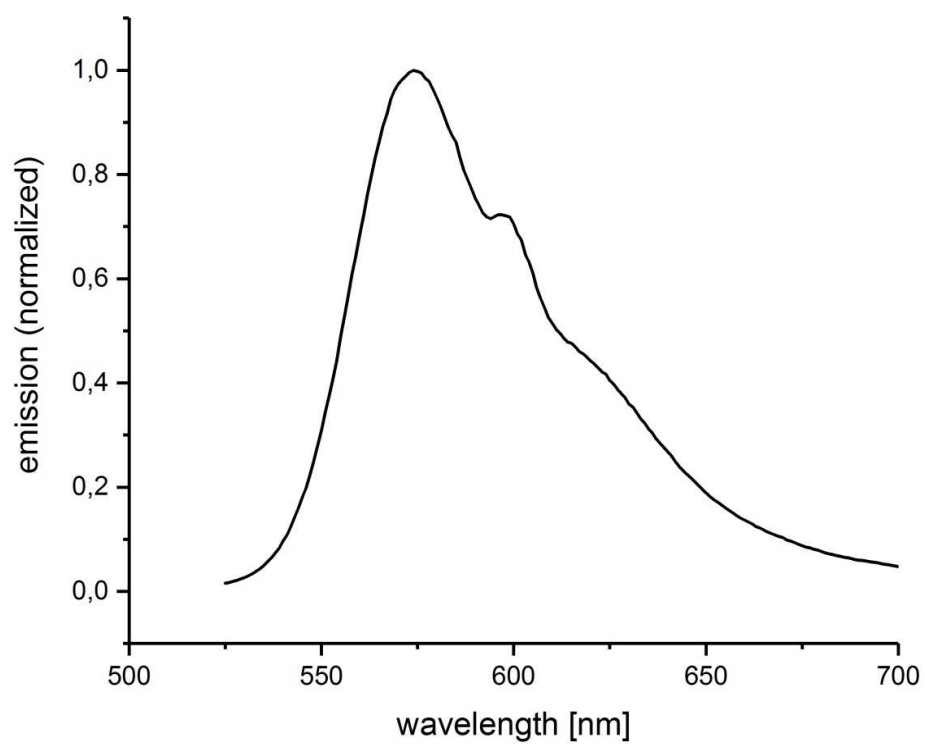
Compound 4:
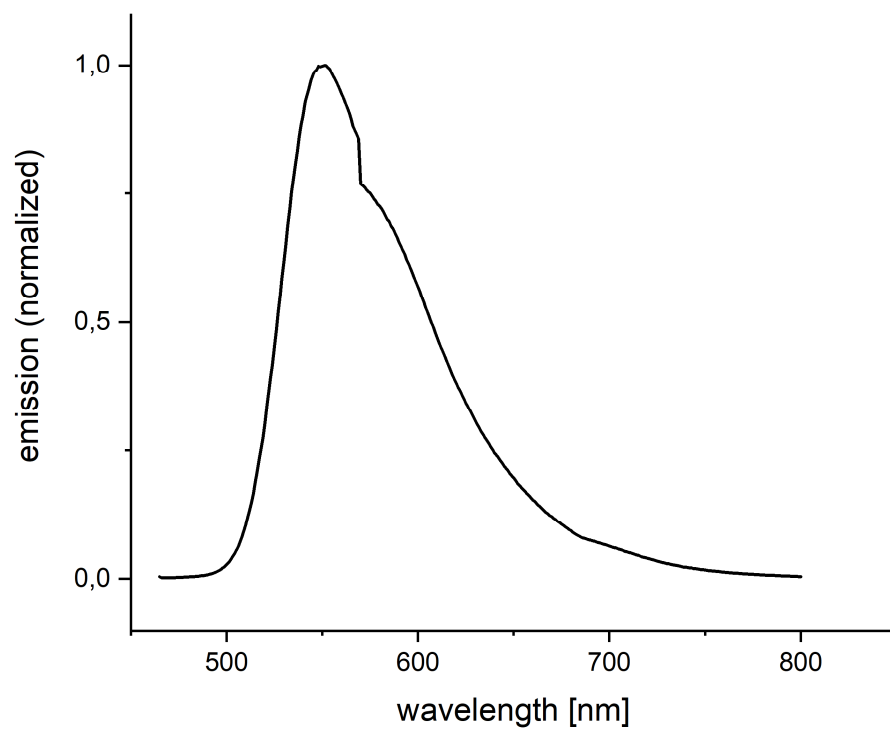
Compound 5:

Cyclic Voltammograms of Compounds 2-5, 8, 10, 12
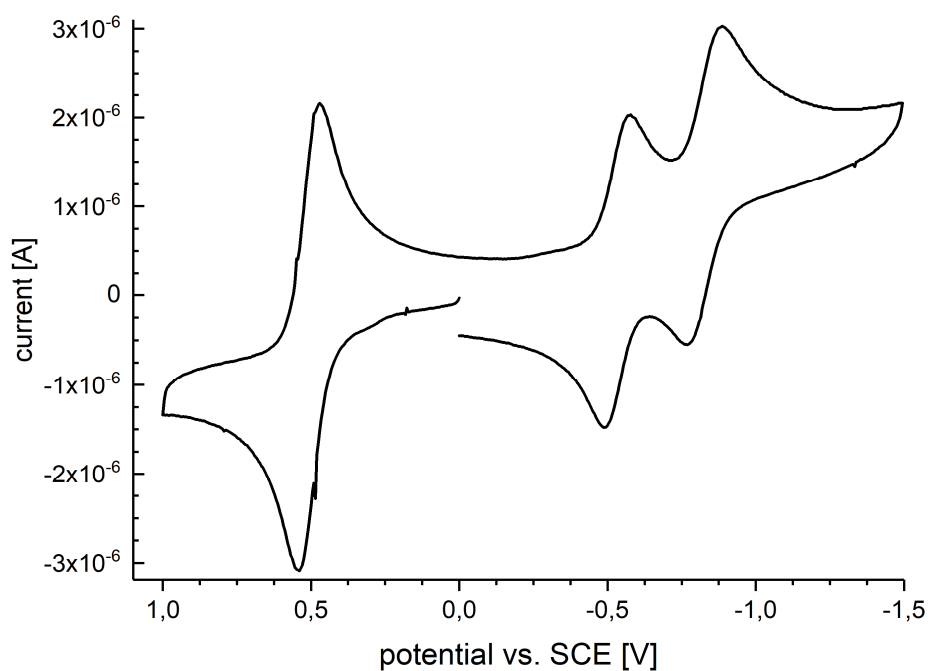
Compound 2:
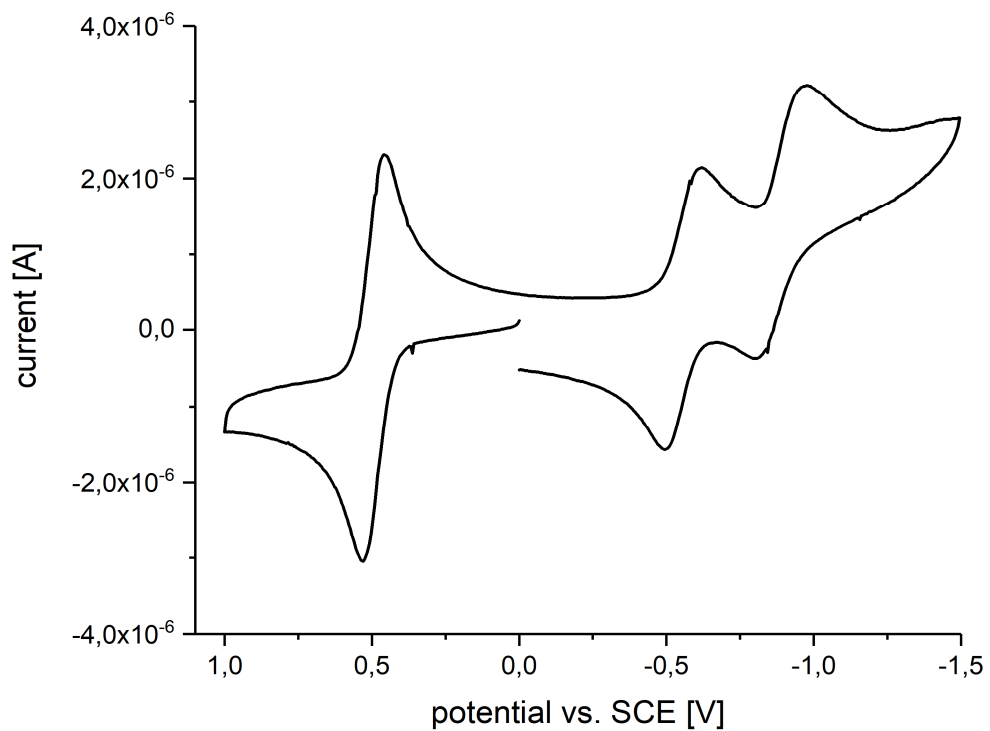
Compound 3:
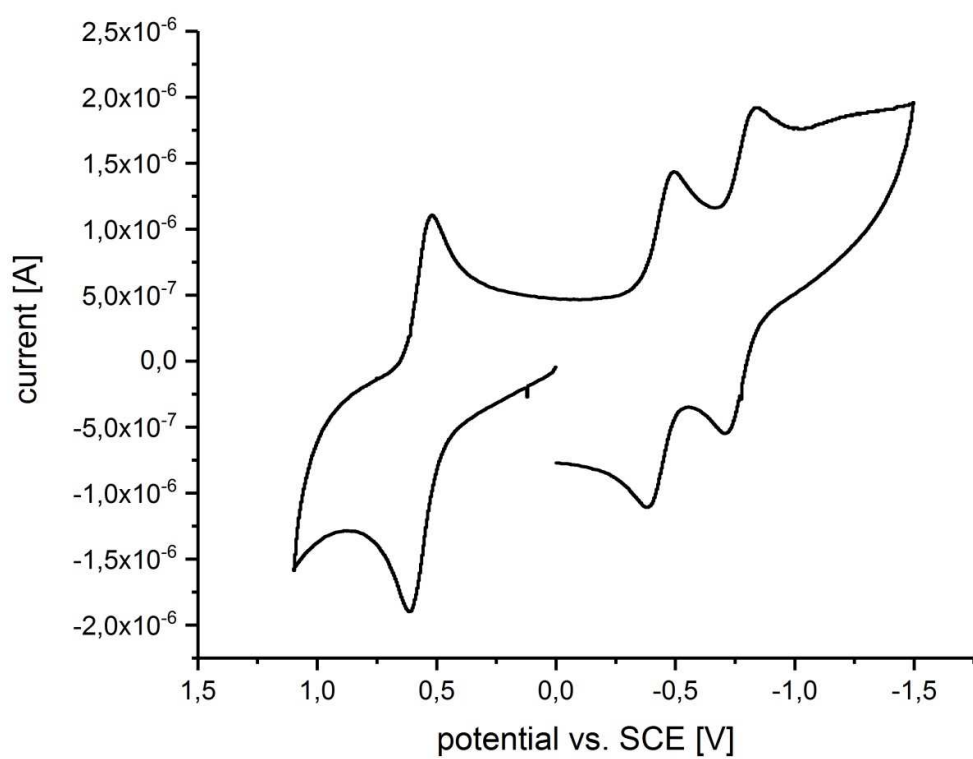
Compound 4:
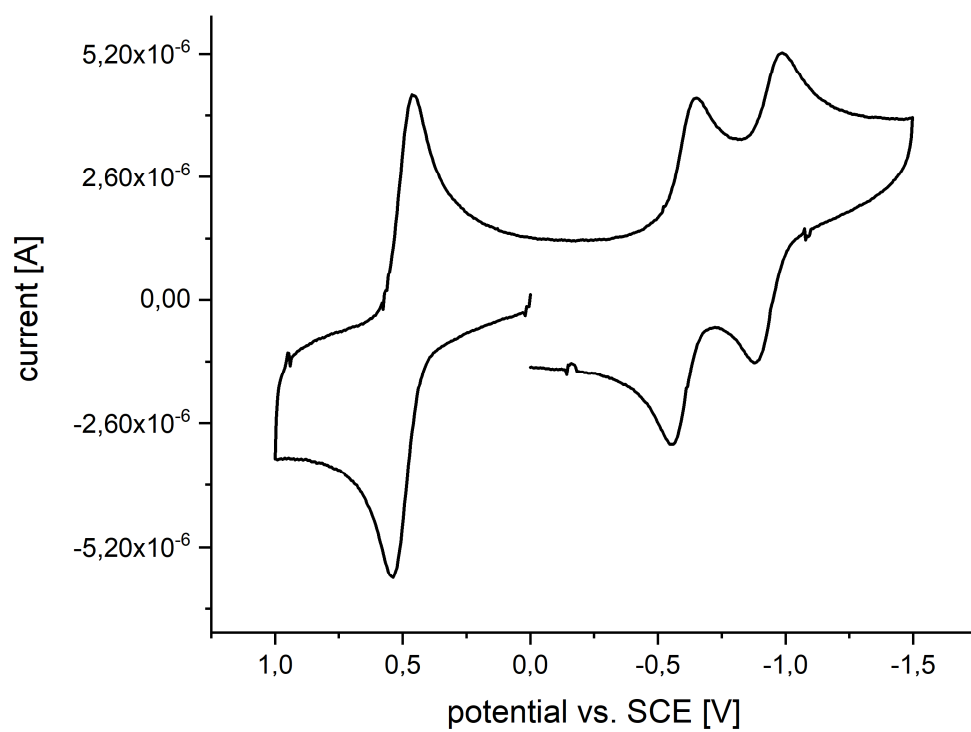
Compound 5:
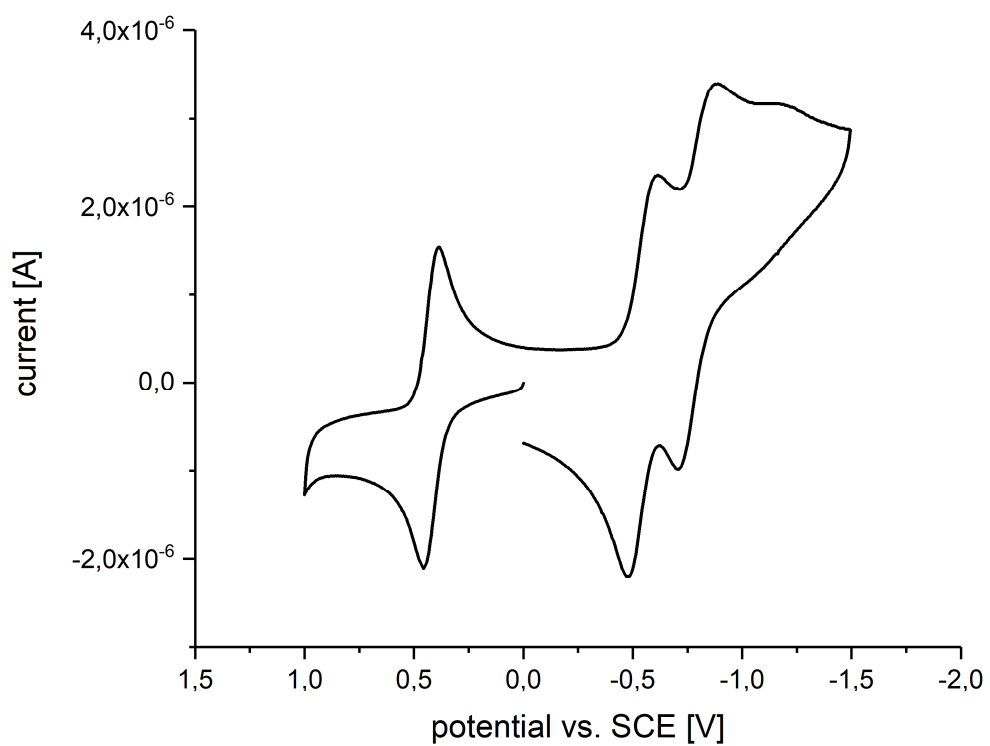
Compound 8:
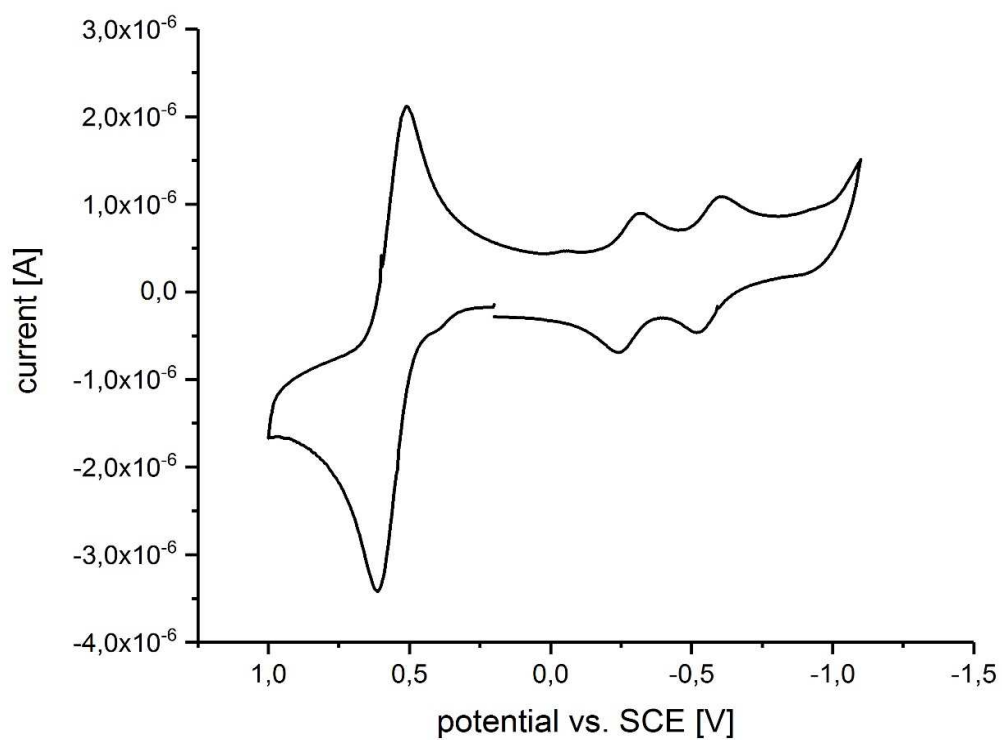
Compound 10:

Compound 12:
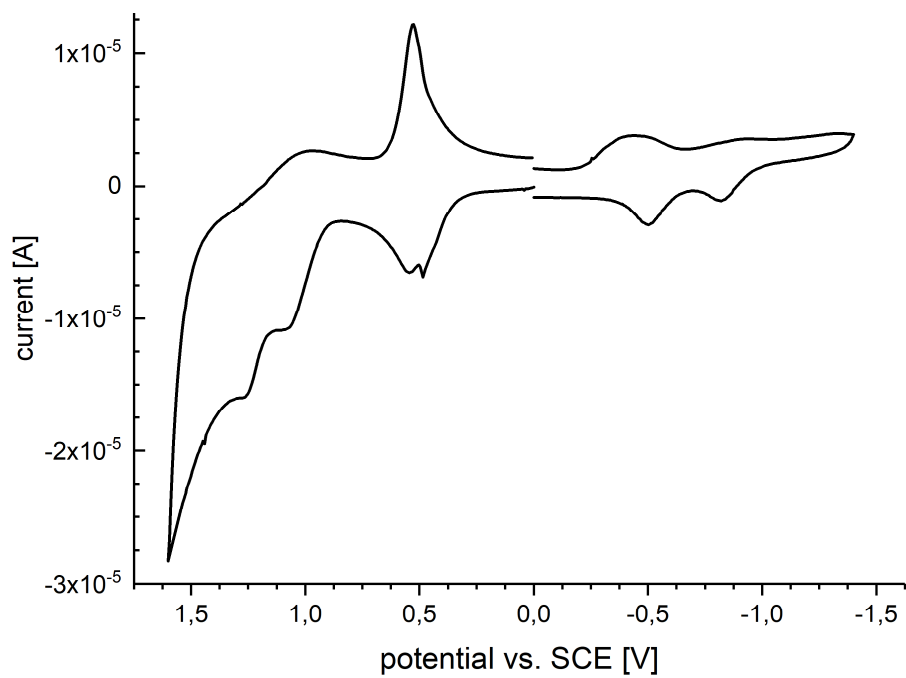
Computational Methods.

The DFT calculations were carried out using ORCA 3.0.1 program package.[1] B3LYP was employed as functional[2]a def2-SVP basis set was used for all atoms during geometry optimizations[3]. All other properties were calculated using a def2-QZVPP basis set.[4]

Compound 1:
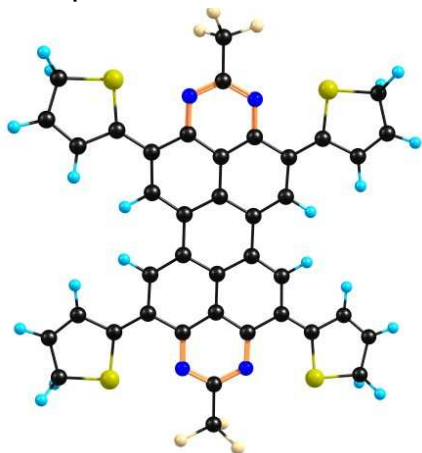
Coordinates of 1:

Atomic Type	Coordinates (Angstroms)		
	X	Y	Z
F	4.688535	2.874021	10.315876
F	5.319944	4.862439	10.898074
N	2.001917	3.658746	10.464108
N	2.904407	5.360417	11.842306
C	0.779579	3.848929	10.984107
C	-0.340634	3.074653	10.482427
C	4.356652	4.174235	10.280981
C	-2.164417	6.184619	14.260426
C	-0.720158	5.017685	12.599149
C	0.563954	4.819669	12.006402
C	-1.604160	3.303740	11.109491
H	-2.447965	2.712676	10.764302
C	1.557982	6.636145	13.388567
C	1.700257	5.586541	12.395730
C	-0.845074	6.012139	13.622761
C	0.258627	6.784009	13.969967
H	0.135532	7.549002	14.733414

C	2.991630	4.412701	10.922134
C	-0.187722	2.151107	9.428791
C	-0.913948	0.572754	7.813418
H	-1.624872	-0.027608	7.240793
C	-1.271986	1.433557	8.791722
H	-2.310619	1.602024	9.077968
C	2.643890	7.466151	13.741546
C	3.736700	9.251880	14.864937
H	3.833239	10.117593	15.524850
C	2.580300	8.579568	14.666498
H	1.648566	8.862404	15.156511
F	-8.666354	7.521522	16.084014
F	-9.297353	5.532981	15.501782
N	-5.979498	6.737425	15.935026
N	-6.881987	5.035781	14.556791
C	-4.757219	6.547454	15.414807
C	-3.637015	7.321778	15.916434
C	-8.334081	6.221401	16.118667
C	-1.813281	4.211963	12.138280
C	-3.257538	5.378892	13.799563
C	-4.541619	5.576809	14.392411
C	-2.373521	7.092788	15.289269
H	-1.529728	7.683892	15.634421
C	-5.535653	3.760367	13.010183
C	-5.677902	4.809875	14.003135
C	-3.132629	4.384463	12.775923
C	-4.236323	3.612592	12.428708
H	-4.113239	2.847645	11.665210
C	-6.969177	5.983366	15.477101
C	-3.789891	8.245277	16.970120
C	-3.063579	9.823516	18.585568
H	-2.352624	10.423819	19.158219
C	-2.705592	8.962763	17.607200
H	-1.666969	8.794271	17.320926
C	-6.621536	2.930330	12.657179
C	-7.714252	1.144588	11.533713
H	-7.810738	0.278884	10.873780
C	-6.557882	1.816942	11.732197
H	-5.626123	1.534159	11.242199
F	-8.323127	5.845332	17.410354
F	4.346187	4.550169	8.989250
C	-4.529610	9.893659	18.847465

H	-4.788983	9.633541	19.890246
H	-4.947423	10.899449	18.653252
C	4.902492	8.727029	14.097998
H	5.339287	9.480239	13.416462
H	5.720918	8.378375	14.755020
C	0.552094	0.502631	7.551571
H	0.969924	-0.503134	7.745879
H	0.811493	0.762673	6.508778
C	-8.880081	1.669369	12.300639
H	-9.698506	2.018015	11.643609
H	-9.316865	0.916120	12.982140
S	-5.329159	8.683283	17.707469
S	4.281570	7.300416	13.105205
S	1.351575	1.713122	8.691492
S	-8.259237	3.095974	13.293488

Final Single Point Energy   --3944.464735431668 E_h
HOMO: -0.209466 E_h -5.6999 eV
LUMO: -0.136821 E_h -3.7231 eV

Compound 2:
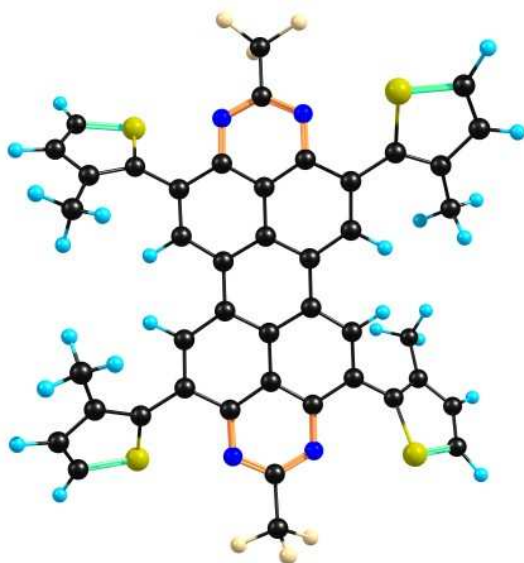
Coordinates of 2:

Atomic Type	Coordinates (Angstroms)		
	X	Y	Z
S	7.594461	14.333895	13.108886
S	8.852790	6.234278	12.493954
F	10.055340	11.479518	14.399920

F	10.096072	9.322575	14.577673
N	7.872543	11.416961	12.829522
N	7.971585	9.038532	12.970254
C	6.915659	11.351276	11.874713
C	6.399754	12.551879	11.275221
C	5.308000	12.424663	10.411244
H	4.870772	13.336018	10.006078
C	4.753081	11.187303	10.016925
C	5.367796	9.985180	10.484779
C	6.413509	10.082594	11.446419
C	7.012539	8.916931	12.020558
C	6.574220	7.617943	11.590425
C	5.591418	7.559090	10.598440
H	5.290871	6.574409	10.245524
C	3.605118	11.078657	9.134632
C	8.315177	10.268801	13.314351
C	9.285824	10.385213	14.485342
C	7.011706	13.867729	11.521456
C	7.219734	14.897247	10.603391
C	7.816347	16.048388	11.208014
H	8.082130	16.945493	10.642719
C	8.053193	15.899285	12.551074
H	8.520579	16.610742	13.231477
C	6.938541	14.836437	9.124039
H	7.032518	13.813752	8.729594
H	7.645227	15.477836	8.574787
H	5.924567	15.192645	8.867975
C	7.137286	6.379706	12.153519
C	6.483883	5.178746	12.423698
C	7.386166	4.158803	12.862586
H	7.056430	3.155470	13.142885
C	8.692016	4.574429	12.927061
H	9.560896	4.004408	13.254579
C	4.997745	4.943176	12.339554
H	4.426918	5.867372	12.514488
H	4.684965	4.202154	13.092330
H	4.683364	4.548109	11.356625
S	2.233776	5.854310	4.928609
S	-0.908728	13.016640	7.441685
F	-1.237239	8.406797	4.454259
F	-1.324948	10.570100	4.387750
N	1.071731	8.456650	5.917119

N	0.579146	10.771697	6.227099
C	1.990074	8.490331	6.911568
C	2.689478	7.296949	7.300971
C	3.650895	7.402589	8.308735
H	4.211536	6.505204	8.564419
C	3.978694	8.607659	8.967418
C	3.300226	9.801646	8.572076
C	2.281808	9.721557	7.579932
C	1.504133	10.865737	7.213992
C	1.703621	12.107697	7.913294
C	2.760554	12.167398	8.827937
H	2.909818	13.093290	9.378820
C	4.974454	8.691752	10.022792
C	0.449448	9.592275	5.641941
C	-0.491736	9.524569	4.441948
C	2.429961	5.994392	6.666238
C	2.380098	4.739512	7.266592
C	2.217788	3.688907	6.308896
H	2.136261	2.636585	6.593245
C	2.146469	4.135101	5.013686
H	1.993054	3.546997	4.109344
C	2.436822	4.461614	8.746862
H	2.133092	5.334467	9.342770
H	1.766070	3.626603	9.007042
H	3.449522	4.171553	9.081027
C	0.808017	13.260831	7.727908
C	1.087697	14.620833	7.859780
C	-0.089367	15.428063	7.761718
H	-0.067658	16.518960	7.829270
C	-1.236428	14.703902	7.562337
H	-2.250405	15.081230	7.429939
C	2.450354	15.241357	8.037566
H	3.248168	14.601793	7.633451
H	2.495919	16.209971	7.514221
H	2.690791	15.439674	9.098047
F	8.601015	10.471999	15.648170
F	0.216378	9.514969	3.290717

Final Single Point Energy   -4101.623171767360 E_h
Homo   -0.210617 E_h -5.7312 eV
Lumo   -0.131061 E_h -3.5664 eV

Compound 4:
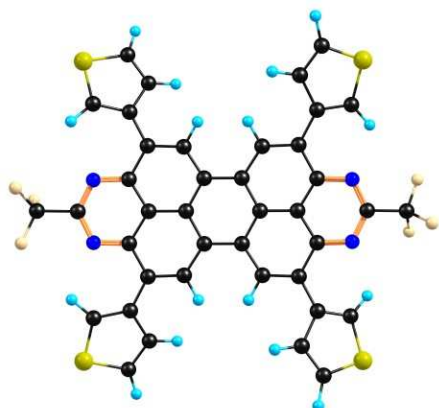
Coordinates of 4:

Atomic Type	Coordinates (Angstroms)		
	X	Y	Z
S	0.572072	0.404774	7.615285
S	4.930936	8.669956	14.181776
F	4.614767	2.878741	10.275444
F	5.288907	4.834817	10.917777
N	1.965509	3.683384	10.432042
N	2.867434	5.409407	11.790986
C	0.742450	3.865861	10.953845
C	-0.383347	3.065700	10.491075
C	4.318868	4.188665	10.263443
C	-2.152577	6.187446	14.230936
C	-0.737461	5.033112	12.581436
C	0.537326	4.850454	11.972778
C	-1.595045	3.259793	11.126592
H	-2.428050	2.634978	10.815298
C	1.514178	6.682899	13.360375
C	1.668355	5.639095	12.354710
C	-0.876582	6.023740	13.597234
C	0.263421	6.812076	13.937281
H	0.142205	7.561927	14.714429
C	2.946491	4.446118	10.889149
C	-0.283090	2.091585	9.384929
C	0.878352	1.520472	8.889267
H	1.892237	1.712210	9.226185
C	-1.133434	0.685207	7.702112
H	-1.815463	0.179322	7.020111
C	-1.439877	1.595084	8.675324
H	-2.460487	1.933922	8.854652

C	2.612841	7.582746	13.773701
C	3.962379	7.427341	13.489040
H	4.417355	6.640205	12.896417
C	3.545866	9.447111	14.867703
H	3.650935	10.373028	15.431278
C	2.396996	8.768903	14.572180
H	1.420676	9.129046	14.896088
S	-4.552912	10.002016	18.771801
S	-8.905496	1.715899	12.229670
F	-8.592729	7.516464	16.123895
F	-9.266017	5.559807	15.482478
N	-5.943335	6.714293	15.964985
N	-6.844374	4.985221	14.609402
C	-4.720477	6.532204	15.442614
C	-3.595218	7.334069	15.903564
C	-8.296023	6.206717	16.136147
C	-1.825519	4.210123	12.165778
C	-3.240439	5.363951	13.815859
C	-4.515041	5.546381	14.424960
C	-2.383371	7.139254	15.268666
H	-1.550670	7.765010	15.578872
C	-5.490910	3.710861	13.040876
C	-5.645499	4.756034	14.045040
C	-3.101210	4.372833	12.800504
C	-4.240673	3.582735	12.462503
H	-4.119281	2.831836	11.686378
C	-6.923832	5.949833	15.509789
C	-3.696257	8.310586	17.007429
C	-4.858065	8.883529	17.500006
H	-5.871592	8.691466	17.162167
C	-2.847454	9.720268	18.688172
H	-2.166117	10.227274	19.370031
C	-2.540163	8.808017	17.717453
H	-1.519530	8.468035	17.540401
C	-6.588670	2.808260	12.631185
C	-7.938138	2.962402	12.917033
H	-8.393655	3.750625	13.507780
C	-7.520008	0.938879	11.544407
H	-7.624251	0.011012	10.983904
C	-6.371881	1.619954	11.836196
H	-5.395365	1.260412	11.512166
F	-8.316468	5.801275	17.414929

F	4.340197	4.594439	8.984783

Final Single Point Energy	-3941.040844369229 E_h		
HOMO	-0.211787 E_h	-5.7630 eV	
LUMO	-0.130715 E_h	-3.5569 eV	

Compound 5:
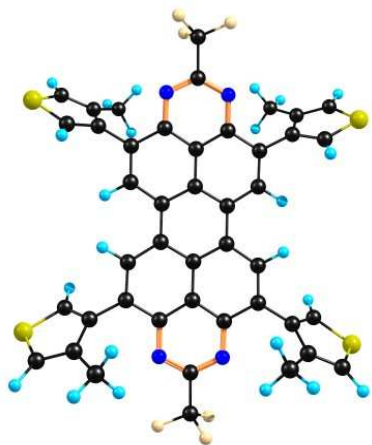
Coordinates of 5:

Atomic Type	Coordinates (Angstroms)		
	X	Y	Z
S	-0.582908	9.470236	2.025635
S	5.373558	4.181412	11.608226
F	3.823082	5.625870	3.878891
F	4.148794	4.216346	5.489557
N	2.388615	7.142972	5.512337
N	3.487630	6.144481	7.377304
C	1.577839	7.836582	6.331390
C	0.600803	8.763191	5.789346
C	-0.283954	9.351152	6.669045
H	-1.004027	10.054594	6.252163
C	-0.109195	8.625390	10.916200
C	0.729634	8.277872	8.630910
C	1.653724	7.654536	7.745086
C	2.694063	6.807143	8.231971
C	2.874443	6.653651	9.663973
C	1.946746	7.238513	10.496343
H	2.090580	7.110752	11.569281
C	0.845593	8.033205	10.032977
C	3.265953	6.329016	6.081602
C	4.175645	5.514004	5.160371

C	0.503215	9.063455	4.339565
C	-0.703036	8.978615	3.672147
H	-1.648118	8.611458	4.070142
C	1.100454	9.820985	2.216863
H	1.672764	10.216647	1.378376
C	1.564719	9.557940	3.483214
C	2.989935	9.797410	3.900319
H	3.046240	10.352032	4.851616
H	3.528592	10.381186	3.139415
H	3.519439	8.843552	4.043653
C	4.019164	5.889236	10.218320
C	3.862173	4.829099	11.086696
H	2.927523	4.376437	11.415456
C	6.240688	5.355706	10.681258
H	7.330364	5.375000	10.709308
C	5.414019	6.203030	9.985143
C	5.908269	7.336418	9.130869
H	5.850982	7.073789	8.062141
H	6.952075	7.586421	9.372774
H	5.301405	8.243905	9.285061
S	0.185387	8.267730	16.973028
S	-5.767621	13.564787	7.391742
F	-4.218103	12.117882	15.121065
F	-4.542249	13.528436	13.510990
N	-2.784322	10.600526	13.487254
N	-3.882448	11.600361	11.622478
C	-1.973845	9.906716	12.668071
C	-0.997390	8.979360	13.209902
C	-0.112595	8.391586	12.330134
H	0.607185	7.687741	12.746846
C	-0.286990	9.117960	8.083107
C	-1.125596	9.465768	10.368473
C	-2.049438	10.089305	11.254413
C	-3.089244	10.937425	10.767681
C	-3.269617	11.091167	9.335702
C	-2.342380	10.505755	8.503186
H	-2.486198	10.633760	7.430277
C	-1.241535	9.710517	8.966407
C	-3.660980	11.415332	12.918153
C	-4.570250	12.230640	13.839550
C	-0.900277	8.678018	14.659493
C	0.306030	8.760995	15.327049

H	1.251523	9.127485	14.929416
C	-1.498334	7.918895	16.781397
H	-2.071082	7.522999	17.619475
C	-1.962300	8.183723	15.515307
C	-3.387735	7.946122	15.097868
H	-3.444527	7.391875	14.146377
H	-3.927242	7.362749	15.858476
H	-3.916041	8.900674	14.954734
C	-4.413962	11.856308	8.781558
C	-4.256512	12.916158	7.912921
H	-3.321653	13.368024	7.583661
C	-6.635272	12.391478	8.319468
H	-7.724977	12.373070	8.291929
C	-5.808959	11.543706	9.015469
C	-6.303681	10.411064	9.870467
H	-6.245540	10.674061	10.939064
H	-7.347841	10.161849	9.629279
H	-5.697671	9.503006	9.716279
F	-5.844658	11.809044	13.722447
F	5.449753	5.936699	5.276962

Final Single Point Energy: -4101.587009188829 E_h

Homo	-0.226115 E_h	-6.1529 eV
Lumo	-0.133879 E_h	-3.6430 eV

Compound 8:
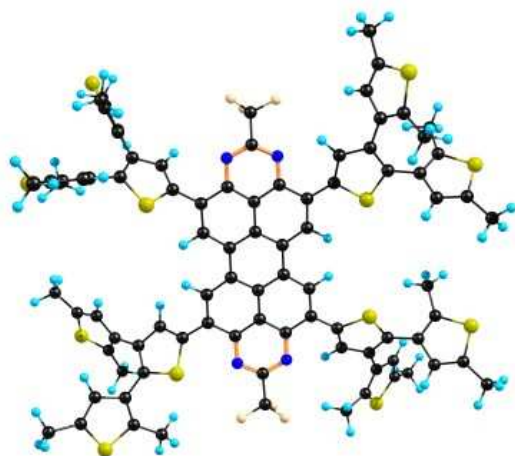
Coordinates of 8:

Atomic Type	Coordinates (Angstroms)		
	X	Y	Z
C	19.680741	-1.230747	4.142699

F	26.372634	-4.887019	1.851326
F	25.252403	-5.965863	3.360193
N	23.031918	-4.100198	1.821851
N	24.082322	-5.919162	0.703860
C	21.974350	-4.170077	0.995840
C	20.829232	-3.297485	1.195363
C	19.819849	-3.335723	0.246068
H	18.988674	-2.642774	0.374895
C	19.817832	-4.212176	-0.883396
C	20.896364	-5.138540	-1.026849
C	21.962726	-5.101068	-0.085335
C	23.067944	-6.002537	-0.169168
C	23.075144	-7.017322	-1.210456
C	22.043753	-7.005071	-2.129071
H	22.051985	-7.780401	-2.894965
C	18.755386	-4.245639	-1.848149
C	24.020509	-4.957875	1.614169
C	25.227683	-4.887683	2.550768
C	20.700974	-2.437420	2.375447
C	19.520197	-2.094020	3.016526
C	21.018559	-0.876823	4.333532
N	16.633854	-6.388870	-5.659542
N	15.523162	-4.615344	-4.525005
C	17.710602	-6.262392	-4.873603
C	18.897230	-7.069814	-5.112650
C	19.903546	-6.997915	-4.167087
H	20.794532	-7.602288	-4.336589
C	19.895901	-6.117848	-3.049518
C	18.799042	-5.220672	-2.889658
C	17.710076	-5.317273	-3.801358
C	16.572038	-4.460030	-3.696915
C	16.584323	-3.398002	-2.696674
C	17.650890	-3.339736	-1.819091
H	17.639734	-2.548125	-1.068736
C	20.954025	-6.088739	-2.089305
C	15.611232	-5.585256	-5.427552
F	25.209671	-3.796207	3.319166
H	18.554451	-2.515419	2.732933
S	22.048495	-1.665787	3.169759
S	16.009588	-0.684564	-2.464662
C	14.358412	-0.126114	-2.574824
C	13.487019	-1.197342	-2.748508

C	15.546706	-2.354839	-2.675470
C	14.180427	-2.450820	-2.809070
H	13.672608	-3.396379	-2.988708
S	24.627349	-8.713610	-2.802277
C	25.697143	-9.860710	-2.035579
C	25.682125	-9.698049	-0.649459
C	24.124459	-8.032418	-1.275264
C	24.794937	-8.653304	-0.242549
H	24.618815	-8.394170	0.798661
S	20.401188	-9.001699	-6.448654
C	20.094816	-9.311652	-8.139908
C	19.023186	-8.551277	-8.600097
C	19.079564	-7.854580	-6.332302
C	18.447511	-7.752711	-7.559747
H	17.608228	-7.081199	-7.726341
C	14.362972	-5.840767	-6.268952
F	14.640583	-6.598028	-7.337469
F	13.442400	-6.492018	-5.539352
F	13.809688	-4.703934	-6.698090
C	27.972395	-10.824425	-2.686182
C	28.609887	-11.587622	-3.626727
S	27.451058	-12.207865	-4.776634
C	26.108537	-11.431270	-3.984337
C	26.546803	-10.709670	-2.883041
H	28.496476	-10.324372	-1.870540
C	26.371309	-10.559951	0.335693
C	27.022980	-10.090881	1.465153
S	27.558355	-11.424172	2.454435
C	26.895801	-12.618460	1.366905
C	26.319024	-11.999655	0.291025
H	25.824916	-12.548272	-0.512959
C	22.412631	-10.137930	-8.793048
C	23.078699	-11.096544	-9.505559
S	21.935996	-12.216144	-10.210879
C	20.560877	-11.373194	-9.543253
C	20.977230	-10.266083	-8.823916
H	22.920563	-9.317624	-8.280927
C	17.105715	-8.487139	-10.290548
C	16.808451	-8.375174	-11.623050
S	18.282133	-8.246827	-12.551437
C	19.290932	-8.330330	-11.130714
C	18.516999	-8.478555	-9.991580
H	16.336336	-8.571981	-9.519344

C	12.012023	-1.145223	-2.882156
C	11.301660	-0.406344	-3.809328
S	9.587659	-0.702443	-3.647813
C	9.816739	-1.837345	-2.340511
C	11.152315	-1.956992	-2.057586
H	11.532345	-2.611962	-1.270535
C	20.992711	1.395167	5.491026
C	21.711911	2.219985	6.312687
S	23.162060	1.408432	6.851025
C	22.791054	-0.043005	5.961546
C	21.598936	0.103410	5.265221
H	20.054629	1.694907	5.021609
C	14.781628	2.280028	-3.335636
C	14.502611	3.588937	-3.045085
S	13.411392	3.674322	-1.682385
C	13.367294	1.940046	-1.491886
C	14.130708	1.327334	-2.470431
H	15.442677	1.981240	-4.151605
C	17.348546	-0.199615	4.539081
C	16.425607	0.071939	5.515968
S	17.023656	-0.464687	7.065384
C	18.517517	-1.052309	6.383601
C	18.555344	-0.826388	5.019515
H	17.189867	0.059163	3.489655
C	26.964329	-14.080922	1.687348
H	26.343262	-14.337692	2.562420
H	26.596071	-14.671371	0.834889
H	27.992451	-14.410726	1.913008
C	27.307829	-8.680693	1.897839
H	28.279370	-8.608726	2.412736
H	27.330272	-8.000887	1.034077
H	26.546153	-8.290008	2.594586
C	30.074592	-11.866204	-3.780420
H	30.500617	-11.335498	-4.649425
H	30.619003	-11.527933	-2.886181
H	30.282434	-12.939499	-3.923554
C	24.717978	-11.633607	-4.515232
H	24.600021	-12.638397	-4.953134
H	23.973457	-11.521014	-3.713593
H	24.461354	-10.904063	-5.302825
C	8.659411	-2.535539	-1.690618
H	8.101250	-3.162504	-2.407466
H	9.024558	-3.192171	-0.886803
H	7.939766	-1.827125	-1.245981
C	11.812472	0.505691	-4.882245
H	11.790726	1.565190	-4.571744
H	12.856289	0.253158	-5.120828

H	11.219808	0.410109	-5.806236
C	23.729635	-1.211731	6.035782
H	24.186688	-1.295197	7.034660
H	23.202350	-2.152154	5.821368
H	24.554877	-1.128892	5.307550
C	21.433569	3.641149	6.702216
H	22.159546	4.335161	6.245420
H	20.430523	3.935832	6.359326
H	21.481348	3.791737	7.793903
C	15.001745	4.825408	-3.731653
H	15.505292	5.511750	-3.029349
H	15.727097	4.551868	-4.512897
H	14.186048	5.391637	-4.213859
C	12.616254	1.316043	-0.355203
H	11.553905	1.150120	-0.603067
H	13.050338	0.335221	-0.113973
H	12.662344	1.944257	0.548532
C	19.513764	-1.743340	7.262778
H	19.016677	-2.452896	7.945086
H	20.230056	-2.307317	6.648516
H	20.094841	-1.033840	7.876359
C	15.082389	0.728256	5.398496
H	14.995384	1.608912	6.055956
H	14.909464	1.064052	4.365107
H	14.265085	0.039888	5.674762
C	15.468239	-8.363837	-12.293446
H	15.352471	-9.200537	-13.002954
H	14.671165	-8.448507	-11.539295
H	15.299356	-7.432357	-12.860798
C	20.778200	-8.212251	-11.279614
H	21.043387	-7.495801	-12.073487
H	21.231339	-7.858929	-10.343051
H	21.252441	-9.176807	-11.527857
C	24.552257	-11.230447	-9.731590
H	24.812694	-11.167002	-10.801913
H	25.086592	-10.422892	-9.209820
H	24.942788	-12.191345	-9.355761
C	19.173728	-11.891897	-9.768957
H	19.101224	-12.964978	-9.522838
H	18.460340	-11.350211	-9.136178
H	18.849019	-11.760835	-10.814907

Final Single Point Energy   -8987.436927424180 E_h
Homo: -0.197201 E_h -5.3661 eV
Lumo: -0.129350 E_h -3.5198 eV

Compound 10:
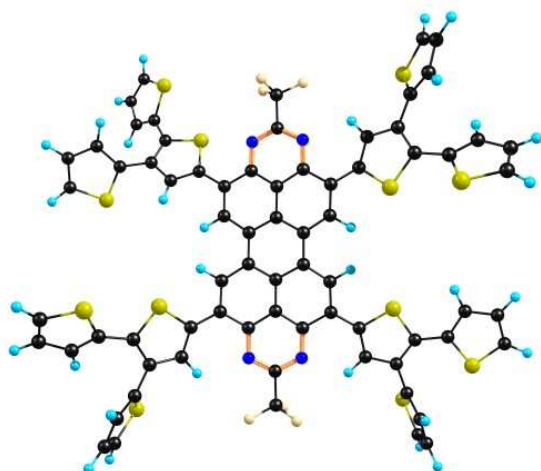
Coordinates of 10:

Atomic Type	Coordinates (Angstroms)		
	X	Y	Z
C	11.438156	6.292075	5.657586
F	16.097756	3.603912	8.946321
F	17.620238	2.094229	8.638208
N	15.783726	3.964395	6.234759
N	17.876707	2.853118	6.083147
C	15.909318	4.435925	4.986645
C	14.843054	5.238278	4.408221
C	14.995317	5.646428	3.088949
H	14.206538	6.259399	2.651872
C	16.146016	5.360163	2.293999
C	17.225952	4.643354	2.894311
C	17.074268	4.143081	4.217612
C	18.059287	3.306714	4.830325
C	19.239549	2.929877	4.063304
C	19.410347	3.543755	2.830787
H	20.316185	3.312528	2.271155
C	16.278885	5.755665	0.916324
C	16.765574	3.209770	6.708461
C	16.521765	2.645394	8.112634
C	13.648182	5.587667	5.180855
C	12.414733	5.964887	4.674016
C	11.958979	6.207687	6.953360
N	19.105244	6.512022	-2.962574
N	16.793799	7.063991	-3.054504
C	18.978555	6.031998	-1.717938
C	20.125763	5.448628	-1.031991

C	19.902692	4.936323	0.237958
H	20.750883	4.500403	0.765089
C	18.653703	4.975658	0.916351
C	17.545719	5.604087	0.275954
C	17.710073	6.081780	-1.056009
C	16.609286	6.604807	-1.803898
C	15.282803	6.603716	-1.200123
C	15.191761	6.246252	0.138583
H	14.209513	6.297227	0.609697
C	18.453671	4.395826	2.213865
C	18.021403	7.004149	-3.545501
F	15.570551	1.697178	8.066329
H	12.176642	5.950982	3.608850
S	13.606244	5.642773	6.932967
C	10.542312	6.588225	10.603064
C	10.045365	7.635769	9.864877
C	10.483971	7.610957	8.510480
C	11.318163	6.544263	8.221913
S	11.551805	5.558314	9.653155
H	9.389055	8.403503	10.278868
H	10.201970	8.354128	7.764240
C	7.972419	5.462450	-2.715434
S	9.582087	4.988684	-2.302958
C	7.941856	6.712072	-3.285431
H	7.024737	7.198440	-3.622226
C	10.243515	6.505032	-2.886990
C	9.231569	7.306443	-3.384231
S	12.556717	6.176123	-1.418190
C	11.671587	6.775279	-2.792127
H	9.416123	8.299835	-3.792333
C	12.511385	7.498102	-3.642873
C	14.068241	6.874004	-1.975463
C	13.859876	7.541794	-3.170232
H	14.668062	8.014792	-3.723617
C	24.417118	-2.401468	2.695068
S	22.928182	-1.565678	2.429988
C	24.913008	-2.166483	3.955212
H	25.844411	-2.599329	4.324225
C	22.963417	-0.866078	4.040123
C	24.089864	-1.292127	4.719876
S	21.272354	1.187802	3.329948
C	21.908664	0.041533	4.477230

H	24.320647	-0.966348	5.734260
C	21.292905	0.197331	5.722570
C	20.175517	1.894116	4.504888
C	20.327494	1.253033	5.721265
H	19.719819	1.507513	6.586466
C	27.597684	3.502087	-2.227172
S	26.529793	4.562627	-3.070640
C	26.986401	2.894827	-1.156207
H	27.488032	2.186059	-0.495701
C	25.209595	4.201630	-1.973296
C	25.631119	3.291964	-1.010945
S	22.684720	4.364568	-0.903563
C	23.887657	4.791682	-2.094563
H	24.975683	2.916208	-0.223398
C	23.347749	5.682774	-3.026478
C	21.453176	5.376887	-1.641264
C	21.983359	5.999405	-2.759204
H	21.396925	6.661540	-3.390519
C	18.267328	7.616582	-4.925843
F	18.939782	8.774347	-4.785392
F	19.011454	6.808403	-5.694075
F	17.129610	7.874679	-5.574492
C	25.056959	6.533824	-6.290731
C	25.298294	7.770866	-5.746071
S	24.675769	7.893157	-4.139001
C	24.076003	6.250548	-4.181471
C	24.353739	5.669753	-5.400243
H	25.369399	6.246498	-7.296331
H	25.805975	8.620018	-6.203043
H	24.054823	4.650211	-5.648053
C	21.646137	-2.033191	6.956245
C	21.522735	-0.659754	6.895167
S	21.630862	0.030618	8.500467
C	21.838361	-1.526317	9.222087
C	21.825866	-2.525849	8.281798
H	21.594182	-2.667448	6.070684
H	21.961512	-1.621407	10.300547
H	21.937395	-3.582595	8.532792
C	7.692989	6.568645	5.322204
C	7.928466	7.443999	4.290497
S	9.622872	7.682922	4.034205
C	10.036681	6.585610	5.332040
C	8.893321	6.080419	5.915764
H	6.694365	6.272118	5.648728
H	7.202994	7.960142	3.662968

H	8.922767	5.373382	6.746093
C	11.112406	8.460013	-7.018045
C	11.517866	9.739550	-6.729687
S	12.292341	9.829235	-5.186591
C	12.071289	8.116454	-4.906785
C	11.428311	7.535711	-5.979772
H	10.605565	8.181275	-7.943842
H	11.410377	10.635048	-7.340772
H	11.177851	6.474248	-6.015144
H	10.365008	6.356098	11.652741
H	24.843544	-3.019295	1.905360
H	28.621011	3.376850	-2.580427
H	7.139141	4.790102	-2.514305

Final Single Point Energy:	8358.560644524268 E_h	
Homo:	-0.197049 E_h	-5.3620 eV
Lumo:	-0.134977 E_h	-3.6729 eV

Compound 12:

Coordinates of 12:

	Coordinates (Angstroms)		
Atomic Type	X	Y	Z
S	-17.209399	25.007113	16.550027
S	-13.788104	31.852640	26.130237
F	-15.472020	30.503427	18.912436
F	-15.186600	31.658214	20.720541
N	-15.900130	28.224225	20.300363
N	-15.449905	29.489080	22.271623
C	-15.874533	27.078269	21.001377
C	-16.106179	25.806621	20.342926
C	-16.145564	24.668354	21.117484

H	-16.320813	23.723880	20.604851
C	-15.654432	24.811907	25.398064
C	-15.704638	25.901526	23.191712
C	-15.648787	27.092626	22.410879
C	-15.406036	28.365353	23.007323
C	-15.128759	28.433683	24.427359
C	-15.195713	27.273553	25.162960
H	-15.003695	27.350679	26.233077
C	-15.503254	25.990129	24.602120
C	-15.704323	29.351076	20.977133
C	-15.872265	30.648716	20.179956
C	-16.311354	25.713147	18.875980
C	-17.393327	25.060440	18.286731
C	-15.676547	25.844804	16.607328
C	-15.362887	26.175253	17.910497
C	-14.863356	29.727842	25.115312
C	-13.676428	30.456164	25.079989
C	-15.405949	31.447016	26.641996
C	-15.826120	30.296518	26.003332
S	-15.491358	24.669443	31.537870
S	-17.780874	17.356863	22.358267
F	-17.806357	19.505485	29.126919
F	-18.495594	18.554179	27.307054
N	-16.549830	21.426029	27.727261
N	-17.050974	20.184787	25.757199
C	-16.190230	22.489145	26.986145
C	-15.754160	23.717681	27.624939
C	-15.504325	24.810117	26.823118
H	-15.176348	25.723815	27.315753
C	-15.990170	24.661416	22.541131
C	-16.006670	23.587471	24.754257
C	-16.267277	22.442995	25.560731
C	-16.677195	21.208445	24.980974
C	-16.747419	21.082969	23.536310
C	-16.493149	22.204536	22.778308
H	-16.580706	22.109538	21.695737
C	-16.148584	23.482461	23.335957
C	-16.985136	20.359028	27.068245
C	-17.449114	19.155300	27.889156
C	-15.571240	23.803199	29.095201
C	-16.061588	24.836732	29.894529
C	-14.556735	23.245610	31.153392

C	-14.737615	22.900278	29.829871
C	-17.242426	19.826429	22.922940
C	-16.795926	18.532008	23.192087
C	-18.829581	18.582149	21.692272
C	-18.385249	19.834829	22.062028
F	-16.459898	18.245623	27.982053
F	-17.171408	31.004037	20.161421
H	-18.920213	20.748310	21.797967
H	-14.239346	22.046643	29.371217
H	-16.818077	29.867378	26.149763
H	-14.464490	26.730255	18.180324
C	-15.693458	18.041291	24.007342
C	-15.681482	16.935571	24.837838
S	-14.129975	18.828962	24.023542
C	-14.434403	16.737056	25.495975
H	-16.563877	16.314976	25.001848
C	-13.501533	17.686087	25.159258
H	-14.239081	15.930713	26.205062
H	-12.478286	17.780786	25.520964
C	-19.996685	18.252884	20.887507
C	-20.535223	18.977881	19.840153
S	-20.978959	16.841160	21.217203
C	-21.722999	18.400185	19.306297
H	-20.067597	19.886191	19.458199
C	-22.082164	17.238843	19.945593
H	-22.284880	18.822597	18.471301
H	-22.928766	16.586622	19.734122
C	-18.607872	24.496994	18.868217
C	-19.301428	23.371330	18.458039
S	-19.464895	25.285594	20.178183
C	-20.498404	23.140948	19.197172
H	-18.947688	22.727389	17.650751
C	-20.712691	24.089920	20.167222
H	-21.173976	22.302366	19.017963
H	-21.537543	24.155230	20.876738
C	-14.876887	26.045981	15.406948
C	-13.503707	26.190592	15.318301
S	-15.596060	26.111530	13.810680
C	-13.037190	26.341985	13.981035
H	-12.850908	26.156859	16.191714
C	-14.052135	26.311045	13.057849
H	-11.986872	26.459887	13.707520

H	-13.978411	26.399553	11.974193
C	-13.736867	22.587886	32.162915
C	-13.478408	21.238310	32.315210
S	-12.871075	23.512556	33.374739
C	-12.593483	20.953483	33.396652
H	-13.936015	20.479143	31.678826
C	-12.187655	22.082779	34.064895
H	-12.276388	19.948421	33.680755
H	-11.531721	22.156832	34.931657
C	-16.987279	25.930193	29.616896
C	-17.000661	27.187630	30.197569
S	-18.373264	25.741805	28.559839
C	-18.105135	27.989359	29.788971
H	-16.226522	27.523087	30.890244
C	-18.926139	27.345723	28.895982
H	-18.284144	29.004076	30.147315
H	-19.828051	27.724377	28.415945
C	-12.395552	30.200997	24.436170
C	-11.143279	30.552077	24.917129
S	-12.232222	29.379377	22.898197
C	-10.073133	30.149930	24.071806
H	-11.001692	31.060849	25.871859
C	-10.508634	29.494003	22.946305
H	-9.021704	30.335568	24.300032
H	-9.913877	29.073370	22.136215
C	-16.130088	32.240042	27.623405
C	-17.154873	31.829451	28.459073
S	-15.789128	33.937921	27.877806
C	-17.658300	32.870326	29.289589
H	-17.520751	30.802184	28.486047
C	-17.010611	34.065241	29.095093
H	-18.466082	32.734642	30.011082
H	-17.186657	35.017695	29.593494

Final Single Point Energy: -8358.150806246387 E_h
Homo: -0.202699 E_h -5.5157 eV
Lumo: -0.130190 E_h -3.5427 eV

Schematic Cross-Section of the TFTs

Source (Au)	Drain (Au)
Organic semiconductor	
Gate dielectric (thermally grown SiO$_2$)	
Substrate and gate electrode (Si)	
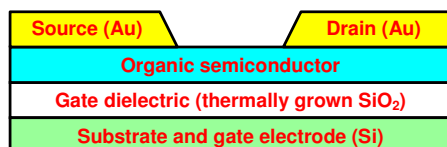
## X-ray Crystal Structure Determinations

Crystal data and details of the structure determinations are compiled in Tables S1 and S2. Full shells of intensity data were collected at low temperature with a Bruker AXS Smart 1000 CCD diffractometer (Mo-K_a radiation, sealed X-ray tube, graphite monochromator, compound **5**·2 CHCl$_3$) or an Agilent Technologies Supernova-E CCD diffractometer (Mo- or Cu-K_a radiation, microfocus X-ray tube, multilayer mirror optics, all other compounds). Detector frames (typically w-, occasionally j-scans, scan width 0.4...1°) were integrated by profile fitting.[5-7] Data were corrected for air and detector absorption, Lorentz and polarization effects[5] and scaled essentially by application of appropriate spherical harmonic functions.[7-10] Absorption by the crystal was treated with a semiempirical multiscan method (as part of the scaling process), (and) augmented by a spherical correction (compounds **2**, **5**·2 CHCl$_3$, **11**·0.75 CHCl$_3$),[8-10] or numerically (Gaussian grid, all other compounds).[7,11] For datasets collected with the microfocus tube(s) an illumination correction was performed as part of the numerical absorption correction.[10]

The structures were solved by "intrinsic" phasing[12] (compound **11**·0.75 CHCl$_3$) or by the charge flip procedure[13] (all other compounds) and refined by full-matrix least squares methods based on F^2 against all unique reflections.[14] All non-hydrogen atoms were given anisotropic displacement parameters. Hydrogen atoms were generally input at calculated positions and refined with a riding model. When justified by the quality of the data the positions of some hydrogen atoms were taken from difference Fourier syntheses and refined. When found necessary, disordered groups and/or solvent molecules were subjected to suitable geometry and adp restraints.

Crystal Structures of Compounds 2-5, 11

Crystals of compounds **2**-**5** and **11** were grown by slow evaporation of saturated solutions of the compounds in THF (**2**-**4**) or $CHCl_3$ (**5**, **11**), respectively. Crystals of **11** could also be grown by slow evaporation of a pentane solution.

Compound 2:
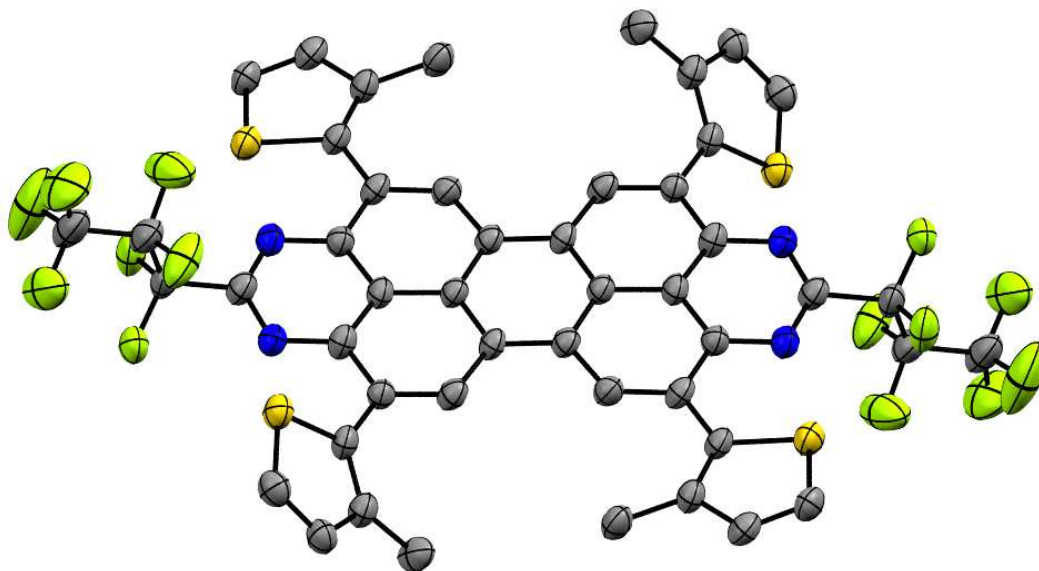
Ortep view (50% probability level) of **2** (C = grey ,N = blue, F = green, S = yellow). Hydrogen atoms are omitted for clarity. Only one of the independent molecules is shown.
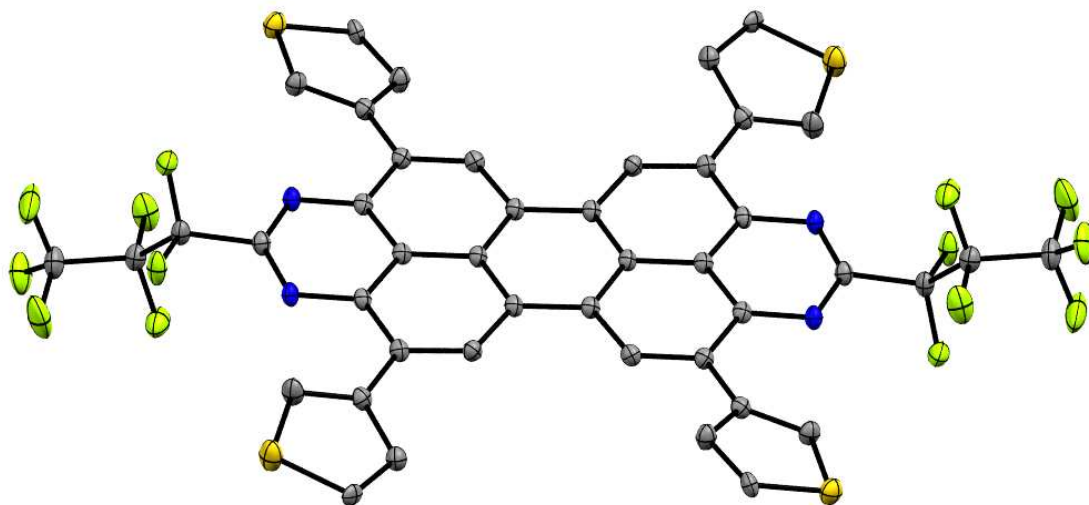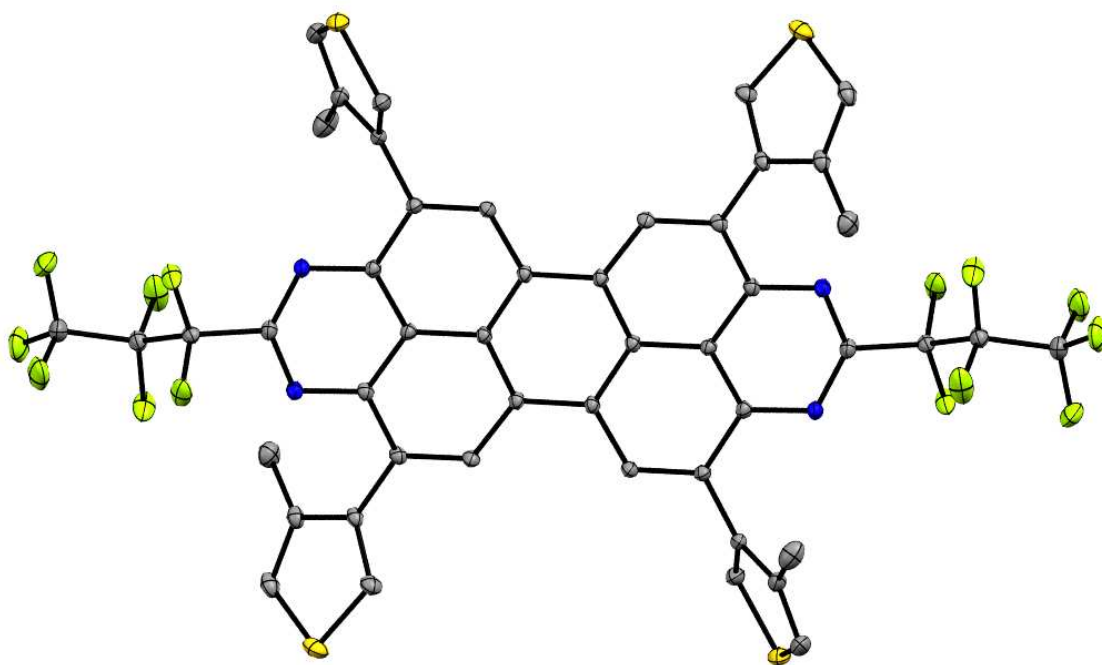
Compound 3:
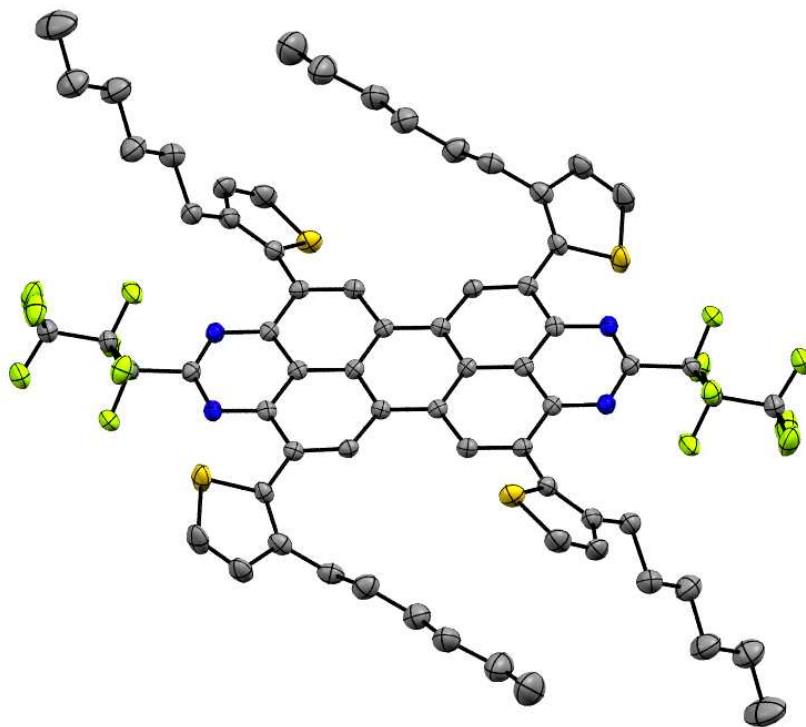
Ortep view (50% probability level) of **3** (C = grey ,N = blue, F = green, S = yellow). Hydrogen atoms are omitted for clarity. Only one of the independent molecules is shown.

Compound 4:

Ortep view (50% probability level) of **4** (C = grey ,N = blue, F = green, S = yellow). Hydrogen atoms and solvent molecules are omitted for clarity.

Compound 5:
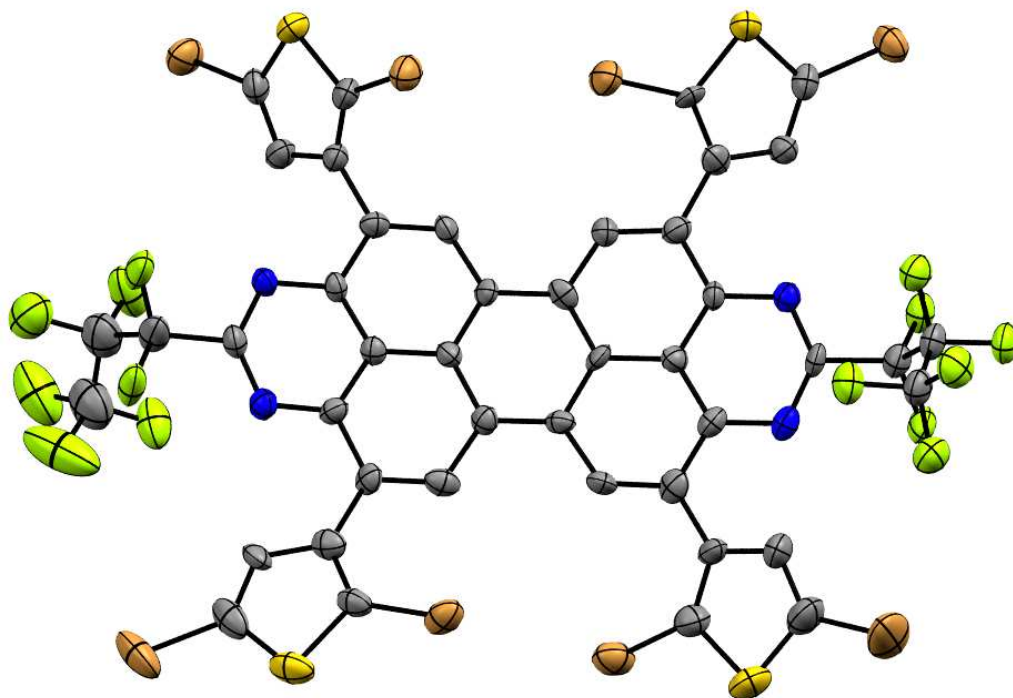

Ortep view (50% probability level) of **5** (C = grey ,N = blue, F = green, S = yellow). Hydrogen atoms and solvent molecules are omitted for clarity.

Compound 11:

Ortep view (50% probability level) of **11** (C = grey ,N = blue, F = green, S = yellow, Br = brown). Hydrogen atoms and solvent molecules are omitted for clarity. **O**nly one of the independent molecules is shown.

Table S1. Details of the crystal structure determinations of compounds **2**, **3**, **4**·2 thf and **5**·2 CHCl$_3$.

	2	3	4·2 thf	5·2 CHCl$_3$
formula	C$_{48}$H$_{24}$F$_{14}$N$_4$S$_4$	C$_{68}$H$_{64}$F$_{14}$N$_4$S$_4$	C$_{52}$H$_{32}$F$_{14}$N$_4$O$_2$S$_4$	C$_{50}$H$_{26}$Cl$_6$F$_{14}$N$_4$S$_4$
crystal system	monoclinic	triclinic	monoclinic	monoclinic
space group	$P\,2_1/n$	P -1	$P\,2_1/c$	$P\,2_1/c$
a /Å	16.6520(8)	15.3304(3)	16.1364(3)	14.764(8) [a]
b /Å	19.7591(6)	17.3728(4)	5.19816(7)	8.872(5) [a]
c /Å	20.6578(11)	21.0398(4)	26.6969(5)	19.004(9) [a]
α /°		107.5526(18)		
β /°	112.774(6)	100.5745(16)	98.5684(17)	91.194(15) [a]
γ /°		111.0829(18)		
V /Å^3	6267.1(6)	4708.83(17)	2214.33(6)	2489(2)
Z	6	3	2	2
M_r	1050.95	1331.47	1139.05	1289.69
F_{000}	3180	2070	4146	1292
d_c /Mgm^{-3}	1.671	1.409	1.708	1.721
μ /mm^{-1}	3.052	2.147	2.967	0.610
max., min. transmission factors	1.000, 0.606 [b]	0.909, 0.808 [c]	0.925, 0.554 [c]	0.746, 0.709 [b]
X-radiation, λ /Å	Cu-$K\alpha$, 1.54184	Cu-$K\alpha$, 1.54184	Cu-$K\alpha$, 1.54184	Mo-$K\alpha$, 0.71073
data collect. temperat. /K	120(1)	120(1)	120(1)	100(1)
θ range /°	3.6 to 69.6	4.0 to 71.0	4.0 to 71.0	1.4 to 31.5
index ranges h,k,l	±19, ±23, -25 ... 24	±18, ±21, ±25	±19, ±6, -32 ... 30	±21, -12 ... 13, ±27
reflections measured	220936	126219	168031	60977
unique (R_{int})	11252 (0.2395)	17947 (0.0641)	4258 (0.0860)	8212 (0.0419)
observed ($I\geq2\sigma(I)$)	5632	13532	4146	6564
data / restraints /parameters	11252 / 284 / 1007	17947 / 0 / 1240	4258 / 18 / 357	8212 / 0 / 354
GooF on F^2	0.966	1.024	1.125	1.032
R indices ($F>4\sigma(F)$) $R(F)$, $wR(F^2)$	0.0758, 0.1728	0.0533, 0.1368	0.0403, 0.0938	0.0430, 0.1072
R indices (all data) $R(F)$, $wR(F^2)$	0.1595, 0.2277	0.0751, 0.1507	0.0415, 0.0945	0.0580, 0.1164
largest residual peaks /eÅ^{-3}	0.534, -0.574	0.865, -0.509	0.434, -0.391	0.954, -0.520

[a] su include systematic error contributions from Monte Carlo simulations. [b] empirical absorption correction. [c] numerical absorption correction.

Table S2. Details of the crystal structure determinations of compounds **11**·0.75 $CHCl_3$ and **11**·0.667 *n*-pentane.

	11·0.75 $CHCl_3$	**11**·0.667 *n*-pentane
formula	$C_{44.50}H_{8.75}Br_8Cl_{2.25}F_{14}N_4S_4$	$C_{47.33}H_{16}Br_8F_{14}N_4S_4$
crystal system	triclinic	monoclinic
space group	P -1	$P\,2_1/n$
a /Å	15.2196(7)	15.36041(17)
b /Å	15.3694(5)	25.7224(2)
c /Å	24.0731(6)	20.8946(2)
α /°	101.545(2)	
β /°	102.351(3)	110.8723(13)
γ /°	105.027(3)	
V /Å^3	5113.9(3)	7713.83(16)
Z	4	6
M_r	1712.59	1674.16
F_{000}	3248	4788
d_c /Mgm^{-3}	2.224	2.162
μ /mm^{-1}	10.950	6.493
max., min. transmission factors	0.7500, 0.7359 [a]	1.000, 0.290 [b]
X-radiation, λ /Å	Cu-$K\alpha$, 1.54184	Mo-$K\alpha$, 0.71073
data collect. temperat. /K	120(1)	120(1)
θ range /°	3.6 to 71.2	2.6 to 26.4
index ranges h,k,l	±18, -18 ... 17, ±29	±19, ±32, ±26
reflections measured	101070	413499
unique (R_{int})	18912 (0.1438)	15801 (0.1026)
observed ($I{\geq}2\sigma(I)$)	10069	13021
data / restraints /parameters	18912 / 476 / 1396	15801 / 24 / 1047
GooF on F^2	1.019	1.022
R indices ($F>4\sigma(F)$) $R(F)$, $wR(F^2)$	0.0783, 0.1761	0.0369, 0.0840
R indices (all data) $R(F)$, $wR(F^2)$	0.1579, 0.2191	0.0500, 0.0894
largest residual peaks /eÅ^{-3}	1.403, -1.309	2.437, -1.008

[a] empirical absorption correction. [b] numerical absorption correction.

References

(1)   Neese, F. *Wiley Interdiscip. Rev. Comput. Mol. Sci.* **2012**, 2, 73-78.

(2)   (a) Becke, A. D. *J. Chem. Phys.* **1993**, *98*, 1372-1377; (b) Becke, A. D. *J. Chem. Phys.* **1993**, *98*, 5648.

(3)   (a) Lee, C.; Yang, W.; Parr, R. G. *Phys. Rev. B* **1988**, *37*, 785-789; (b) Weigand, F.; Häser, M.; Patzelt, H.; Ahlrichs, R. *Chem. Phys. Lett.* **1998**, *294*, 143-152.

(4)   Weigand, F.; Ahlrichs, R. *Phys. Chem. Chem. Phys.* **2005**, *7*, 3297-3305.

(5)   Kabsch, K. in: Rossmann, M. G., Arnold, E. (eds.) *"International Tables for Crystallography" Vol. F*, Ch. 11.3, Kluwer Academic Publishers, Dordrecht, **2001**.

(6)   *SAINT*, Bruker AXS GmbH, Karlsruhe, Germany **1997**-**2013**.

(7)   CrysAlisPro, Agilent Technologies UK Ltd., Oxford, UK 2011-2014 and Rigaku Oxford Diffraction, Rigaku Polska Sp.z o.o., Wrocław, Poland 2015-2017.

(8)   Blessing, R. H. *Acta Cryst.* **1995**, *A51*, 33.

(9)   (a) Sheldrick, G. M. *SADABS*, Bruker AXS GmbH, Karlsruhe, Germany **2004**-**2014**;   (b) Krause, L; Herbst-Irmer, R.; Sheldrick, G. M.; Stalke, D. *J. Appl. Cryst.* **2015**, *48*, 3.

(10)   *SCALE3 ABSPACK, CrysAlisPro*, Agilent Technologies UK Ltd., Oxford, UK **2011**-**2014** and Rigaku Oxford Diffraction, Rigaku Polska Sp.z o.o., Wrocław, Poland **2015**-**2017**.

(11)   Busing, W. R.; Levy, H. A. *Acta Cryst.* **1957**, *10*, 180.

(12)   (a) Sheldrick, G. M. *SHELXT*, University of Göttingen and Bruker AXS GmbH, Karlsruhe, Germany, **2012**-**2014**; (b) Ruf, M; Noll, B. C. *Application Note SC-XRD 503*, Bruker AXS GmbH Karlsruhe, Germany **2014**; (c) Sheldrick, G. M. *Acta Cryst.* **2015**, *A71*, 3.

(13)   (a) Palatinus, L. *SUPERFLIP*, EPF Lausanne, Switzerland and Fyzikální ústav AV ČR, v. v. i., Prague, Czech Republic, **2007**-**2014** (b) Palatinus, L.; Chapuis, G. *J. Appl. Cryst.* **2007**, 40, 786.

(14)   (a) Sheldrick, G. M. *SHELXL-20xx*, University of Göttingen and Bruker AXS GmbH, Karlsruhe, Germany **2012**-**2017**; (b) Sheldrick, G. M. *Acta Cryst.* **2008**, *A64*, 112; (c) Sheldrick, G. M. *Acta Cryst.* **2015**, *C71*, 3.